CORROSION INHIBITION OF DOUBLE THERMALLY-AGED HIGH PRESSURE DIE CAST (SSM-HPDC) Al-Si-Mg ALLOY BY NEEM SEED AND GUAVA LEAF EXTRACTS

BY

SANI Lawal Mohammed (B.ENG) Met & Mat, A.B.U (2010)

M.SC/ENG/694/2011-2012

A THESIS SUBMITTED TO THE SCHOOL OF POSTGRADUATE STUDIES, AHMADU BELLO UNIVERSITY, ZARIA, IN PARTIAL FULFILLMENT OF THE REQUIREMENTS FOR THE AWARD OF A MASTER OF SCIENCE IN METALLURGICAL AND MATERIALS ENGINEERING.

DEPARTMENT OF METALLURGICAL AND MATERIALS ENGINEERING,
FACULTY OF ENGINEERING,
AHMADU BELLO UNIVERSITY, ZARIA, NIGERIA.

MARCH 2015

DECLARATION

I declare that the work in this Thesis entitled "Corrosion inhibition of double thermally high pressure die cast (SSM-HPDC) Al-Si-Mg alloy by neem seed and guava leaf extract" has been carried out by me in the department of Metallurgical and Materials Engineering. The information derived from the literature has been duly acknowledged in text and a list of references provided. No part of this thesis was previously presented for another degree or diploma at this or any other Institution.

SANI, Lawal Mohammed _____ _____

Signature Date

CERTIFICATION

This thesis entitled "CORROSION INHIBITION OF DOUBLE THERMALLY-AGED HIGH PRESSURE DIE CAST (SSM-HPDC) Al-Si-Mg ALLOY BY NEEM SEED AND GUAVA LEAF EXTRACTS" by SANI LAWAL MOHAMMED meets the regulations governing the award of degree of Masters of Science of Ahmadu Bello University, and is approved for its contribution to knowledge and literary presentation.

Dr. M. Abdulwahab Chairman, Supervisory Committee	Signature	Date
Prof. S. A. Yaro Member, Supervisory Committee	Signature	Date
Prof. S. A. Yaro Head of Department	Signature	Date
Prof. A. Z. Hassan Dean, School of Post Graduate	Signature	Date

DEDICATION

I dedicate this thesis to Almighty Allah (S.W.T) for giving me the wisdom to carry out this work successfully and my lovely family for their support and contribution towards the completion of my academic pursuit. May God bless you all. Thank you.

ACKNOWLEDGEMENT

In the name of ALLAH the most Gracious, the most Merciful, the Praise Worthy, all thanks are due to Him, the Lord of the heavens and universe, who made everything possible and easier for me, may His peace and Blessings be upon His messenger Prophet Muhammad (S.A.W).

I would like to register my appreciation to my supervisors Dr. M. Abdulwahab and Professor S.A. Yaro for being very accommodating at my unscheduled consultation hours and for their positive criticism and suggestions. To this I would say JazaKallahu Khairan. I also appreciate the help of all academic and non-academic staff of the Department for their supports towards the success of this thesis.

My sincere and special thanks go to my beloved parent Alhaji Sani Isiaku and Malama Hadiza for their guidance, love, encouragement, prayers and financial supports towards the achievement of this academic programme. So also are my brothers and sisters. I remain indebted to them all may Allah reward your efforts abundantly and grant you all your heart desires.

Finally my regards to my friends and all my class members who have contributed either directly or indirectly to the success of this thesis.

ABSTRACT

This study determined the corrosive effect of seawater on as-received and double thermally-aged Al-Si-Mg alloy. It also determined the functional groups present in guava leaf and neem seed extracts and their inhibitive effect on the corrosion of Al-Si-Mg alloy in seawater. This was with a view to enhancing their performance in the aggressive seawater environment. The study involved Fourier transform infrared (FTIR) analysis of the extracts, thermal ageing treatment, hardness measurement, gravimetric based-mass loss test, potentiodynamic polarization test and microstructural examination. The FTIR analysis results showed that the extracts can serve as good corrosion inhibitors due to the presence of aromatic compound and functional group with lone pair of electrons which makes them easily adsorb on surface of the alloy. The thermal ageing treatment employed was Double Thermal Ageing (DTAT) with temper condition at pre-ageing temperature of 105^{o}C at constant time of 2 hrs. The hardness of Al-Si-Mg (SSM-HPDC) alloy was determined using the Rockwell-F scale hardness tester. The hardness value of the alloy increased from 59.1 HRF (as-received sample) to 82.8 HRF (double thermally aged sample) indicating an increase of 40%. Improvement in hardness can be attributed to fine coherent clusters of precipitates which serve as obstacles to dislocation movement. The gravimetric based-mass loss test was carried out at different inhibitor concentrations, time and temperature ranges of 0.1-0.5% v/v, 1-5 hrs and 30-70^{o}C, respectively. From the results obtained the corrosion rate of both the as-received and age-hardened samples decrease with increase in inhibitor concentrations. The maximum inhibition efficiencies of 63.17% and 72.10% were obtained for the as-received and age-hardened samples, respectively, in the presence of guava leaf extract. While in the presence of neem seed extract maximum inhibition efficiencies of 60.49% and 64.26% were obtained for the as-received and age-hardened samples, respectively. The

mechanism of inhibition was elucidated by kinetic and thermodynamic models. The polarization curves showed that the extracts act as mixed-type inhibitors. Results obtained from the potentiodynamic polarization technique indicate higher potential value for guava (*Psidium guajava*) leaf extract and lower potential value for neem (*Azadirachta indica*) seed extract. The Tafel plot showed an increase in polarization resistance (R_p) and lower corrosion current density (j_{corr}) for inhibited samples as compared with uninhibited samples. From the results, IE of 90.48% and 98.88% was obtained for as-received and age-hardened samples respectively in the presence of guava (*Psidium guajava*) leaf extract. While in the presence of neem seed extract IE of 96.55% and 80.68% were obtained for the as-received and age-hardened samples respectively. The two methods used for the corrosion evaluation were in agreement and a mixed type corrosion inhibition exist which obeys the Langmuir adsorption isotherms. From OPM result, the microstructure of the age-hardened sample showed finer grains and enhanced grain boundaries than the as-received sample. This was as a result of increase in volume of precipitated intermetallic compounds during ageing process and also refinement of precipitated constituent particles. The surface morphology of as-corroded samples was assessed with scanning electron microscope. Results showed severe damage and pits formation for as-corroded uninhibited condition than as-corroded inhibited condition.

TABLE OF CONTENTS

Page

LIST OF FIGURES

Page

LIST OF PLATES

Page

LIST OF TABLES

Page

LIST OF ABBREVIATIONS, NOTATIONS AND UNITS

T4 temper- This involves solution heat treatment and ageing at room temperature

T6 temper- This involves solution heat treatment and conventional ageing at 180^{o}C /2hr.

HRF-Rockwell micro-hardness number

hr-hour

mm-Millimeter

mpy-mils per year

FTIR-Fourier Transform Infrared Spectroscopy

OPM-Optical Microscopy

SEM-Scanning Electron Microscopy Equipped with Energy Dispersive Spectroscopy

SSM-HPDC-Semi Solid Metal High Pressure Die Cast

Al-Si-Mg alloy-Aluminium + Silicon + Magnesium alloy

G.M-Gravimetric based-mass loss method

PP-CR -Potentiodynamic polarization corrosion rate

PP-Jcorr-Potentiodynamic polarization corrosion current density

LPR-Linear Polarization Resistance

CHAPTER ONE

1.0 INTRODUCTION

Aluminum is the second widely used metal due to its desirable chemical, physical and mechanical properties. It is alloyed with elements like Si, Mg, Cu, Mn, Fe etc. Addition of silicon to aluminum can improve its fluidity as well as castability and mechanical properties (Asuke *et al.,* 2009). Addition of Magnesium to Al-Si alloy improves its strength to weight ratio and yield stress by combining with silicon to form the age hardening phase (Mg_2Si) which precipitates from a super saturated solid solution during heat treatment (Birol, 2009).

Semi-solid metal processing has gained increasing interest from automotive industry and to a lesser extent the aerospace industry because it demonstrate the capability of producing near –net shaped components with good mechanical properties (Govender *et al.,* 2008).The application of this technique is still in its early stage and some brake cylinders and pistons have been manufactured by this process (Haizhi, 2003).

Aluminium and its alloy find application in many industries due to high strength to weight ratio, good corrosion resistance, excellent workability, high electrical and thermal conductivity. However the ability of aluminium and its alloy to resist attack in aggressive corrosive environment have been reported to be poor (Mohammed *et al.,* 2013).The use of inhibitors for corrosion control of materials, which are in contact with aggressive environment is an accepted practice (Stephen *et al.,* 2014). Although synthetic inhibitors when used for corrosion control, have been reported to indicate an excellent performance. But majority of these inhibitors are not eco-friendly and are expensive (Popoola *et al.,* 2012). Therefore effort towards identifying any potential eco-friendly and less expensive corrosion inhibitors remain relevant and important. The growing interest among researchers for green inhibitors remained a top research focus. In this

direction, plant extracts and oil have gained acceptance as corrosion inhibitors that are considered safe, eco -friendly, available and less expensive for most metals and alloys (Popoola *et al*, 2012). Accordingly, the present study involves the use of neem seed and guava leaf extracts as corrosion inhibitors for high pressure die cast (SSM-HPDC) Al-Si-Mg alloy in the as-received and age-hardened condition.

1.1 Aim and Objectives

The aim of this research is to investigate the possibility of using neem seed and guava leaf extracts as corrosion inhibitors for high pressure die cast (SSM-HPDC) Al-Si-Mg alloy in the as-received and age-hardened conditions. To achieve this aim, the following specific objectives were pursued.

1. Determination of the functional groups present in the extracts using the Fourier transform infrared spectroscopy (FTIR) machine;
2. Thermal ageing treatment of the Al-Si-Mg (SSM-HPDC) alloy (double thermal ageing treatment);
3. Hardness measurement of alloy in the as-received and age-hardened conditions;
4. Corrosion testing using the gravimetric based-mass loss and potentiodynamic polarization methods; and
5. Study of inhibition kinetics of neem seed and guava leaf extracts on the alloy and microstructure analysis of the as-received, thermally aged and corroded samples using OPM and SEM.

1.2 Justification of the study

Aluminium and its alloys are widely used for different applications in industries and marine environment because of their excellent properties (Popoola *et al.*, 2012). However, the alloys still

exhibit insufficient and poor performance in service condition that requires high hardness, wear and aggressive corrosion environment (Abdulwahab *et al*., 2012). They are usually heat treated to obtain the desired combination of strength and ductility, since the alloy may find applications in ship building, automobile and aerospace industries. In aggressive environment such as chloride and acidic, their protective layers are locally destroyed and corrosive attack takes place (Cabot *et al.*, 1991). Due to different industrial applications and economic importance of aluminium and its alloys, their protection against corrosion by inhibiting the working environment is worth studying (Sanni *et al*., 2014; Ayeni *et al.*, 2012). The safety and environmental issues of corrosion inhibitors arising in industries has always been a global concern (Rekha *et al.*, 2010). This has necessitated the search for naturally occurring substances as corrosion inhibitors to be a subject of great practical significance. Hence, the availability, non toxic nature, cheap and environmental friendliness of neem seed and guava leaf satisfy the use of their extracts as inhibitors.

1.3 Scope of work

The scope of this research covers

1. Fourier transform infrared spectroscopy (FTIR) analysis of the extracts,
2. Double thermal ageing treatment of as-received high pressure die cast Al-Si-Mg (SSM-HPDC) alloy.
3. Hardness measurement with the use of Rockwell indenter hardness testing machine.
4. Corrosion analyses using the gravimetric and potentiodynamic polarization technique.
5. Micro-structure characterization of the alloy using OPM and SEM.

1.4 Contribution to knowledge

To the best of my knowledge, no previous work has been carried out on the corrosion inhibition of double thermally-aged high pressure die cast Al-Si-Mg (SSM-HPDC) alloy using neem seed and guava leaf extracts. This research has

1. Improve the hardness of the alloy by 40% employing the double thermal ageing treatment.
2. Established inhibitive values of guava leaf and neem seed extracts on corrosion resistance of Al-Si-Mg alloy in seawater environment.

CHAPTER TWO

2.0 LITERATURE REVIEW

2.1 General Properties of Aluminium and its Alloy

The relative low price of aluminium along with its many useful properties e .g appearance, non-sparking, non magnetic and ease of fabrication makes it useful in a wide range of industrial applications (Rawajfel *et al.,* 2009). Aluminum and its alloys are characterized by a relatively low density (2.7g/cm^3 as compared to 7.9g/cm^3 for steel and 8.86g/cm^3 for copper), high electrical and thermal conductivities , and resistance to corrosion in some common environment such as atmosphere, water and salt water (Fontana and Greene, 1987).

2.1.1 Classification system of aluminium alloy

Most commercial Aluminium alloys belong to one of two families i.e. wrought alloys and casting (foundry) alloys.

Wrought alloys are cast into billets and then wrought into their final shape by forging, extrusion, rolling, or drawing while Casting or foundry alloys are cast right into their final shape. Many Aluminum alloys respond to thermal treatments based on phase solubility. These treatments include solution heat treatment, quenching and precipitation or age hardening. For either casting or wrought alloys such alloys are described as heat treatable, while those alloys in which no significant strengthening can be achieved by heating and cooling are generally referred to as non heat treatable alloys (Adams, 2012).

2.1.2 Aluminium cast alloys designation

The Aluminium Association system uses a designation by four digits. The first one indicates the principal elements and the second ones indicate the other elements in the alloy. The last one

digit, positioned after a dot, indicates the alloy type (0 for casting, 1 and 2 ingot) (Fracasso, 2010). The principal types of alloys are summarized in the table below.

Table 2.1 American Aluminum casting Alloys Designation

Aluminium, 99.00%	1xx.x
Alluminium alloys grouped by major alloying elements:	
Copper	2xx.x
Silicon with added copper and/or magnesium	3xx.x
Silicon	4xx.x
Magnesium	5xx.x
Zinc	7xx.x
Tin	8xx.x
Other element	9xx.x
Unused series	6xx.x

Source: Fracasso, 2010

2.2 Semi-Solid Metal (SSM) Processing

This process is a unique manufacturing method to produce near-net shape product for various industrial applications (Atkinson, 2005).The aim is to obtain a semi-solid structure (which is free of dendrites) with the solid present in a near spherical form. This semi solid mixture flows homogeneously, behaving as thixotropic fluid with viscosity depending on the shear rate and fraction of solid (Moller *et al.*, 2010). There are two main different SSM processing methods namely rheocasting and thixocasting. With thixocasting, a specially prepared billet of solid material with globular structure is reheated into the semi-solid range, followed by a forming process such as high pressure die casting (HPDC). Rheocasting on the other hand involves preparation of the SSM slurry directly from the liquid, followed by HPDC. Rheocasting has become the preferred semi-solid process, due to the higher costs that are associated with thixocasting (Moller *et al.*, 2010; Flemings *et al.*, 2006).

2.3 Ternary and Multi Component Alloy

Al-Si-Mg is an alloy with ternary phase diagram. Composition in ternary system is usually represented as points on or in an equilateral triangle, ABC (Figure 2.1). The corners of the triangle correspond to the three pure components, and the edges represent the three binary systems. Each point within the triangle corresponds to a definite composition; the ratio of the three components for P is equal to the ratio of distance a, b, c of P from the three sides of triangle. The sum of these three distances is constant for a given triangle (Abdulwahab, 2011)

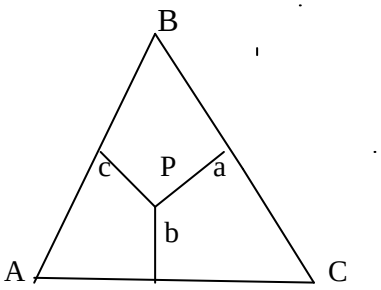

$$Pa + Pb + Pc = Constant$$

Figure 2.1: Representation of ternary composition (Abdulwahab, 2011).

The equilateral triangle can be divided up as in (Figure 2.2) and the composition corresponding to any point can be read directly. The side AB will represent binary alloys of element A and B, while the first line parallel to this side will represent alloys containing 10% C. The composition of the ternary alloy at point X is 40% A, 40% B and 20% C while at point Y is 20% A, 30% B, 50% C. (Umaru, 2013).

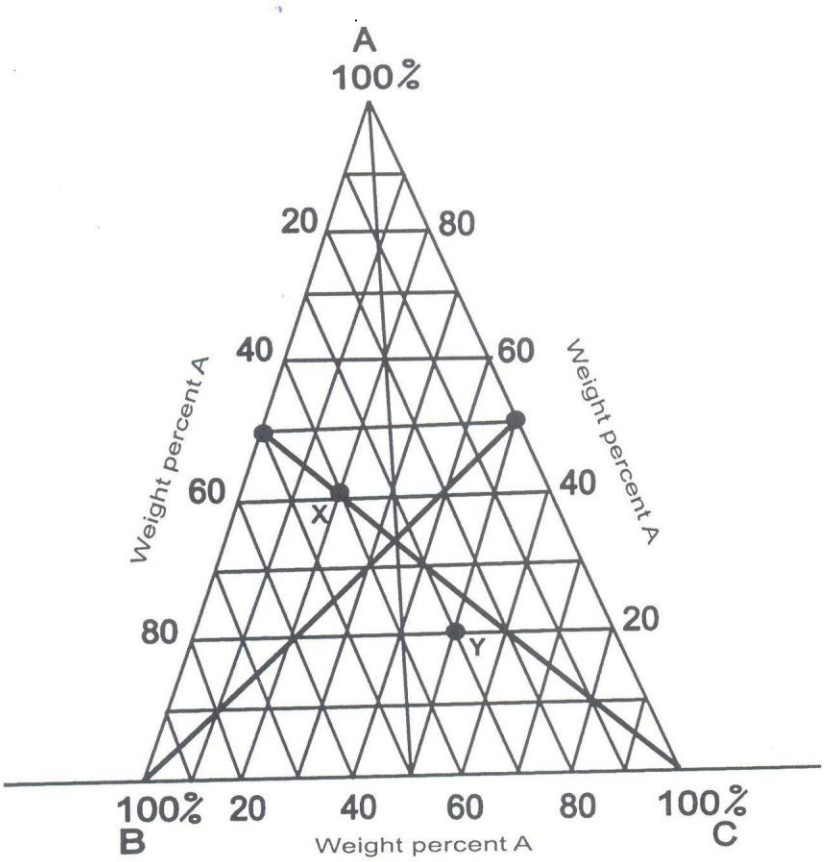

Figure 2.2: Ternary phase diagram for composition base for an ABC (Umaru, 2013)

2.4 Heat Treatment of Cast Al-Si-Mg alloys

Heat treatment indicates a sequence of controlled heating and cooling which leads to microstructure modifications and thus changes in the properties of a material (Fracasso, 2010).

Heat treatment is one of the major factors used to enhance the mechanical properties of heat-treatable Al-Si-Mg alloys, through an optimization of both solution and ageing heat treatments given to this alloy (Tash *et al*., 2007). Typical heat treatment process for cast Aluminum alloy A356 is the single thermal ageing treatment (T6-temper condition), which consist of a solution heat treatment, quenching and ageing at an elevated temperature (Ma, 2006).

2.4.1 Solution treatment

Solution heat treatment is carried out at a temperature range of 400-560^{o}C in order to dissolve hardening agents in the Al matrix, homogenize the casting and modifies the morphology of eutectic silicon to improve ductility (Tavitas *et al.,* 2014; Hossain and Kurny, 2014).

2.4.2 Quenching

The objectives of quenching are to suppress the precipitation, to retain solute atoms and quenched-in vacancies in solution. If the cooling rate is fast enough to avoid the formation of second phases, the final structure will be a unique solution made up of uniformly distributed solute atoms inside the matrix (Fracasso, 2010). Water quenching is mostly used for aluminum alloys, but it causes distortion, cracking and residual stresses (Ma, 2006). However, hot water quenching is recommended for Al-Si-Mg alloy since it minimizes quenching stresses and distortion (Tash *et al.,* 2007).

2.4.3 Ageing treatment

The age hardening can take place either at room temperature (natural, T4- temper) or at elevated temperature (artificial, T6- temper) (Ma, 2006). During natural ageing of Al-Si-Mg alloys hardening occurs due to the precipitation of solute clusters and Guinier-Preston(G.P) zones which during artificial ageing temperature (usually between 90^{o}C and 230^{o}C) these clusters and G.P zones transform as follows :

$$SSS \longrightarrow GP\ (I)_{Spherical} \longrightarrow GP\ (II)\beta''_{needles} \longrightarrow \beta'_{rods} \longrightarrow \beta\ (Mg_2Si)_{platelet}$$

SSS is the super saturated solid solution, β is the equilibrium Mg_2Si and β' and β'' are metastable precursors of β.

2.5 Hardness Measurement

Hardness is a measure of the resistance of a metal to a permanent plastic deformation by indentation. (Tash *et al.*, 2006). The hardness of Al-Si alloy is measured by compressing an indenter on its surface. The indenter is usually a sphere, pyramid of a cone, is constituted by a material harder than the material on test. The materials commonly used for indenters, for example, are tempered steel, tungsten carbide or diamond. There are three different methods for hardness measurement: Brinell, Vickers and Rockwell.

2.5.1 Rockwell hardness test

The test consist of penetrating into piece at two times and with two different loads (initial and total), a unified indenter (diamond cone or tempered steel sphere) and to measure the increase of depth between the initial imprint and final in suitable time. Four sizes of hard ball from $^{1}/_{16}\,in$ to $^{1}/_{12}\,in$ ball and the diamond penetrators are most commonly used. The penetrator chuck is mechanically connected to a dial indicator which responds to vertical motion of the penetrator. Since the penetrators are small, the specimen should be ground smooth and clean. The specimen is placed on the anvil of the machine and the penetrator seated by means of 10 kg minor load. The dial indicator is zeroed and then a major load of 60, 100 or 150 kg is applied, forcing the penetrator into the specimen. Upon removal of major load, the indented specimen recovers slightly, and the final depth of penetration is registered directly on the dial indicator as a hardness number (Umaru, 2012)

2.6 Mechanism of Electrochemical Corrosion

Electrochemical corrosion involves two half cell reactions; an oxidation reaction at the anode and a reduction reaction at the cathodes (Abdulwahab, 2011).

For corrosion of aluminum in water with a near neutral pH, these cell reactions can be represented as:-

Anode reaction

$Al \longrightarrow Al^{3+} + 3e$ ……..……..(2.1)

Cathode reaction

$O_2 + 2H_2O + 4e^- \longrightarrow 4(OH)^-$ ……..(2.2)

Over all reaction

$4Al + 3O_2 + 6H_2O \longrightarrow 4Al^{3+} + 12\,(OH)^-$……..……(2.3)

There are obviously different cathodic reactions for different alloys exposed to various environments. These half cell reactions are thought to occur (at least initially) at microscopic anodes and cathodes covering a cathodic surface. Microscopic anodes and cathodes can develop as corrosion damage progress with time (Perez, 2004; Abdulwahab *et al.*, 2011).

In seawater environment, the dissolved aluminium ions then combine with the chloride ions to form aluminium chloride.

$Al^{3+} + Cl^- \longrightarrow Al^{3+}\,Cl^-$ …….(2.4)

Subsequently, $Al^{3+}\,Cl^-$ is hydrolyzed by water molecules as follows

$2Al^{3+}\,Cl^- + O_2 + 4H_2O \longrightarrow 2Al(OH)_3 + 2\,H^+\,Cl^-$ …….. (2.5)

The free acid $H^+\,Cl^-$, migrates to the bottom of the pits which increases the acidity at these locations thereby increasing the size of the pits and hence corrosion rate.

2.7 Corrosion Prevention and Control Method

The main methods of preventing and controlling corrosion are cathodic/anodic protection, use of inhibitors, coating (both organic and inorganic), proper design of structures, alteration of environment, material selection, use of galvanically compatible metal/alloy system.

2.8 Corrosion Inhibitors

Corrosion inhibitors are substances which when added in small concentrations to corrosive media decrease or prevent the reaction of the metal with the media (Stephen *et al.,* 2014).

Corrosion protections by inhibitors have been employed in many systems namely; cooling system, refinery units, chemicals, oil and gas production units, boiler e.t.c. They are also used in numerous systems, from water supply system to the protection of microelectronics and contemporary military equipment (Kuznetsov, 2014).

Inhibitors reduce the corrosion rate in a number of ways: by modifying the corrosion potential, retarding the cathodic or anodic corrosion reactions via polarization or passivation (Stephen *et al.,* 2014). Inhibitors can be classified into three groups: anodic, cathodic and adsorption.

2.8.1 Anodic inhibitors

These inhibitors increase polarization of anode by reacting with the ions of the corroding metals to produce either thin films or layers of limited solubility which coat the anode e.g. molybdates, phosphates, nitrates, nitrites, chromates e.t.c

2.8.2 Cathodic inhibitors

They affect the usual cathodic reactions. In the first

$$2H_2O + O_2 + 4e^- \longrightarrow 4OH^- \quad \text{.....(2.6)}$$

The inhibitors reacts with the hydroxyl ion to precipitate compound on the cathode site, thus blanketing the cathode from the electrolyte, preventing access of oxygen to the site e.g. salts of zinc and magnesium which form insoluble hydroxides.

In the second cathodic reaction

$$2H^+ + 2e \rightleftharpoons 2H \rightleftharpoons H_2 \quad \text{.....(2.7)}$$

The evolution of hydrogen is controlled by increasing the overvoltage (polarization) of the system.

2.8.3 Adsorption inhibitors

These are long organic molecules with side chains which are adsorbed and desorbed from the metal surface. The bulky molecules can limit the diffusion of oxygen to the surface or trap the metal ions on the surface, stabilize the double layer and reduce the rate of dissolution. Example- organic amines.

2.9 Organic Inhibitors

Organic inhibitors have been found to function by adsorption of their ions or molecules onto the metal surface. Accurate elucidation of the mechanism of adsorption of inhibitor on metal surface is essential for the design and development of new corrosion inhibitors as well as for a detailed understanding of mechanism of the inhibition processes (Stephen *et al.,* 2014).

The action of inhibitors is always associated with changes in the state of the surface being protected due to adsorption or formation of poorly soluble compounds with metal cations. Such compounds decrease the area of active metal surface and/or increase the corrosion energy (Ayeni, 2012). The adsorption of inhibitors on the metal/alloy surface retards the cathodic or anodic electrochemical processes that accompany corrosion of the metal/alloy (Ebenso *et al.,* 2003). The performance of organic inhibitor is related to the chemical structure and physiochemical properties of the compound like functional groups, electron density at the donor atom, P-orbital character and the electronic structure of the molecule (Amitha and Bharathi, 2012). Some factors that contribute to the action of inhibitors include: carbon chain length, size of the organic molecule, aromatic/conjugate bonding, strength of bonding to the substrate, cross linking ability and solubility in the environment (Amitha and Bharathi, 2012).

Hetero atoms such as nitrogen, oxygen and sulphur are capable of forming coordinate covalent bond with metal owing to their free electron pairs and thus acting as inhibitor. Compounds with π–bonds also generally exhibit good inhibitive properties due to interaction of π-orbital with metal surface (Toliwal *et al.,* 2010).

2.10 The Use of Natural Plant Extracts as Corrosion Inhibitors

Plant extracts have become important because they are environmentally acceptable, inexpensive, readily available and renewable sources of materials, and ecologically accepted (Olusegun *et al.*, 2013).

The use of plant extract and oils has gained acceptance as corrosion inhibitors that are considered safe, eco-friendly, available and less expensive for most metal and alloys (Popoola *et al*., 2012). In the search for more environmentally friendly and readily available inhibitors, researchers have reported the use of local plants such as *vernonia amygdalina* (Ayeni, 2012), *azadirachta indica* leaf (Loto *et al.*, 2011), black pepper extracts (Quraish *et al.*, 2009), *sorghum bicolor* leaf extract (Stephen *et al*., 2014), pulverized *jatropha curcas* leaves (Omotoyinbo *et al*., 2013), *piper guinensis* (Ebense *et al*., 2008) e.t.c.

Loto *et al* (2011) investigated the corrosion inhibition performance of neem leaf (*Azadirachta indica*) extract on the corrosion of mild steel test specimen immersed in 0.5M HCl and H_2SO_4 acid, respectively, at ambient temperature of 30^oC and elevated temperature of 80^oC using the weight loss and potential measurement technique. In the result obtained, the leaf extract, in sulphuric acid medium gave the best corrosion inhibition performance at 0.5g/l extract concentration at 30^oC. A more appreciable inhibition performance was achieved in the dilute hydrochloric acid at 0.25g/l extract concentration also at 30^oC.

Nnanna *et al* (2012) studied the inhibition effect of *Newbouldia leavis* extract on the corrosion of aluminium in 0.2-1.0M HCl and 0.1-1.0M H_2SO_4 solutions using the gravimetric technique. The result show that the extract inhibited the corrosion of aluminium in the test solutions and inhibition efficiency depends on the concentration of the plant extract as well as on the time of exposure of aluminium samples in the solutions containing the extract. The adsorption of *Newbouldia leavis* on aluminium surface obeys Langmuir adsorption isotherm.

Howida *et al.* (2014) investigated the effect of aqueous extracts of Damsissa, Lupine and Halfbar on the corrosion of 7075-T6 aluminium alloy in aqueous solution of 0.5M sodium chloride. The polarization curves showed that the three extracts act as cathodic inhibitors.

The effects of corrosion inhibition on AA 2024-T3 using cerium cation and cinnamate anion by Hongwei *et al.* (2014). It was found that cerium ion and cinnamate group has synergistic inhibiting effects. The results show that CeCin is an effective inhibitor pigment for improving the corrosion resistance of epoxy coatings on AA2024-T3, as reflected by much higher coating resistance than that of the blank epoxy coating.

2.10.1 Neem tree (*Azadirachta indica*) / Neem seed extracts as corrosion inhibitors

Neem tree (*Azadirachta indica*) is a native to tropical and semi-tropical regions with origin in Europe and later domesticated in Asian. It is extensively found in India and Indonesia (Liauw *et al*., 2008). It is also ubiquitous in Northern Nigeria, and fairly found in Western Nigeria, where it is popularly referred to as Dogon yaro (Awolu *et al.,* 2013). All parts of neem plant such as leaves, bark, flower, fruit, seed and root have advantages in medical treatment and industrial products. Neem seed is a part of neem tree which has high concentration of oil (Maria *et al.,* 2008).

Peter *et al*., (2010) studied the inhibitive action of leaves (LV), root (RT) and seeds (SD) extracts of *Azadirachta indica* on mild steel using weight loss and gasometric techniques. The results obtained indicate that the extracts functioned as good inhibitors in H_2SO_4 solutions. Inhibition efficiency was found to increase with extracts concentration and temperature, and followed the trend: SD □ RT □ LV. The experimental data fit into the Freundlich adsorption isotherm.

Ajanaku *et al*., (2015) studied the adsorption properties of *Azadirachta indica* on corrosion of Aluminium in 1.85M Hydrochloric acid by gasometric techniques. The inhibition efficiency of the extracts and adsorption isotherm of the process were calculated using Frumkin, Freundlich, Langmuir and Temkin adsorption theories and the surface morphology studied using Scanning Electron Microscopy (SEM). It was observed that the plant extract retarded the acid induced corrosion of aluminium and the volume of hydrogen gas evolved reduced with increasing extract concentration. The adsorption studies revealed that Langmuir isotherm is the best model for the adsorption of *Azadirachta indica* (R^2= 0.999) on aluminium surface.

2.10.2 Guava tree (*Psidium guajava*) / Guava leaf extracts as corrosion inhibitors

Guava is a small tropical tree that grows up to 35 feet tall. It is widely grown in tropics. The leaves and bark of *psidium guajava* tree have a long history of medical uses that are still employed today (Nwinyi *et al.,* 2008).The leaves and bark of guava plant have been used to treat diarrhea, other gastrointestinal disorder, toothaches, cold and swelling (Fagbohum *et al*., 2013).

Noyel et al., (2015) investigated the adsorption and corrosion inhibition property of the alcoholic *Psidium guajava* (guava) leaf extract on mild steel in 1M Phosphoric acid medium using weight loss, potentiodynamic polarization and electrochemical impedance spectroscopy techniques. The studies showed that the inhibition efficiency increases with inhibitor concentration upto 800 ppm and decreases signicantly at 1200 ppm. The adsorption obeys the both the Langmuir and the

Temkin adsorption isotherm equations. The adsorption was found to follow a comprehensive type adsorption dominated by chemisorptions. Potentiodynamic polarization studies showed that the inhibitor acted as a mixed-type inhibitor.

2.11 Adsorption Consideration

Adsorption of organic compounds depends upon the charged and nature of the metal surface, electronic characteristics of the metal surface, ionic species, temperature of the corrosion reaction and the electrochemical potential at the metal-solution interface (Obot *et al.,* 2008 ; Umoren *et al.,* 2010). The first one is weak undirected interaction due to electrostatic attraction between inhibiting organic ions and the electrically charged surface of the metal. This interaction is termed physical adsorption. The second type of interaction involves charge sharing or charge transfer from the adsorbate to the atoms of the metal surface in order to form coordinate coordinate type bond and is termed chemical adsorption (Dahmani *et al.,* 2010).

The adsorption isotherms provide important clues regarding the nature of metal-inhibitor interaction. Inhibitor molecules adsorb on the metal surface if the interaction between molecule and metal surface is higher than that of water molecule and the surface (Ating *et al.,* 2010). In order to obtain the adsorption isotherm, the degree of surface coverage θ, for various concentrations must be known. The most frequently used isotherms are Langmuir, Frumkin, Temkin, Hill De-Boer, Parsons, Freundlich, Dhar-Flory-Huggin, El-Awady and Bockris-Swinkels. All these isotherms are of the general form (Dahmani *et al.,* 2010);

$f\ (\theta, x)\ \exp\ (-2a\theta) = KC$ …….2.8

Where $f\ (\theta, x)$ is the configurational factor which depends upon the physical model and the assumption underlying the derivation of the isotherm, θ is the surface coverage degree, C is the inhibition concentration in the bulk solution, a is the lateral interaction term describing the

molecular interaction in the adsorbed layer and the heterogeneity of the surface, x is the size ratio and K is the adsorption-desorption equilibrium constant.

2.11.1 Langmuir isotherm model

The Langmuir isotherm is sometimes is sometimes evaluated with plot of degree of surface coverage (θ) against concentration of inhibitor (C). If a linear relationship is obtained the adfsorption is said to obey the Langmuir isotherm, meaning a monolayer physical adsorption occurred.

2.11.2 Temkin and Frumkin adsorption model

Temkin (1984) and Frumkin (1926) while studying the adsorption isotherm of various organic inhibitors showed if the adsorption obeyed the following equation:

$\theta = \frac{1}{F}\, In\, (I_oC)$ ……..2.9

Where C is the additive concentration, I_o is the value of Langmuir constant, F is a constant depending on intermolecular interactions in the adsorption layer and on heterogeneity of the surface.

Then the Temkin or Frumkin adsorption model may be obeyed. These isotherms are usually evaluated with a plot of degree of surface coverage (θ) against logarithm of concentration of inhibitor (log C). If it has a linear relationship it is in line with the Temkin adsorption, while if the plot gives an S-shape it is in line with Frumkin adsorption isotherm. These models suggest a double layer adsorptiuon.

2.12 Application of Aluminium and its Alloys

Aluminum and its alloys find a wide variety of used because of its remarkable combination of characteristics such as low density, high corrosion resistance, high electrical and thermal conductivity, ease of fabrication, low cost, good castability, good machinability, desirable

appearance and high strength to weight ratio (Rawaj *et* al., 2009; Hulya *et al*., 2007; Sheng *et al*., 2012).

The wide variety of uses of aluminum and its alloy includes (Djurdjevic *et al.*, 2001; Umaru, 2013; Tavitas *et al.*, 2008; Abdulwahab, 2011).

1. Pure aluminum is used as electrical conductor cables e.g. in electricity transmission lines due to its high electrical conductivity.
2. Used extensively in the manufactured of packaging products such as cartons for fruit juice and packaging in pharmaceuticals.
3. It is used for the manufacture of domestic cooking utensils such as kettles, cooking pots, frying pans, spoons and plates.
4. In alloy form, it is used in automotive and aerospace industries for the manufacture of engine blocks, pistons, brake calipers, carburetor parts, helicopter desks, wing skins etc.
5. In construction it is used in sheet product for roofing and wall cladding, in extrusions for windows and doors and in castings for builders' hardware.
6. Used in oil and gas industries as, refining equipment such as air-cooled heat exchangers.

CHAPTER THREE

3.0 MATERIALS AND METHOD

3.1 Materials and Equipment

3.1.1 Materials

The materials used in this research include: as- received high pressure die cast (SSM-HPDC) Al-Si-Mg alloy, neem seed and guava leaf extracts, sodium chloride, distilled water, ethanol, etchants e.t.c

3.1.2 Equipment

The equipment used in this research work include: FTIR machine (8400S Shimadzu Japan), Heat treatment electric resistance furnace (SX-5-12), water heater, Indenter hardness testing machine (8187.5KLV), electronic/digital weighing balance (BL-410S), optical microscope (NJF-120A), scanning electron microscope (Phenom Pro X), series of grit paper, desiccators for sample storage, measuring cylinder, electrochemical potentiostat corrosion kit.

3.2 Methods

3.2.1 Extraction of neem seed and guava leaf

Samples of neem seed and guava leaf were dried, ground and soaked in a solution of ethanol for 48 hours. The samples were cooled, filtered and the filtrates were further subjected to evaporation using rotary evaporator (ROTOVAP) in order to leave the samples free of ethanol. The oily residues which resulted from the evaporation process were used as inhibitor.

3.2.2 Fourier transform infrared spectroscopy (FTIR) analysis of the extracts

Extracts of neem seed and guava leaf were placed and exposed under range of infrared ray beams. The transmittance and reflectance of the infrared (IR) rays at different frequencies was translated into IR absorption plot consisting of reverse peaks. The spectra pattern was analyzed

and matched according to IR absorption table to identify the functional group present in the extracts.

3.2.3 Sample preparation

The Al-Si-Mg alloy with chemical composition as shown in Table 3.1 was sectioned into small specimen (coupons) of dimension 12×12×2 mm each. The coupons were mechanically polished with series of grit papers down to 800 grit size. The abraded coupons were then washed, degreased in ethanol, dried and weighed using an analytical balance and stored in a desiccator to prevent their further interactions with the environment.

Table 3.1 Chemical Composition of the as received Al-Si-Mg alloy

Element	Al	Si	Mg	Fe	Cu	Mn	Zn	Ti	Sr
%	92.28	7.14	0.36	0.10	0.01	0.01	0.01	0.07	0.02

Source: Centre for Scientific and Industrial Research, nano structure centre, Pretoria-South Africa (Govender and Moller, 2008).

3.2.4. Heat treatment

A total of one hundred and thirty five (135) coupons were solution treated at a temperature of 540^{o}C for 1hr in a heat treatment electric resistance furnace and then rapidly quenched in warm water (65^{o}C). The quenched samples were pre-aged at 105^{o}C for 2hrs, and then finally aged at 180^{o}C for 2hr before cooling in air as shown in Figure 3.1.

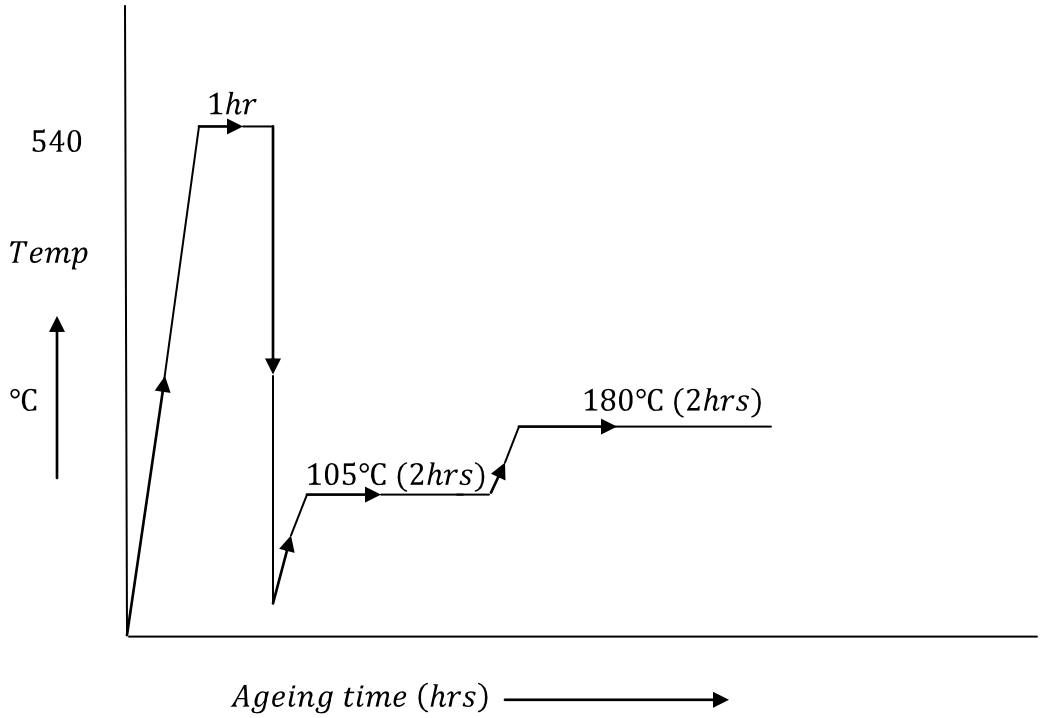

Fig 3.1: Schematic diagram of the double thermal ageing treatment (Abdulwahab, 2011).

3.2.5 Hardness measurement

The hardness of the Al-Si-Mg (SSM-HPDC) alloy in the as-received and age-hardened conditions were measured using Rockwell hardness testing machine with a minor load of 10kg and major load of 60kg (F scale and 2.12mm steel ball indenter). Average of three consistent readings was accepted as the representative hardness value of an alloy in accordance with the report of Hossain *et al*., (2014).

3.3 Corrosion test

3.3.1 Gravimetric – based mass loss method

The gravimetric corrosion test was carried out on the previously weighed coupons with and without inhibitor at 30, 50 and 70^{o}C. Before the commencement of the experiment, the simulated sea water was prepared by dissolving 3.5g NaCl in 100ml of distilled water. Five coupons were suspended into the beaker containing 150ml of the solution with the aid of threads and then placed on a water bath which has provision for regulating the temperatures. The

experiment was first carried out at 30, 50 and 70^{o}C without inhibitor to serve as control and then in solution containing each of neem seed and guava leaf extracts with concentration of 0.1, 0.2, 0.3, 0.5% v/v. The coupons were then retrieved from the corrodent at 1hour interval progressively for 5 hrs, scrubbed with brush in distilled water, washed, dried, reweighed and recorded. The same procedure was repeated for the double thermally aged coupons with their final weight measured and recorded. The weight loss, corrosion rate, inhibitor efficiency, free energy of adsorption, activation energy and heat of adsorption were determined.

3.3.2 Corrosion Rate Determination

The weight loss was determined by finding the difference between the initial weight of the coupons and the final weight after one hour interval using the following relationship (Ayeni *et al* ., 2012)

$W = W_0 - W_f$ ……(3.1)

Where W = Weight loss, W_o= initial weight

W_f = final weight

The corrosion rate was determined in mils per year (mpy) using relationship (Ayeni *et al* ., 2012).

$Corrosion\ rate(mpy) = \frac{534\Delta W}{DAT}$ ……..(3.2)

Where ΔW = weight loss (mg) D = Density of material (g/cm^3)

T = Time of exposure (hours) A = Total surface area (in^2)

3.3.3 Inhibition Efficiency (IE)

The values of inhibition efficiencies were determined for each of the two inhibitors.

$IE = \theta \times 100$ ……..(3.3)

$IE = \frac{CR_O - CR}{CR_O} \times 100$ ……..(3.4)

Where CR_O and CR are the corrosion rates in the absence of and presence of inhibitor, respectively and θ is the degree of surface coverage.

3.3.4 Reaction Kinetics

The activation energy E_a of the corrosion reaction was calculated using the Arrhenius equation given by (Nnanna *et al.*, 2012)

$$\log\frac{CR_1}{CR_2} = \frac{E_a}{2.303R}\left(\frac{1}{T_1} - \frac{1}{T_2}\right) \quad \text{……} \quad (3.5)$$

In which CR_1 and CR_2 are the corrosion rates at any given two temperatures T_1 and T_2, and R is the universal gas constant.

The free energy of adsorption was determined using the equation (Olasehinde *et al.*, 2013).

$$\Delta G_{ads} = -RT\ln(55.5K) \quad \text{……(3.6)}$$

$$K = \frac{\theta}{C(1-\theta)}$$

Where K = Equilibrium constant

θ =is the degree of surface coverage

C =is the concentration of inhibitor (% v/v)

Also the heat of adsorption, Q_{ads} of the inhibitors was calculated using the equation (Ebenso *et al.*, 2008; Nnabuk *et al*., 2011).

$$Q_{ads} = 2.303R\left[\left(log\frac{\theta_2}{1-\theta_2}\right) - \left(log\frac{\theta_1}{1-\theta_1}\right)\right] \times {}^{T_2T_1}/_{T_2 - T_1}\text{(kJ/mol)……(3.7)}$$

Where θ_1 and θ_2 are degree of surface coverage at any two temperatures T_1 and T_2.

3.3.5 Potentiodynamic polarization measurement

The corrosion rates of twenty coupons consisting of ten (10) as-received and ten (10) age-hardened of Al-Si-Mg alloy were determined using the potentiodynamic polarization method in

neem seed extract/simulated-sea water and guava leaf extract/simulated sea-water media. A potentiostat coupled to a computer system, a glass corrosion kit with graphite rods as the counter electrode and a saturated Ag/AgCl 3M Kcl electrode as the reference electrode (SCE) was used. The test coupons were used as working electrode (WE). The samples were positioned at the glass corrosion cell kit leaving 1.14cm^2 surface in contact with the solution. Polarization test was carried out in a 3.5wt% NaCl solution (3.5g in 100ml of distilled water) with variation in concentration of extracts (0.0, 0.1, 0.2, 0.3 and 0.5%v/v) at room temperature in a static solution for a period of 30 minutes each using a potentiostat. The polarization curves were determined by stepping the potential at a scan rate of 0.003v/sec. The polarization curves were plotted using Auto lab data acquisition system, and both the corrosion rate and potential were estimated by the Tafel extrapolation method using both the anodic and cathodic branches of the polarization curves. The data obtained was used to calculate the inhibition efficiencies (IE) for the polarization resistance (R_P), corrosion current density (J_{corr}) and corrosion rate (CR). IE were obtained using the following equations (Wan *et al.*, 2012).

$$IE_{Jcorr} = \left(\frac{J^o_{corr} - J_{corr}}{J^o_{corr}}\right) \times 100 \quad \text{.....(3.8)}$$

$$IE_{Rp} = \left(\frac{R_P - R^o_P}{R_P}\right) \times 100 \quad \text{.....(3.9)}$$

$$IE_{CR} = \left(\frac{CR^o - CR}{CR^o}\right) \times 100 \quad \text{.....(3.10)}$$

Where J_{corr}, R_P and CR are the corrosion current density, polarization resistance and corrosion rate with inhibitor respectively, while J°_{corr}, R°_P and CR° are the corrosion current density, polarization resistance and corrosion rate without inhibitor respectively. The polarization corrosion study was done in centre for scientific and industrial research, nano structure centre, Pretoria-South Africa.

3.4 Micro-structure and surface morphology examination

The samples for the microscopic examination were ground with emery papers of progressively fine grade 80, 220, 600, 800 grits sizes using water as coolant. The ground samples were then polished using one-micro size alumina powder suspended in distilled water, followed by etching in Keller's reagent. The optical microscope (OPM) with an inbuilt camera was used for the microstructure observations. While the Scanning electron microscope (SEM) was used to examine the surface morphology of the as- corroded inhibited and uninhibited samples.

CHAPTER FOUR

4.0 RESULT

Figures 4.1 and 4.2 show the Infrared absorption (IR) spectra of guava leaf and neem seed extracts with their corresponding functional group deduced and recorded in Tables 4.1 and 4.2. The results obtained from hardness measurement are shown in Table 4.3. Figures 4.3-4.30 showed the variation of corrosion rates (CR) and inhibitor efficiencies (%IE) with time at different concentration of extracts on the alloy (as-received and age-hardened) with their Tables in appendix (Tables 1-28). The various thermodynamic parameters (E_a, ΔG_{ads} and ΔH_{ads}) evaluated from mass loss measurements are shown in appendix (Tables 29-38). The adsorption isotherms of the extracts on the alloy (as-received and age-hardened) at different operating temperatures are shown in Figures 4.31-4.34.

The potentiodynamic polarization curves for both as-received and age-hardened Al-Si-Mg (SSM-HPDC) alloy in blank solution of 3.5% NaCl and in presence of different concentration of extracts are shown in Figures 4.35-4.38. The various corrosion parameters are given in appendix (Tables 39-42).

The comparative chart of inhibitor efficiency (IE) for the gravimetric and potentiodynamic polarization technique of the alloy in 3.5% NaCl/ extracts solution are shown in Figure 4.39-4.42 with Tables given in appendix (Tables 43-46). The adsorption isotherms of the extracts on the alloy (as-received and age-hardened) obtained by gravimetric-based mass loss and potentiodynamic polarization techniques are given in Figures 4.43-4.45. The OPM microstructure of the alloy can be found in Plates 1 and 2, while the SEM microstructure of inhibited and uninhibited coupons after corrosion attack are shown in plate 3 and 4.

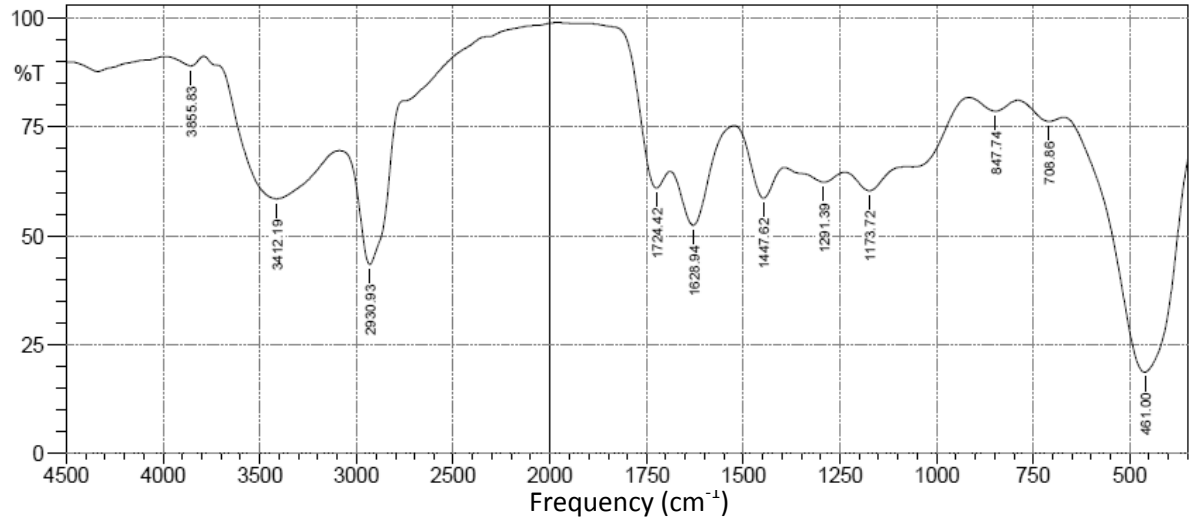

Figure 4.1: FTIR spectrum of guava (*Psidium guajava*) leaf extract.

Table 4.1: Frequencies and peaks of infrared absorption bands of functional groups in guava (*Psidium guajava*) leaf extract

N/S	Frequency (cm^{-1})	Intensity	Assignment
1	3855.83	w	OH stretch
2	3412.19	s, broad	OH stretch
3	2930.93	s, sharp	OH stretch
4	1724.42	s	C=O stretch
5	1628.94	vw-m	C=C stretch
6	1447.67	m	$-CH(CH_3)_2$
7	1291.39	m	O=C-O-C stretch
8	1173.72	s-vs	O=C-O-C stretch
9	847.74	s	C-H bend
10	708.86	s	C-H bend
11	461	s	C-I stretch

Intensity abbreviations: vw = very weak, w = weak, m = medium, s = strong, vs = very strong

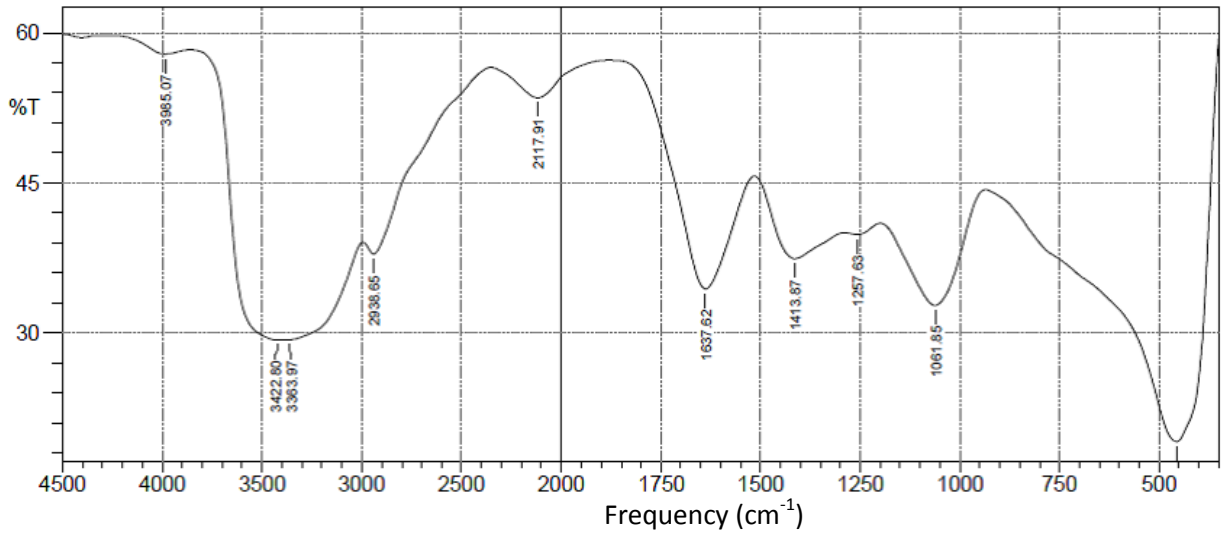

Figure 4.2: FTIR spectrum of neem (*Azadirachta indica*) seed extract.

Table 4.2: Frequencies and peaks of infrared absorption bands of functional groups in neem (*Azadirachta indica*) seed extract

N/S	Frequency (cm^{-1})	Intensity	Assignment
1	3985.01	w-m	OH stretch
2	3422.8	s, broad	OH stretch
3	3363.97	s, broad	OH stretch
4	2938.65	s,sharp	OH stretch
5	2117.91	m	C≡C stretch
6	1637.62	vw-m	C=C stretch
7	1413.87	m	$-CH(CH_3)_2$
8	1257.63	s	O=C-O-C stretch
9	1061.85	vs	C-F stretch
10	456.18	S	C-I stretch

Intensity abbreviations: vw = very weak, w = weak, m = medium, s = strong, vs = very strong

Table 4.3: Variation of Hardness of Al-Si-Mg SSM-HPDC) alloy in the as-received and age-hardened conditions.

Samples	1st HRF	2nd HRF	3rd HRF	Mean HRF
As-received	61.0	58.5	57.8	59.1
Age-hardened	79.3	84.9	84.4	82.8

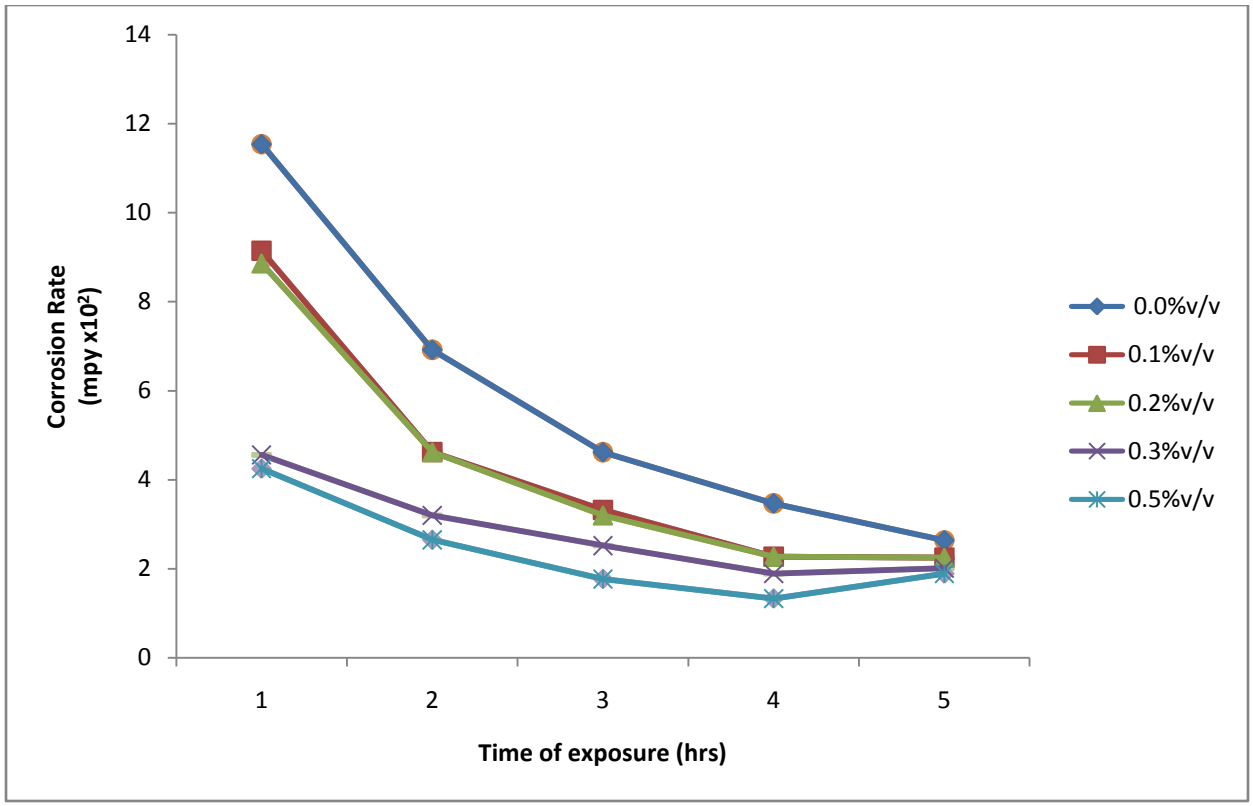

Figure 4.3: Variation of corrosion rate of as-received Al-Si-Mg alloy with time of exposure in the presence of guava (*Psidium guajava*) leaf extract at 30^{o}C.

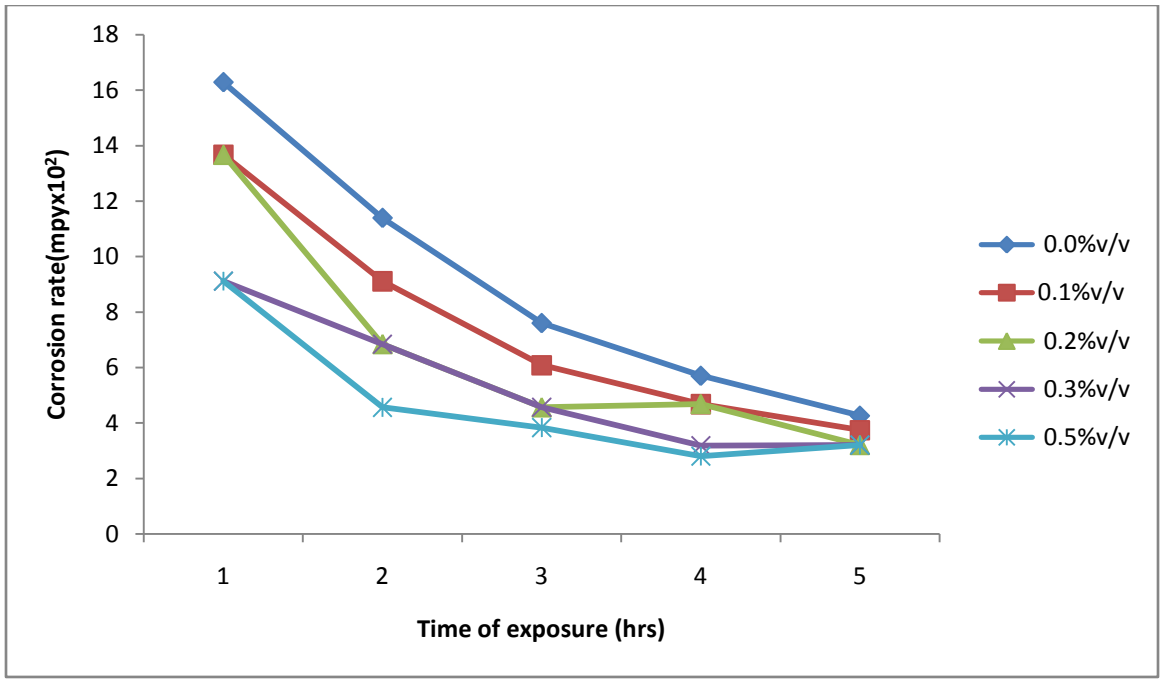

Figure 4.4: Variation of corrosion rate of as-received Al-Si-Mg alloy with time of exposure in the presence of guava (*Psidium guajava*) leaf extract at 50^{o}C.

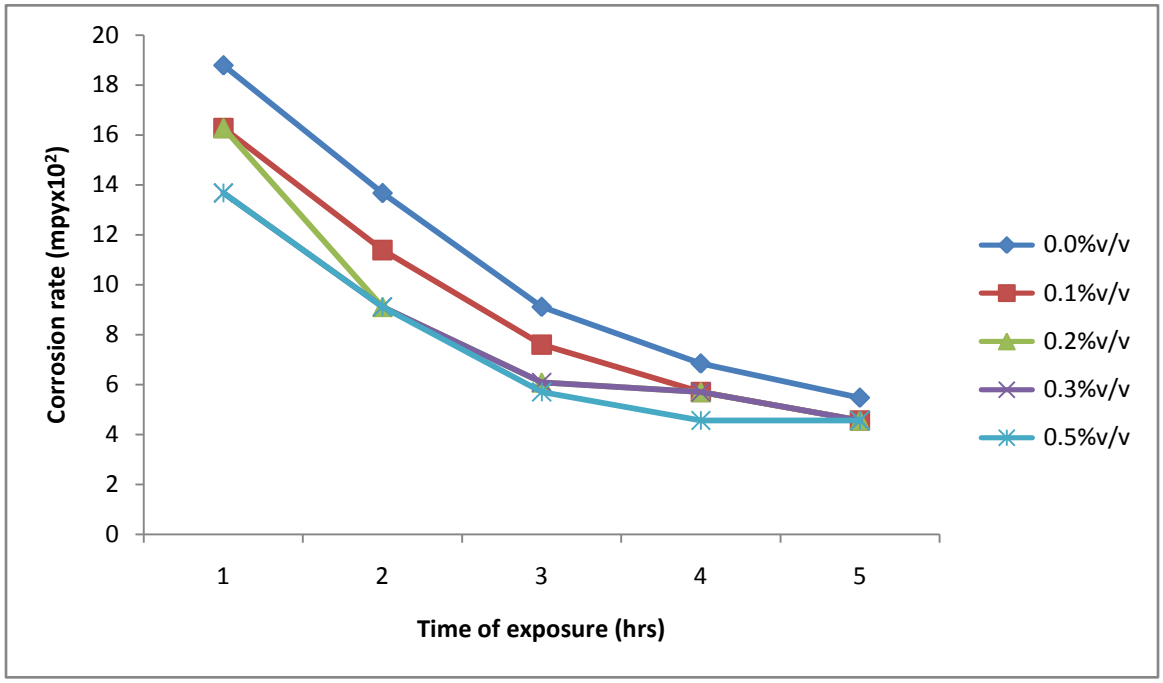

Figure 4.5: Variation of corrosion rate of as-received Al-Si-Mg alloy with time of exposure in the presence of guava (*Psidium guajava*) leaf extract at 70^{o}C.

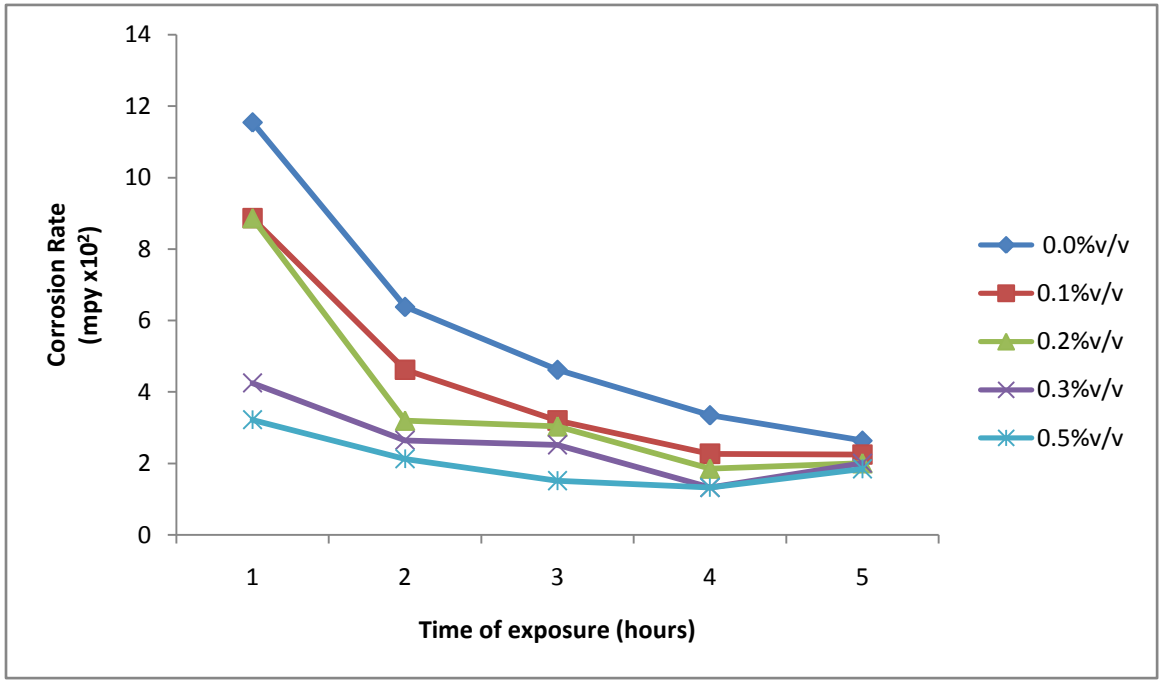

Figure 4.6: Variation of corrosion rate of double thermally aged Al-Si-Mg alloy with time of exposure in the presence of guava (*Psidium guajava*) leaf extract at 30^{o}C.

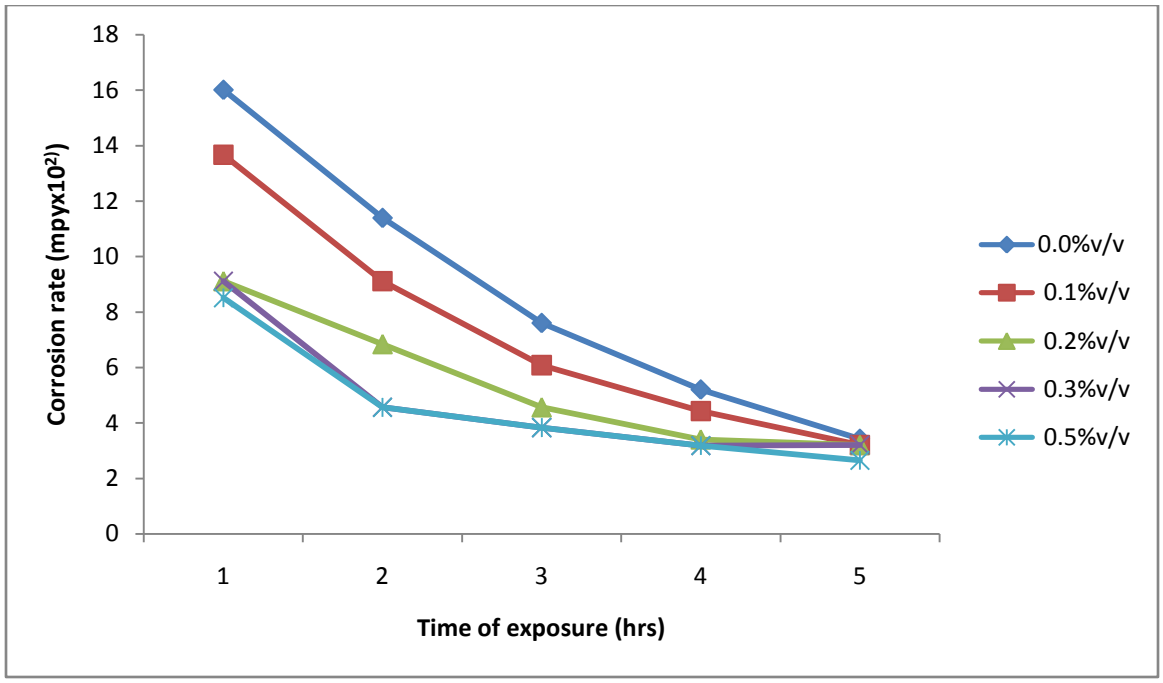

Figure 4.7: Variation of corrosion rate of double thermally aged Al-Si-Mg alloy with time of exposure in the presence of guava (*Psidium guajava*) leaf extract at 50^{o}C.

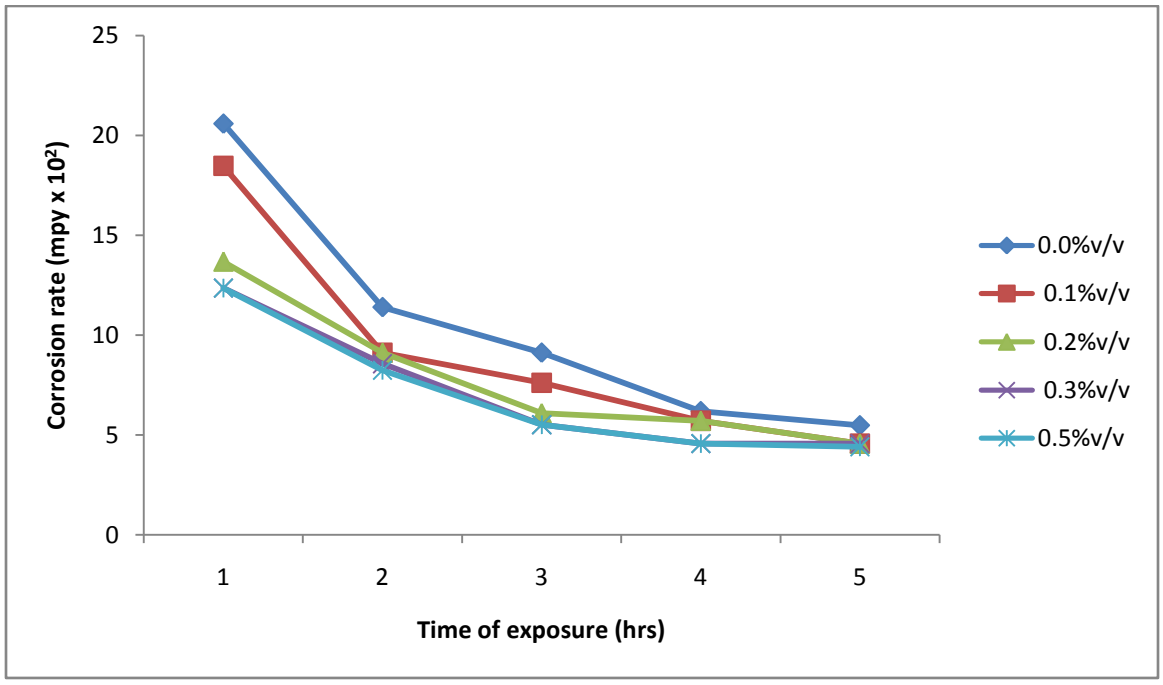

Figure 4.8: Variation of corrosion rate of double thermally aged Al-Si-Mg alloy with time of exposure in the presence of guava (*Psidium guajava*) leaf extract at 70^{o}C.

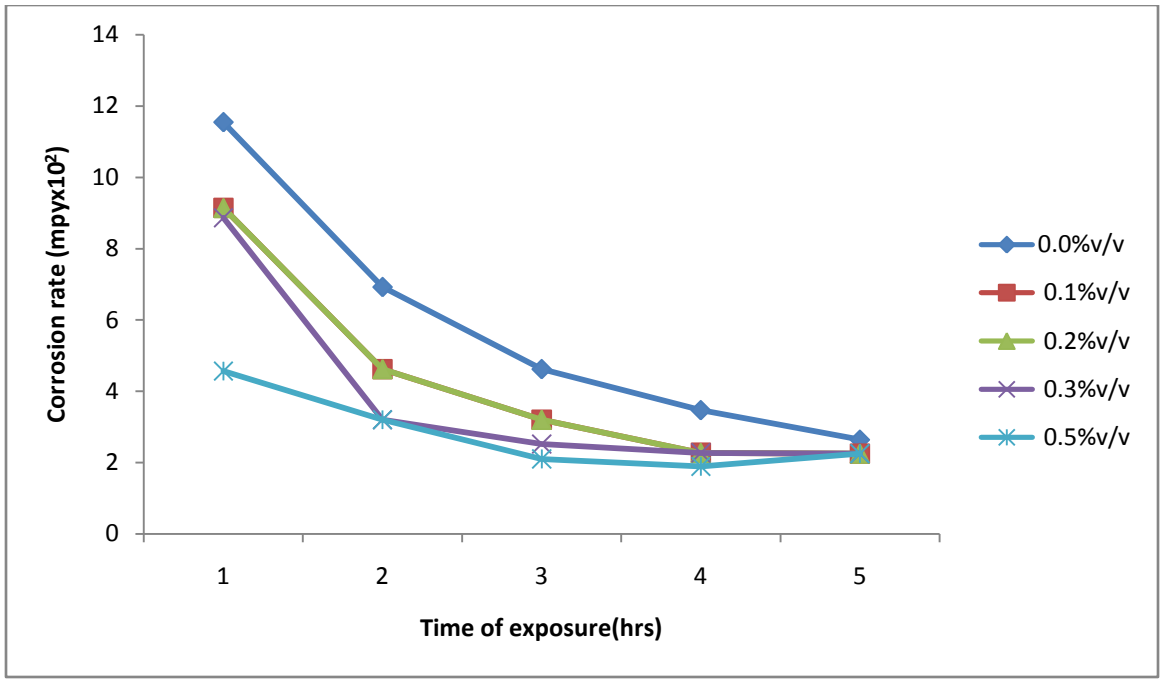

Figure 4.9: Variation of corrosion rate of as-received Al-Si-Mg alloy with time of exposure in the presence of neem (*Azadirachta indica*) seed extract at 30^{o}C.

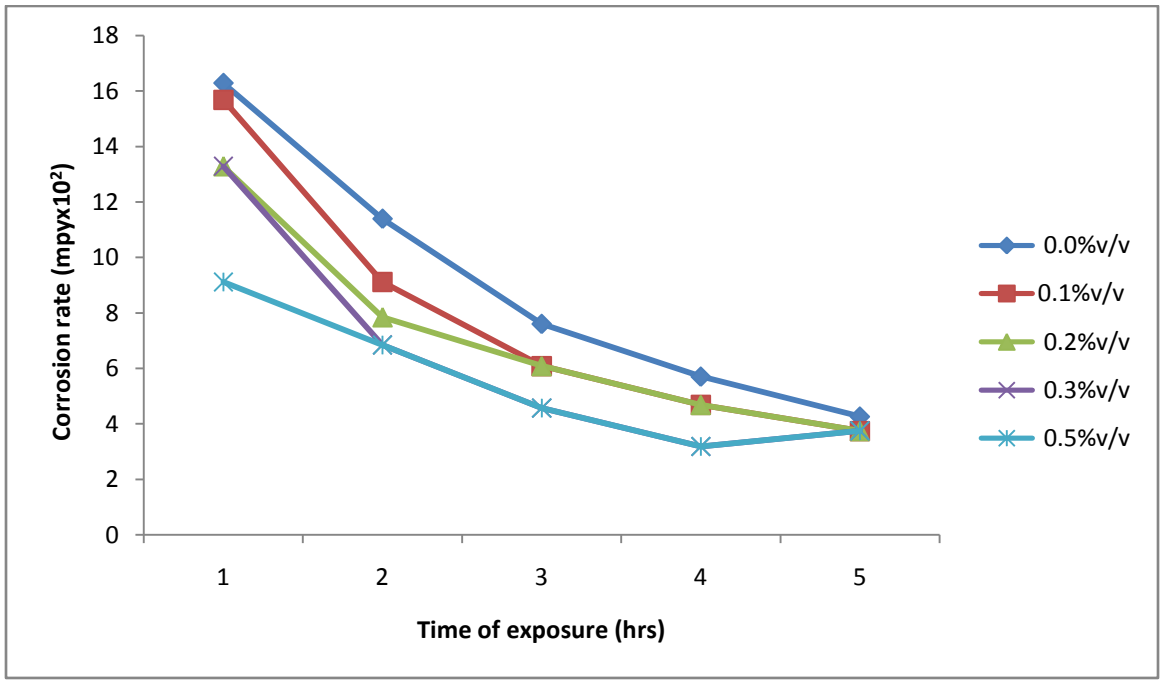

Figure 4.10: Variation of corrosion rate of as-received Al-Si-Mg alloy with time of exposure in the presence of neem (*Azadirachta indica*) seed extract at 50^{o}C.

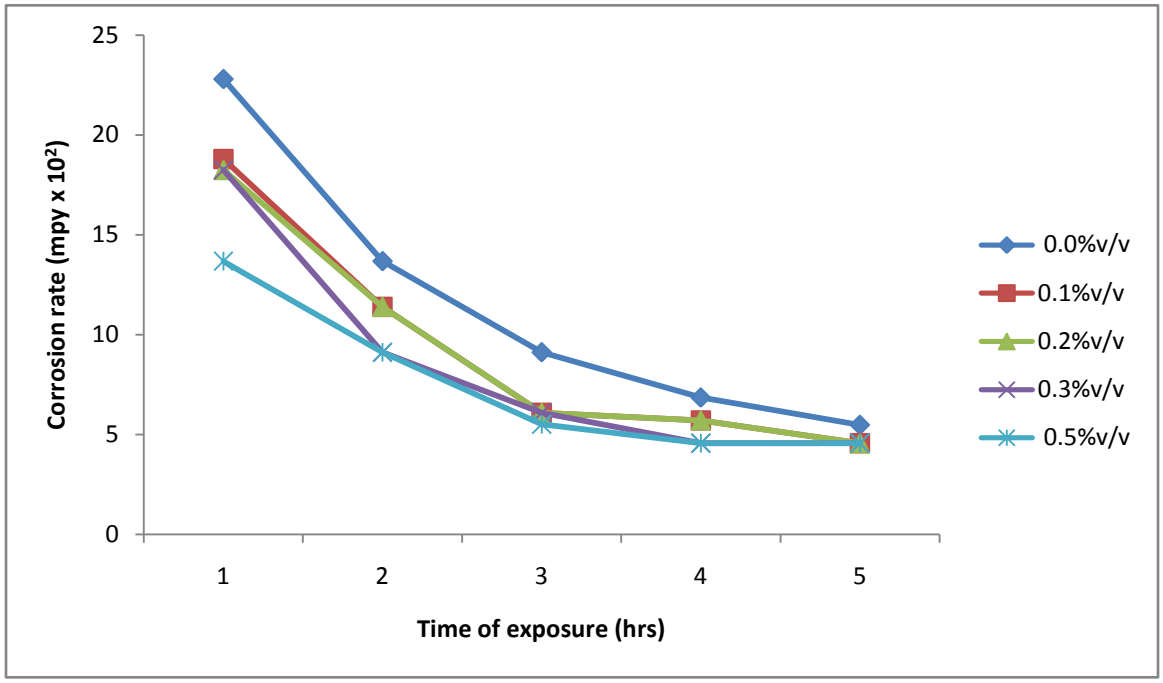

Figure 4.11: Variation of corrosion rate of as-received Al-Si-Mg alloy with time of exposure in the presence of neem (*Azadirachta indica*) seed extract at 70°C.

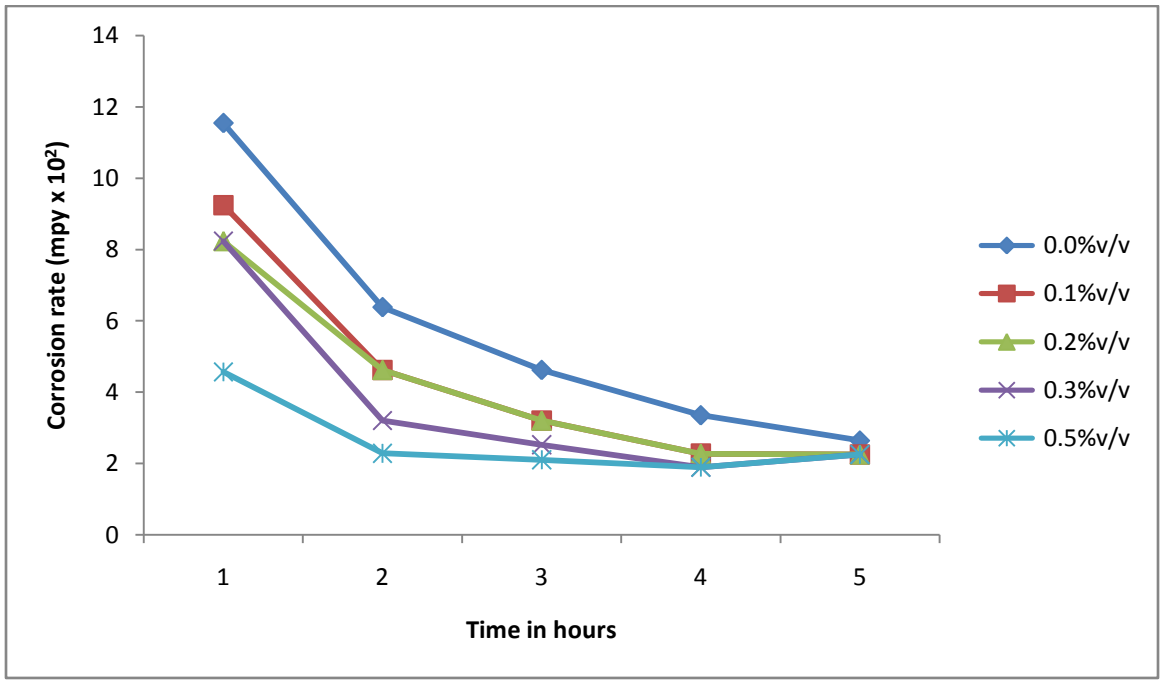

Figure 4.12: Variation of corrosion rate of double thermally aged Al-Si-Mg alloy with time of exposure in the presence of neem (*Azadirachta indica*) seed extract at 30°C.

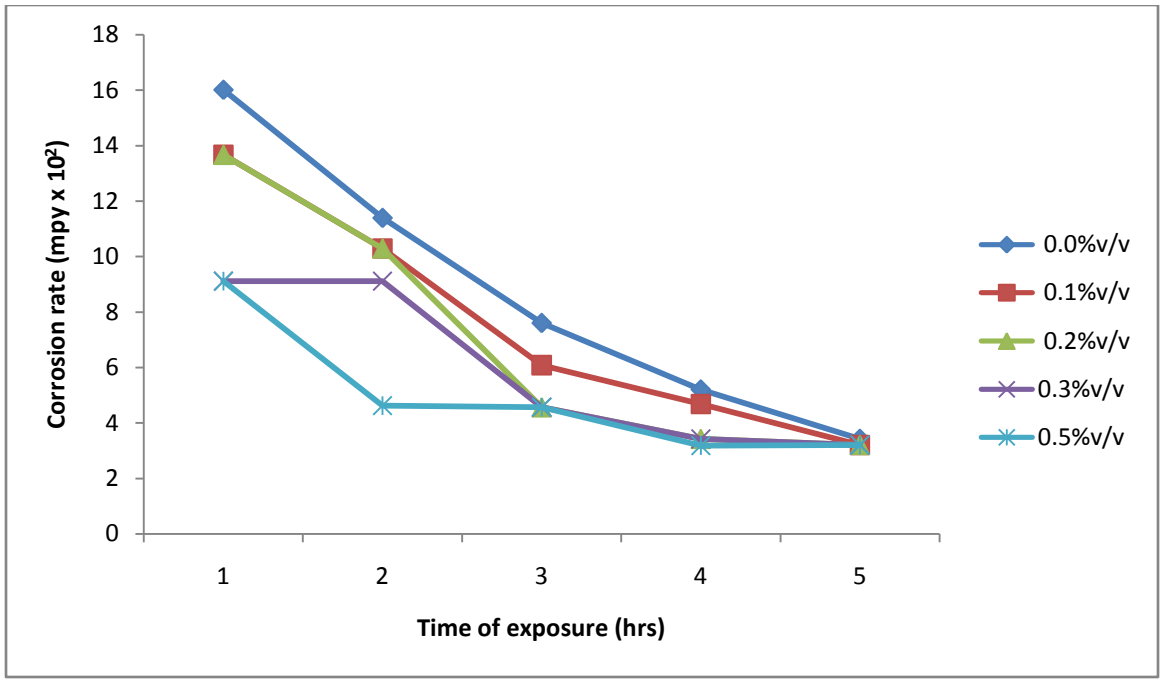

Figure 4.13: Variation of corrosion rate of double thermally aged Al-Si-Mg alloy with time of exposure in the presence of neem (*Azadirachta indica*) seed extract at 50^{o}C.

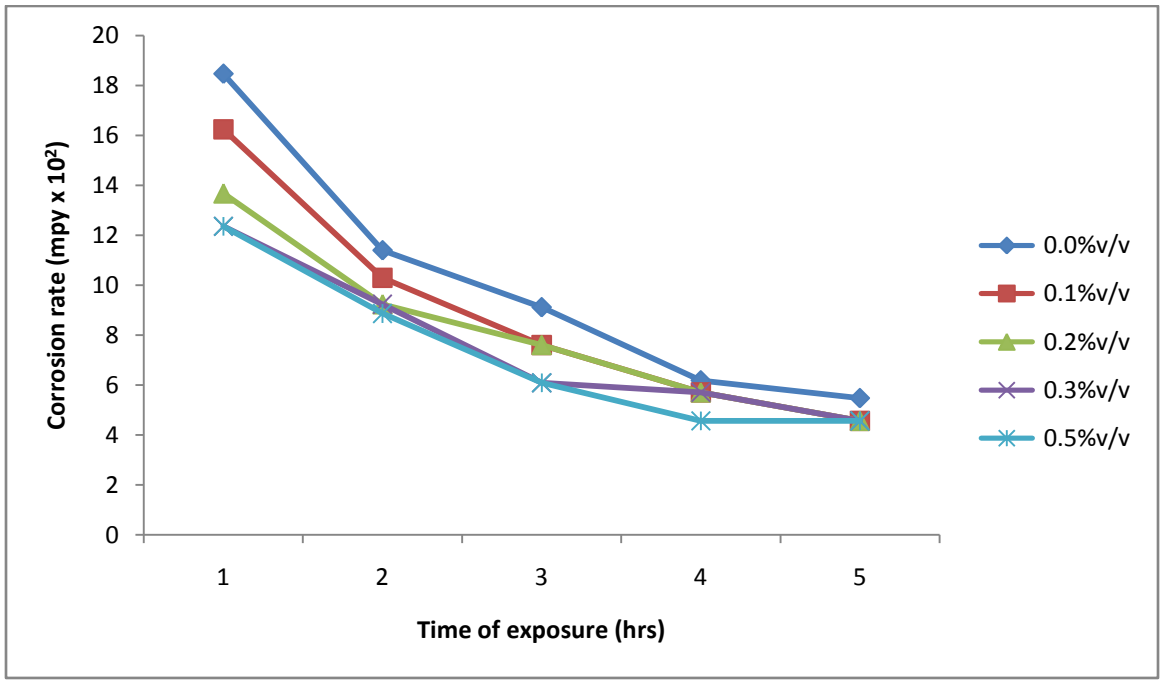

Figure 4.14: Variation of corrosion rate of double thermally aged Al-Si-Mg alloy with time of exposure in the presence of neem (*Azadirachta indica*) seed extract at 70^{o}C.

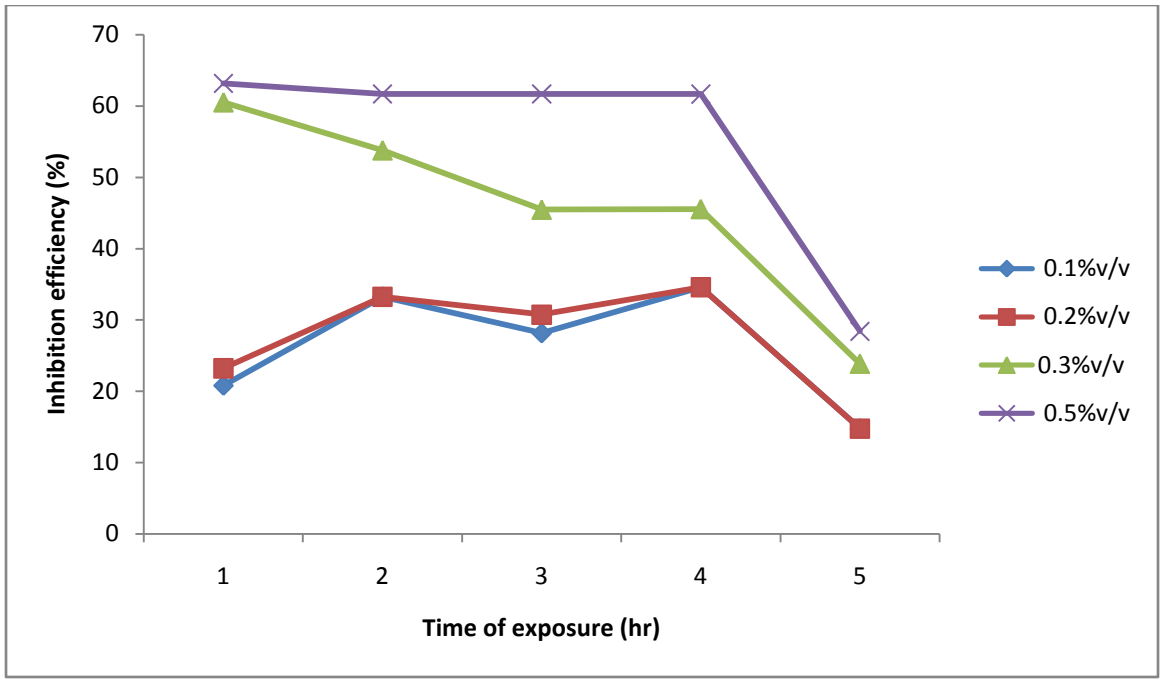

Figure 4.15: Variation of inhibitor efficiency of guava (*Psidium guajava*) leaf extract on as-received Al-Si-Mg alloy with time of exposure at 30^{o}C.

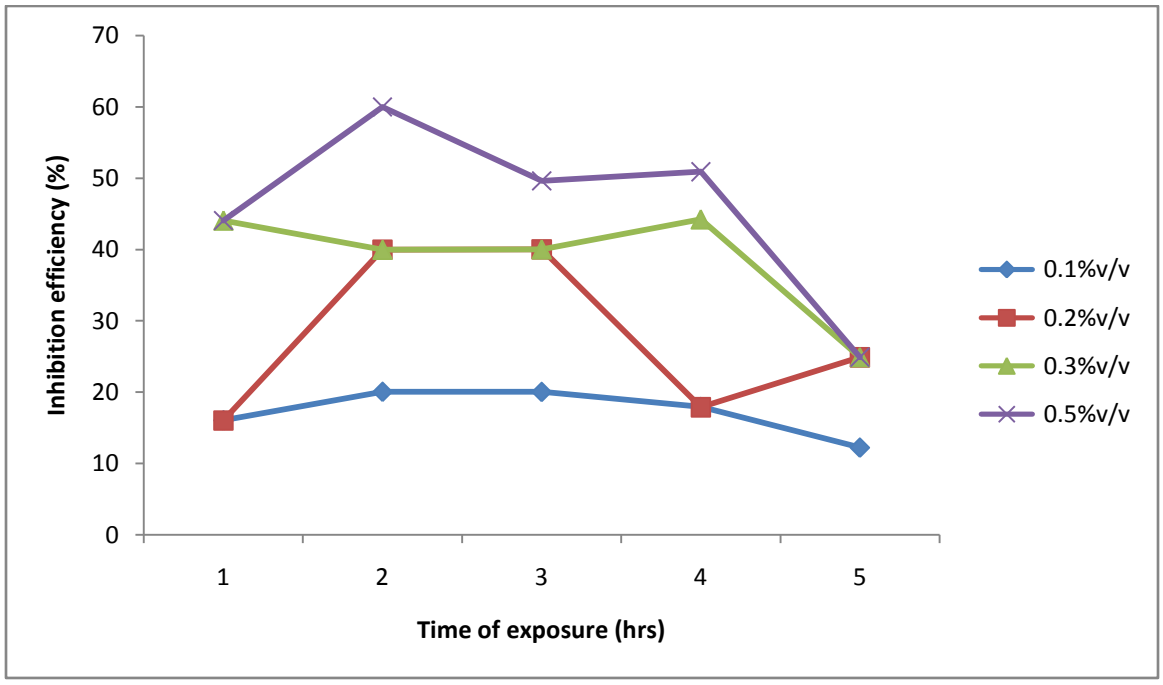

Figure 4.16: Variation of inhibitor efficiency of guava (*Psidium guajava*) leaf extract on as-received Al-Si-Mg alloy with time of exposure at 50^{o}C.

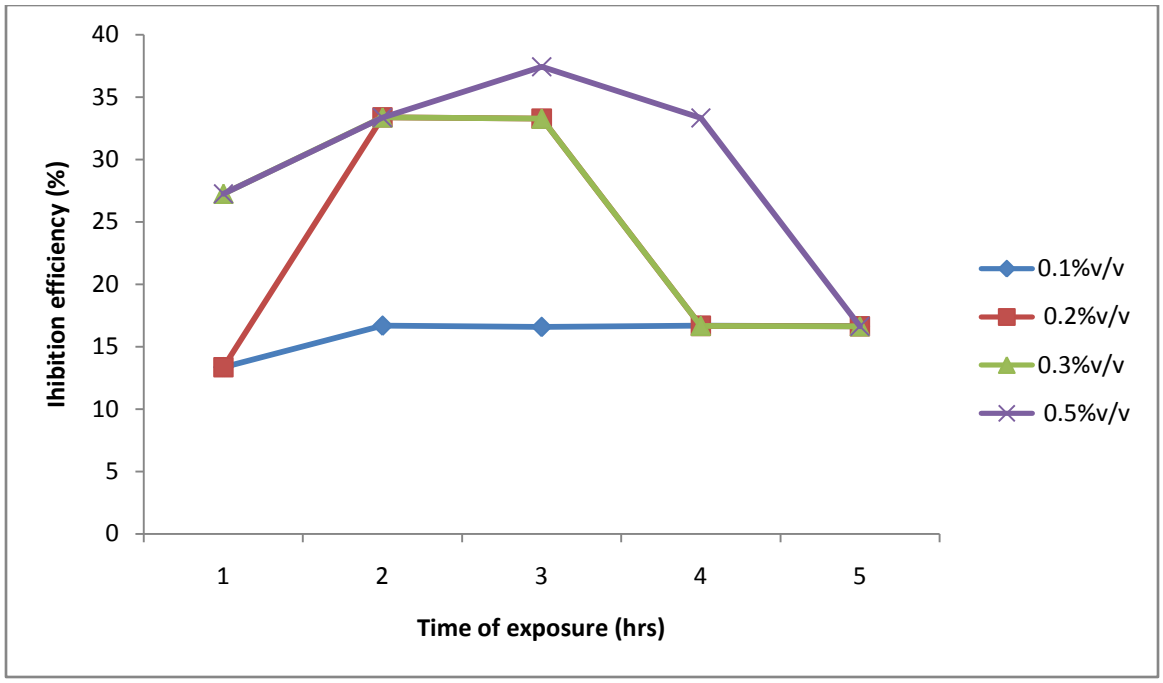

Figure 4.17: Variation of inhibitor efficiency of guava (*Psidium guajava*) leaf extract on as-received Al-Si-Mg alloy with time of exposure at 70^{o}C.

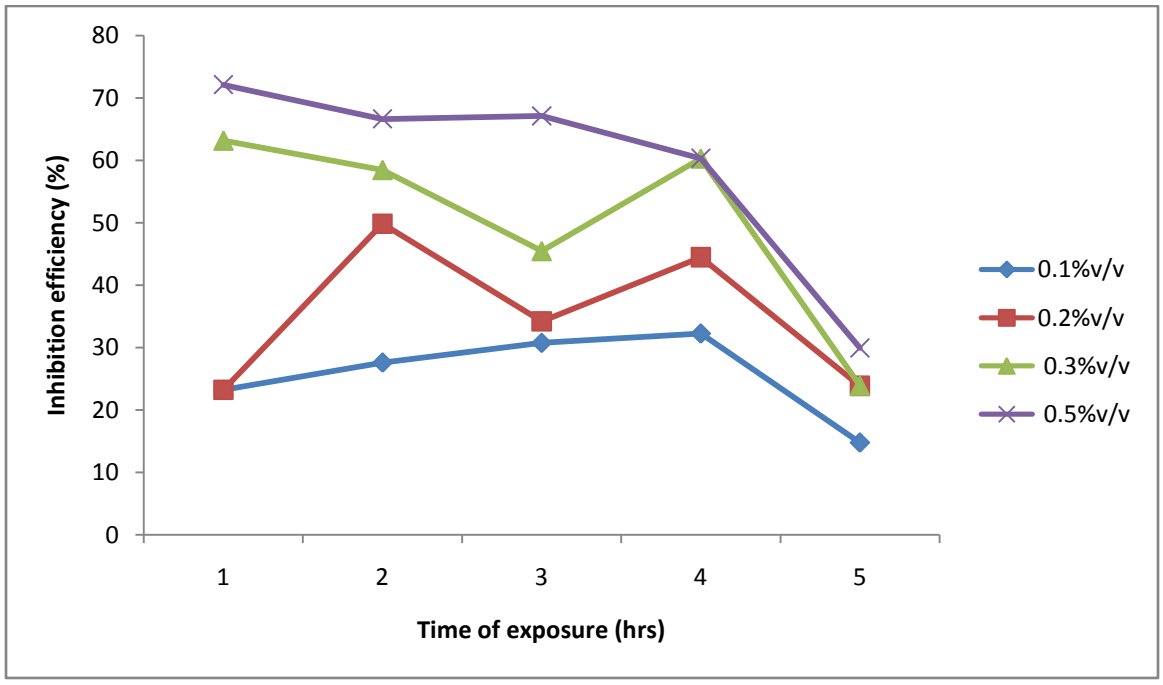

Figure 4.18: Variation of inhibitor efficiency of guava (*Psidium guajava*) leaf extract on double thermally aged Al-Si-Mg alloy with time of exposure at 30^{o}C.

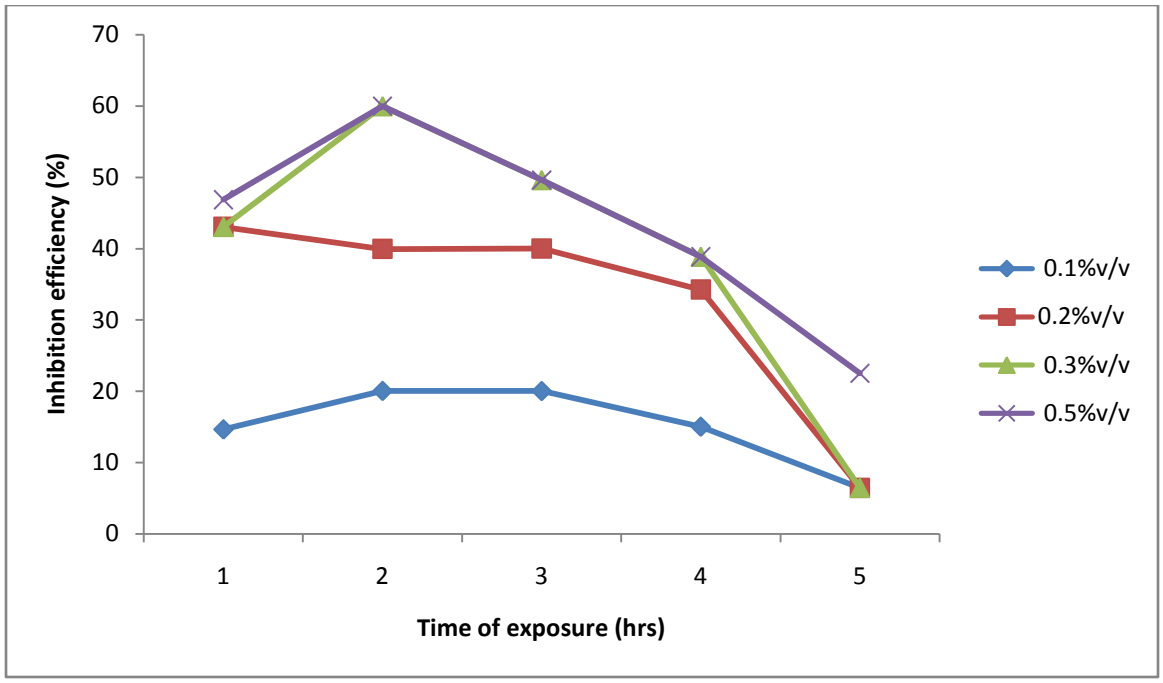

Figure 4.19: Variation of inhibitor efficiency of guava (*Psidium guajava*) leaf extract on double thermally aged Al-Si-Mg alloy with time of exposure at 50^{o}C.

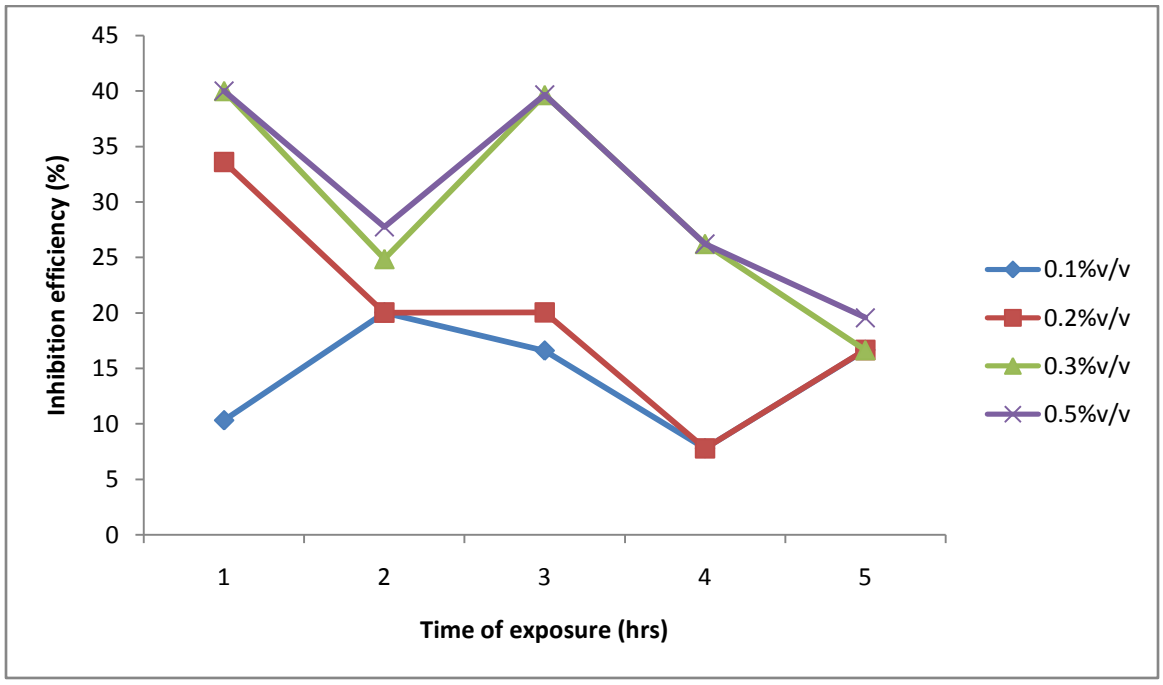

Figure 4.20: Variation of inhibitor efficiency of guava (*Psidium guajava*) leaf extract on double thermally aged Al-Si-Mg alloy with time of exposure at 70^{o}C.

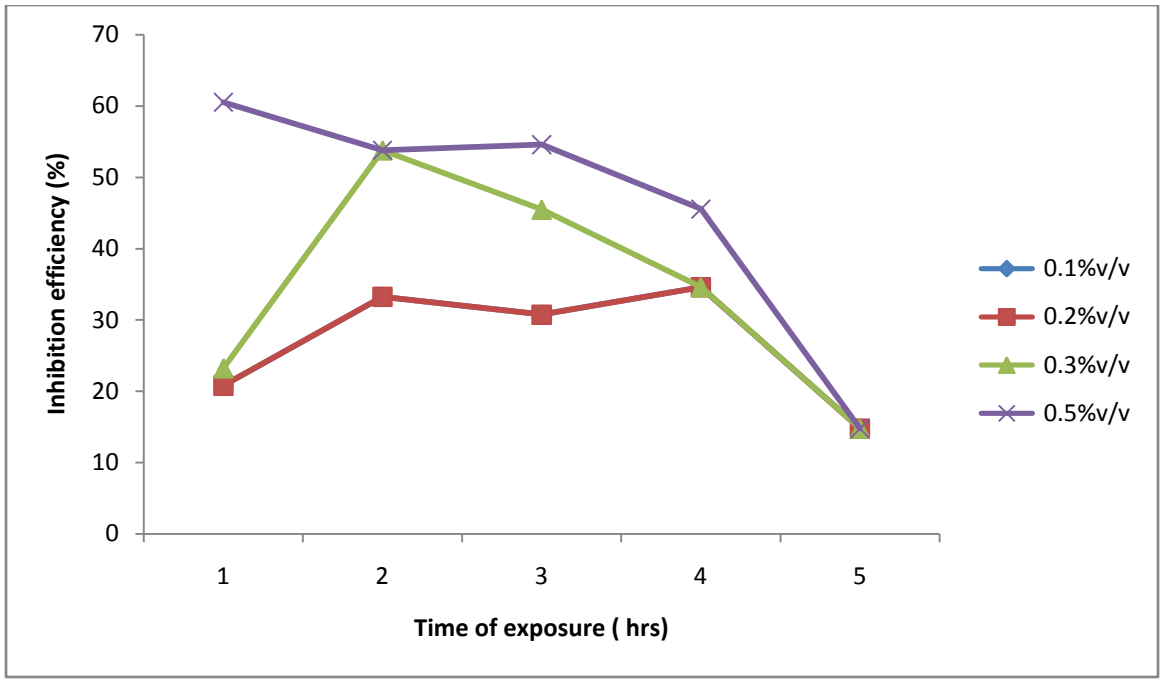

Figure 4.21: Variation of inhibitor efficiency of neem (*Azadirachta indica*) seed extract on as-received Al-Si-Mg alloy with time of exposure at 30^{o}C.

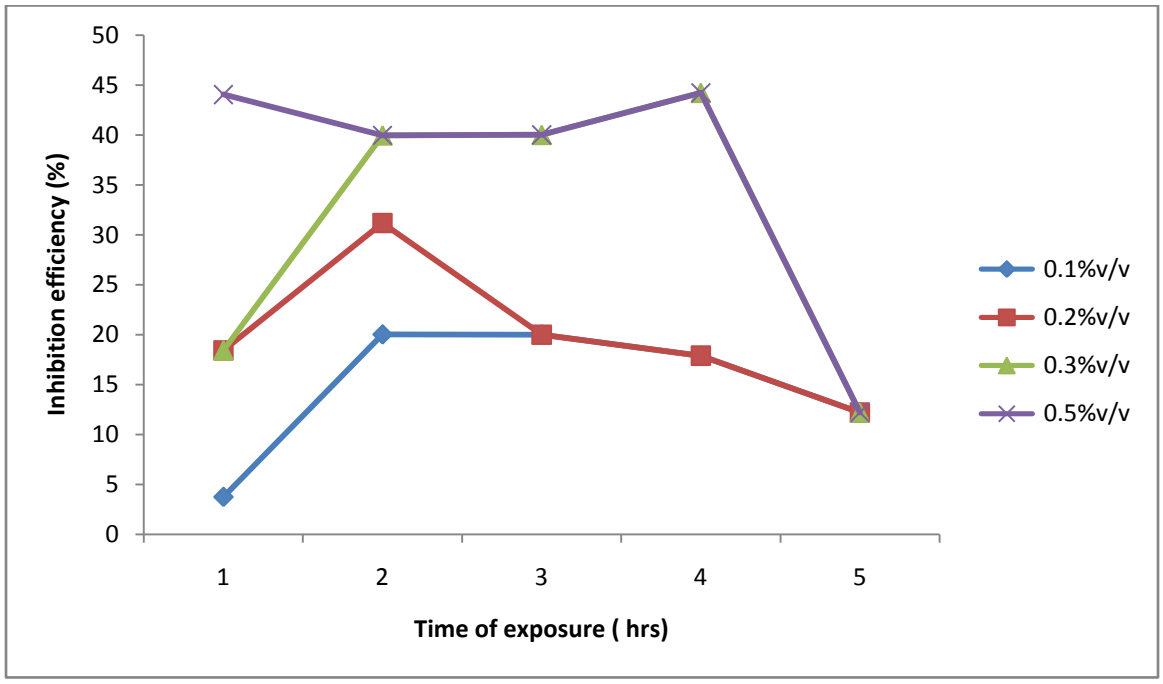

Figure 4.22: Variation of inhibitor efficiency of neem (*Azadirachta indica*) seed extract on as-received Al-Si-Mg alloy with time of exposure at 50^{o}C.

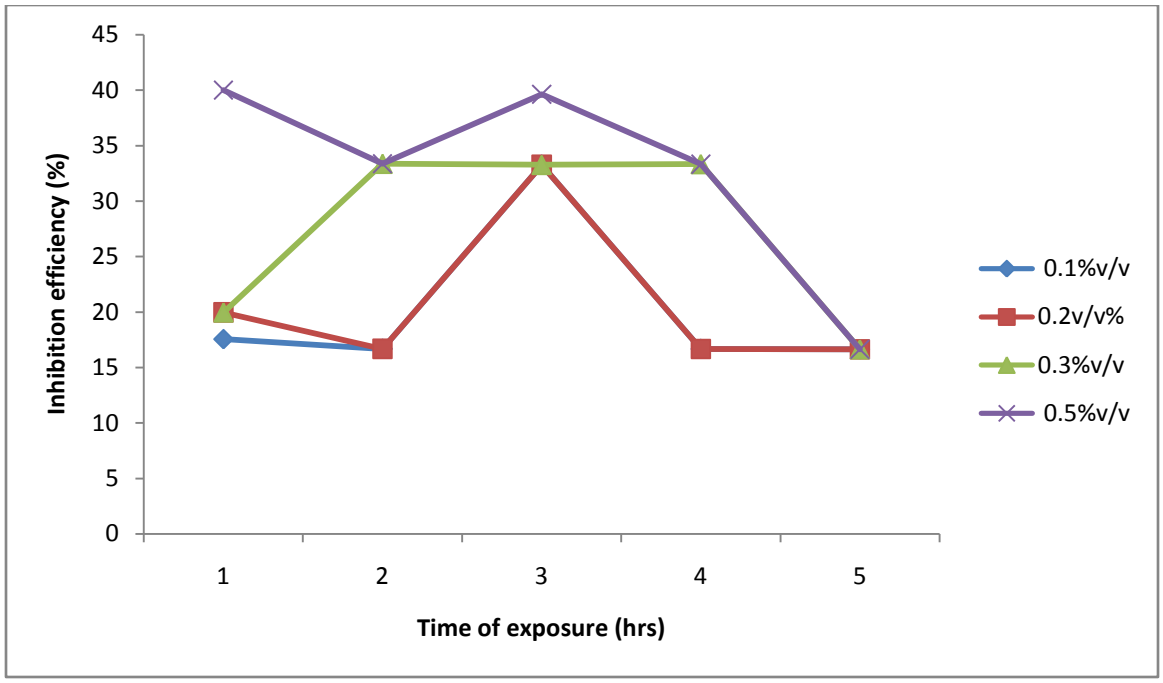

Figure 4.23: Variation of inhibitor efficiency of neem (*Azadirachta indica*) seed extract on as-received Al-Si-Mg alloy with time of exposure at 70^{o}C.

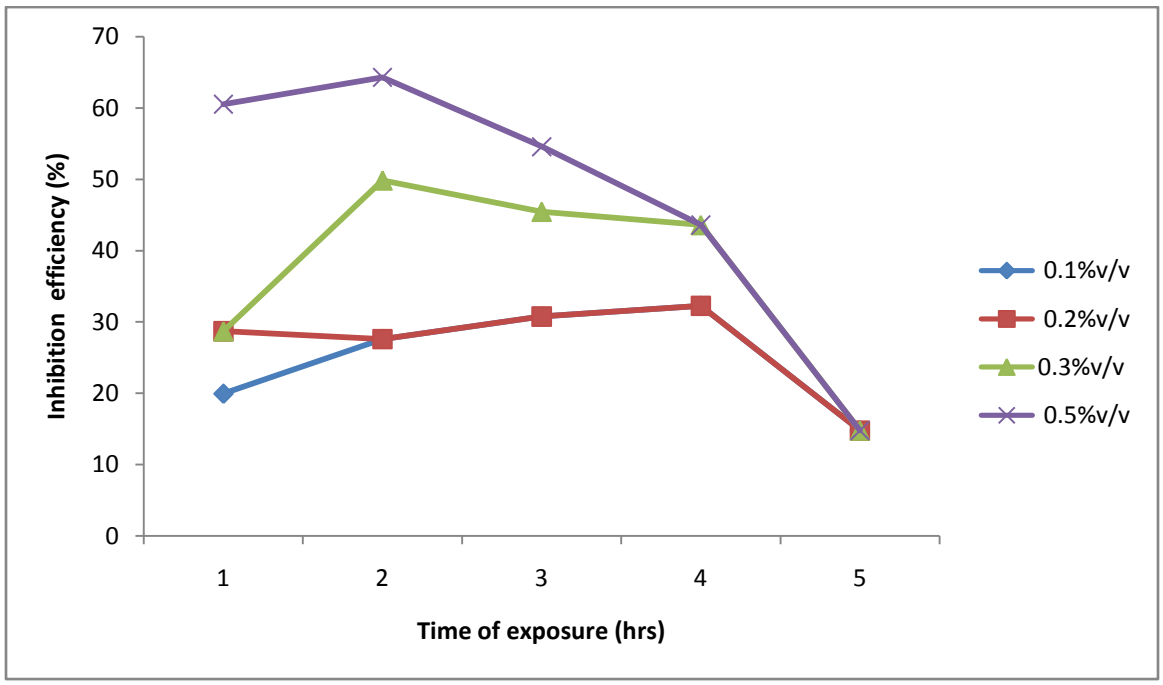

Figure 4.24: Variation of inhibitor efficiency of neem (*Azadirachta indica*) seed extract on double thermally aged Al-Si-Mg alloy at 30^{o}C.

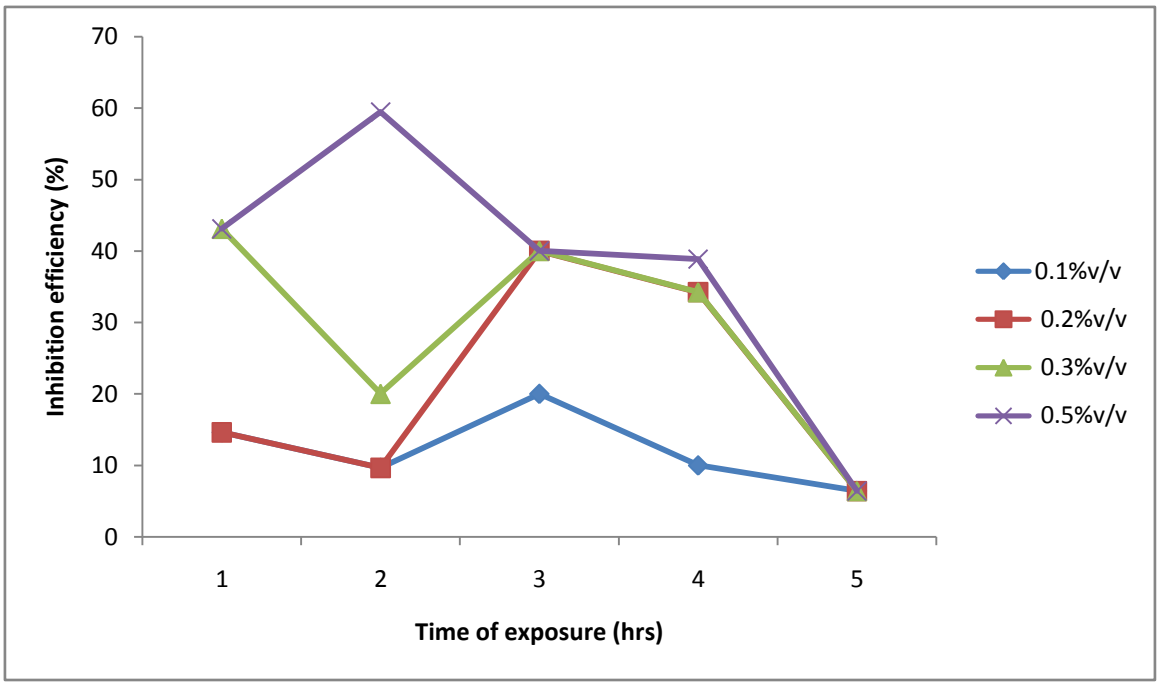

Figure 4.25: Variation of inhibitor efficiency of neem (*Azadirachta indica*) seed extract on double thermally aged Al-Si-Mg alloy with time of exposure at 50^{o}C.

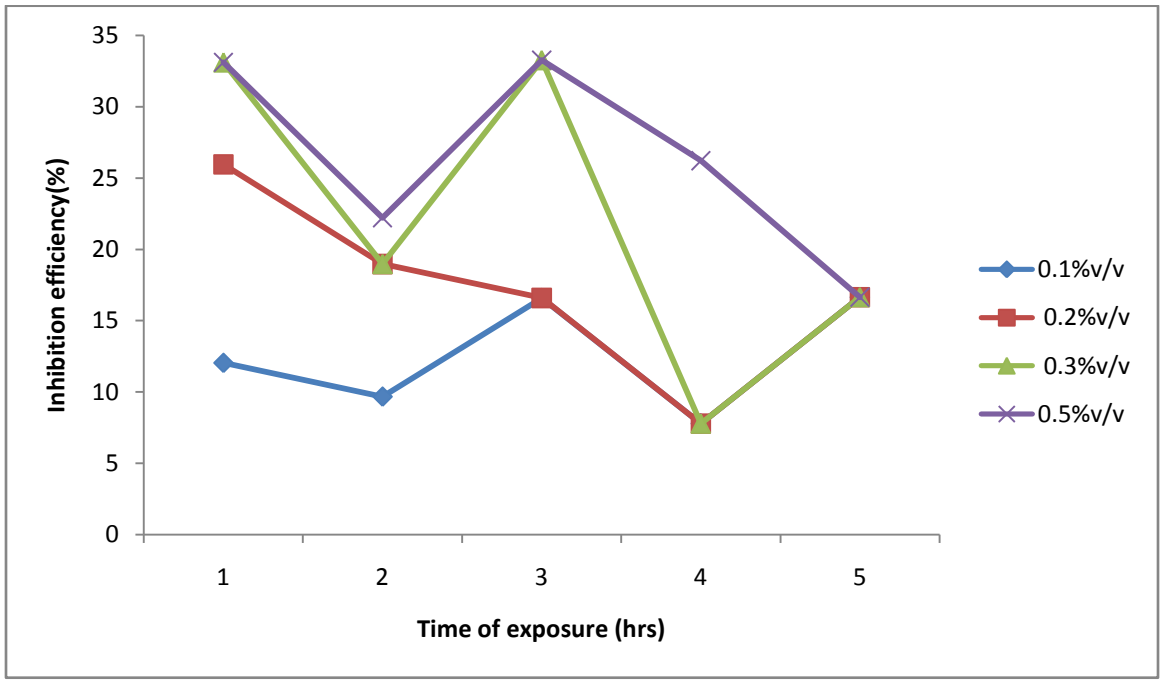

Figure 4.26: Variation of inhibitor efficiency of neem (*Azadirachta indica*) seed extract on double thermally aged Al-Si-Mg alloy with time of exposure at 70^{o}C.

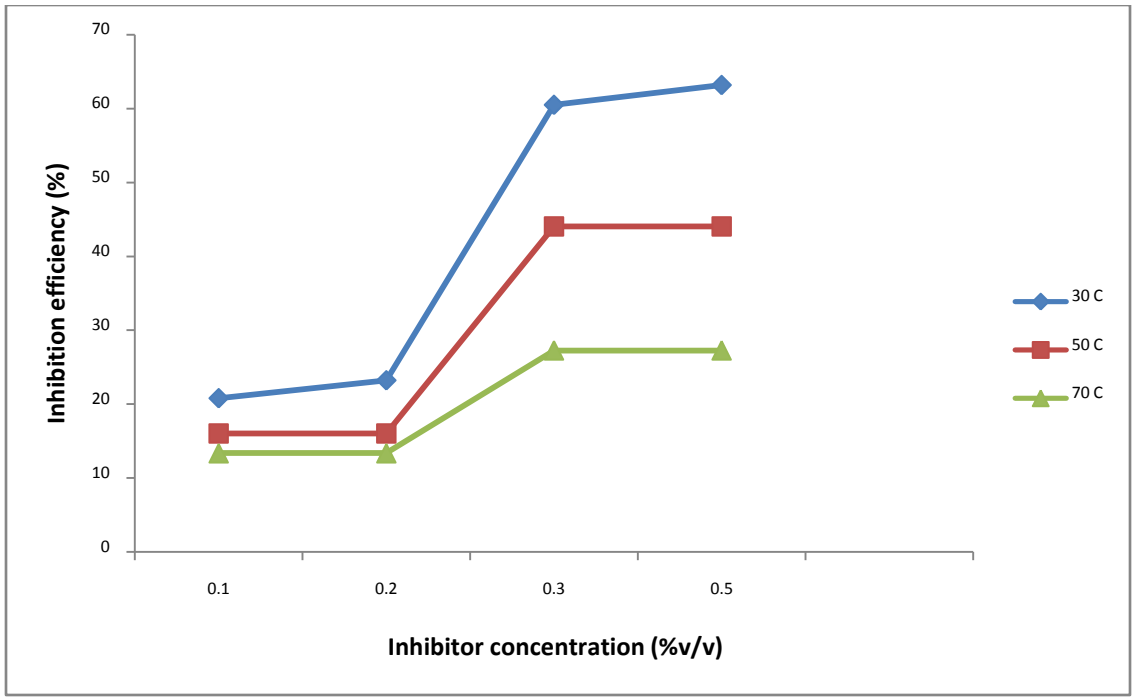

Figure 4.27: Variation of inhibition efficiency on as-received Al-Si-Mg alloy with concentration of guava (*Psidium guajava*) leaf extract for immersion time of 1hr at different operating temperatures.

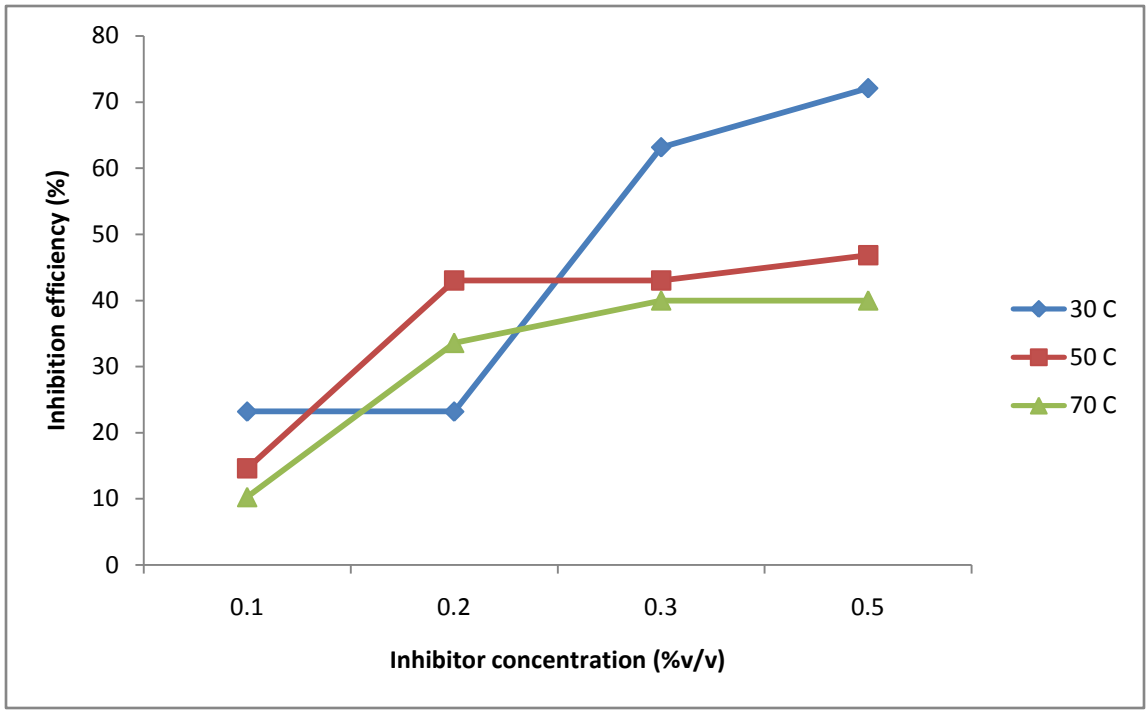

Figure 4.28: Variation of inhibition efficiency on double thermally aged Al-Si-Mg alloy with concentration of guava (*Psidium guajava*) leaf extract for immersion time of 1hr at different operating temperatures.

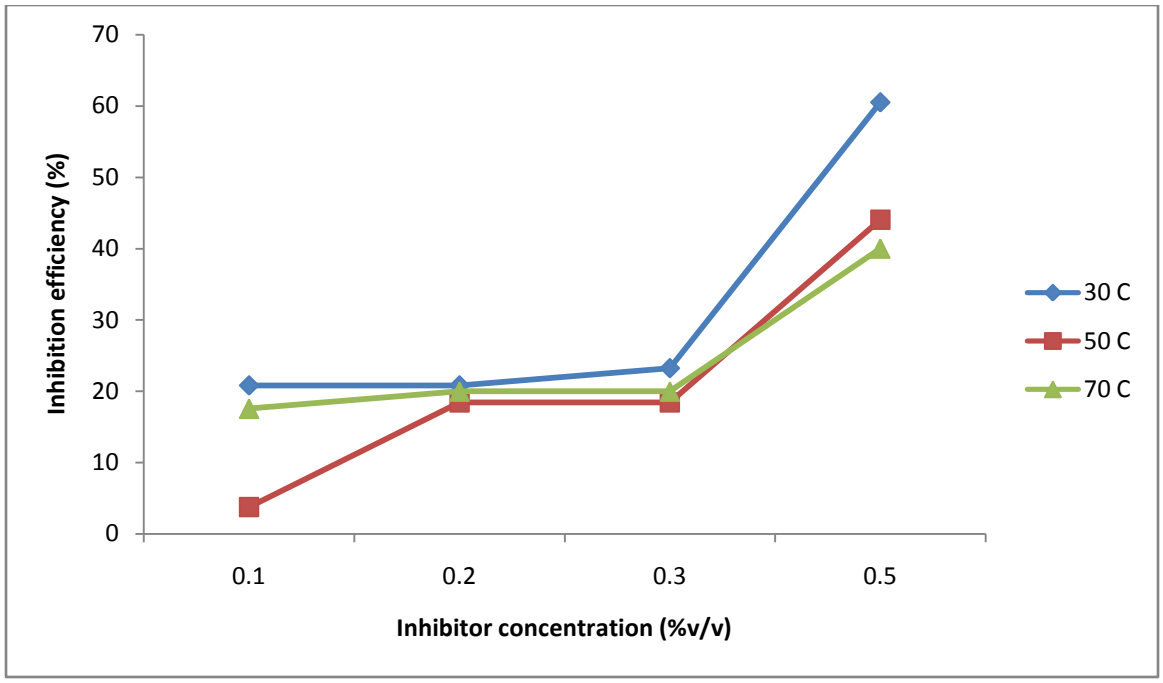

Figure 4.29: Variation of inhibition efficiency on as-received Al-Si-Mg alloy with concentration of neem (*Azadirachta indica*) seed extract for immersion time of 1hr at different operating temperatures.

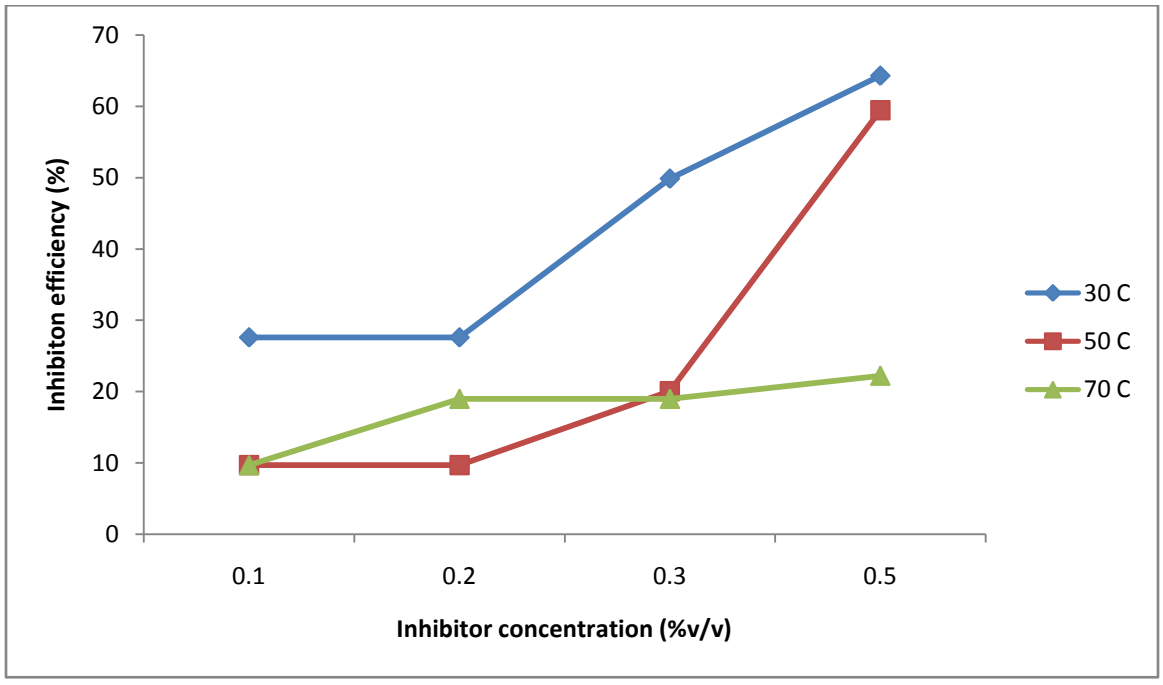

Figure 4.30: Variation of inhibition efficiency on double thermally aged Al-Si-Mg alloy with concentration of neem (*Azadirachta indica*) seed extract for immersion time of 1hr at different operating temperatures.

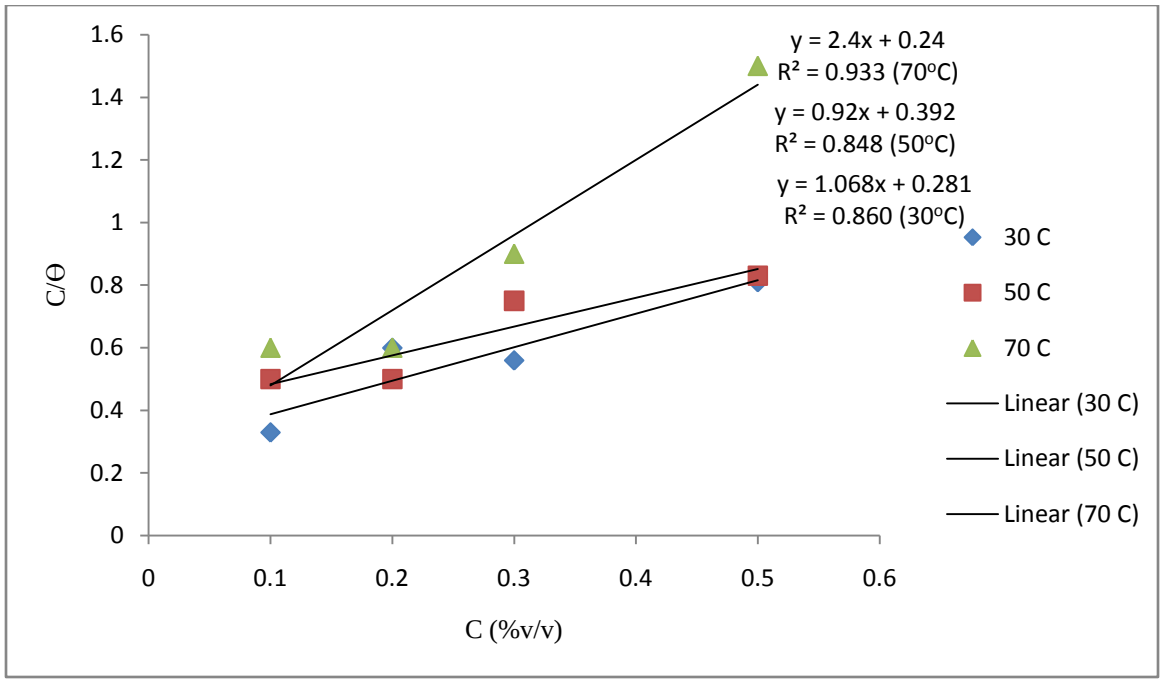

Figure 4.31: Langmuir isotherm for the adsorption of guava (*Psidium guajava*) leaf extract on the surface of Al-Si-Mg (SSM-HPDC) alloy at 2 hrs exposure time.

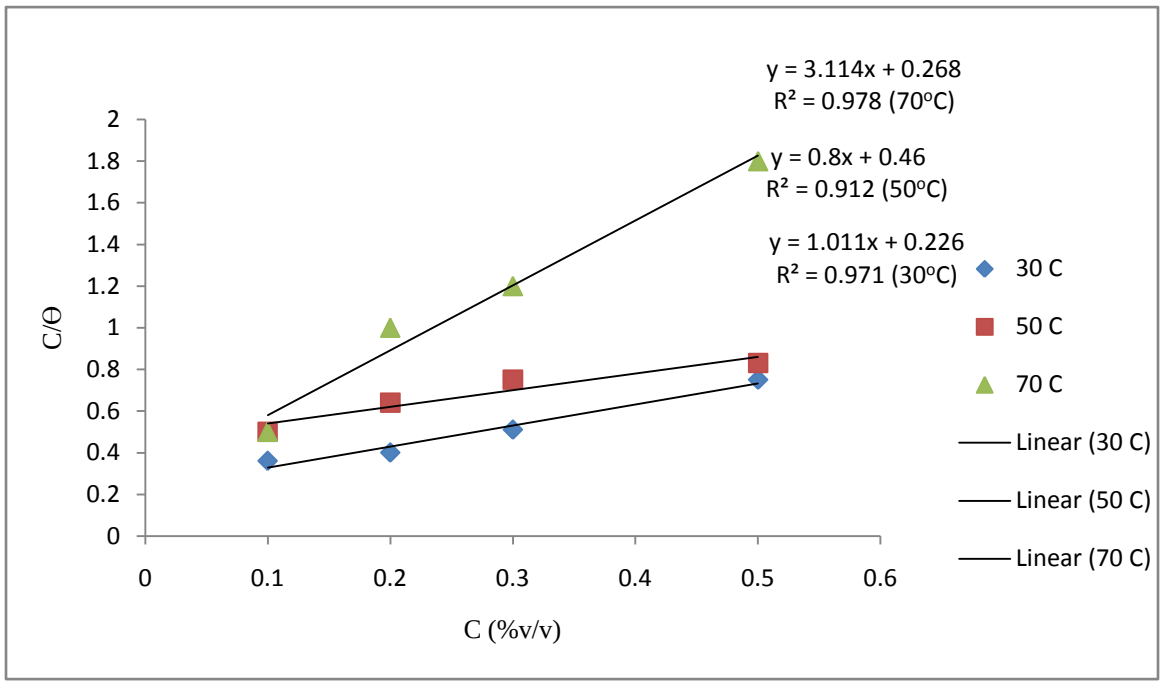

Figure 4.32: Langmuir isotherm for the adsorption of guava (*Psidium guajava*) leaf extract on the surface of double thermally-aged Al-Si-Mg (SSM-HPDC) alloy at 2 hrs exposure time.

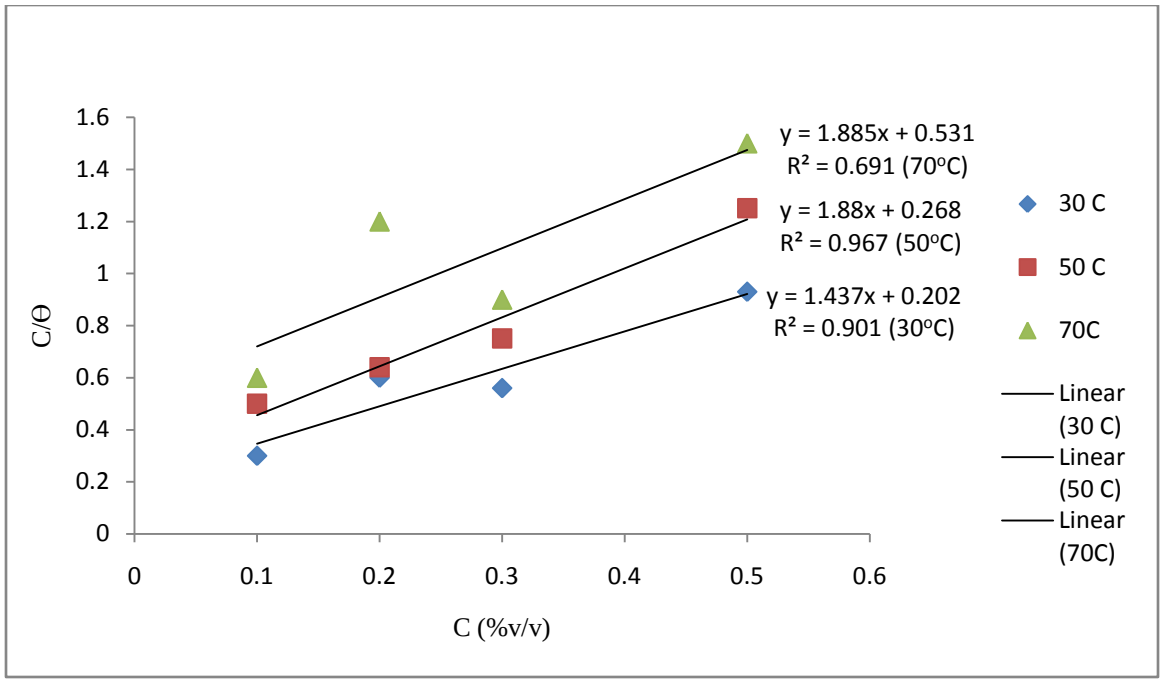

Figure 4.33: Langmuir isotherm for the adsorption of neem (*Azadirachta indica*) seed extract on the surface of Al-Si-Mg (SSM-HPDC) alloy at 2 hrs exposure time.

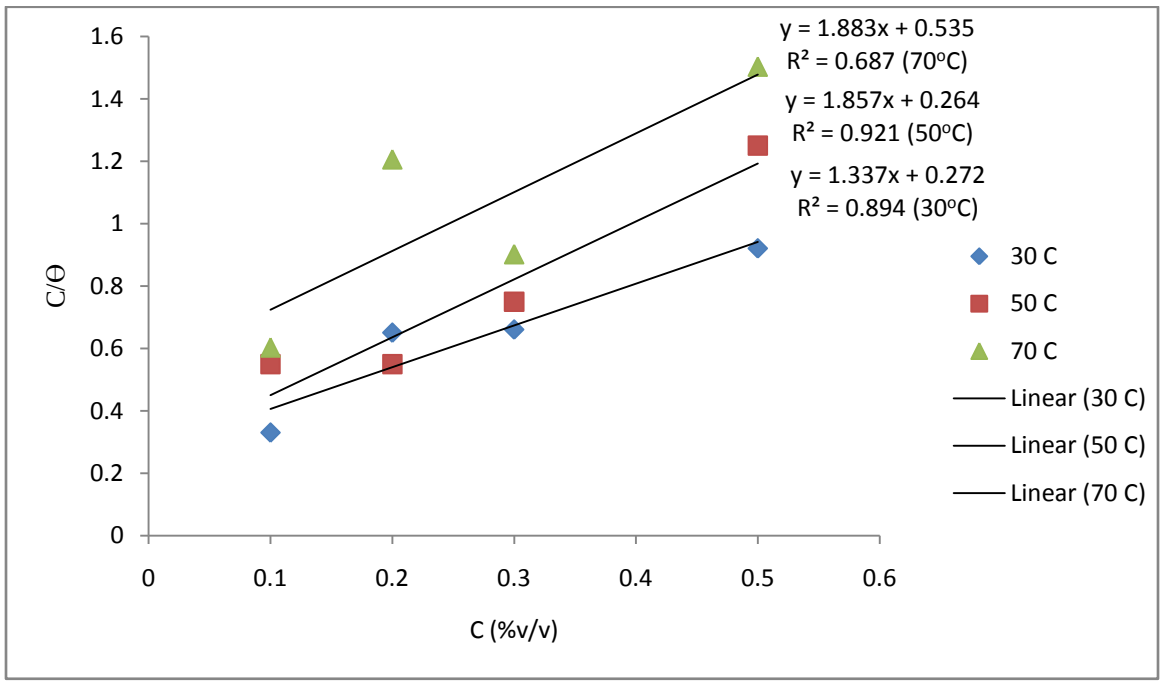

Figure 4.34: Langmuir isotherm for the adsorption of neem (*Azadirachta indica*) seed extract on the surface of double thermally-aged Al-Si-Mg (SSM-HPDC) alloy at 3hrs exposure time

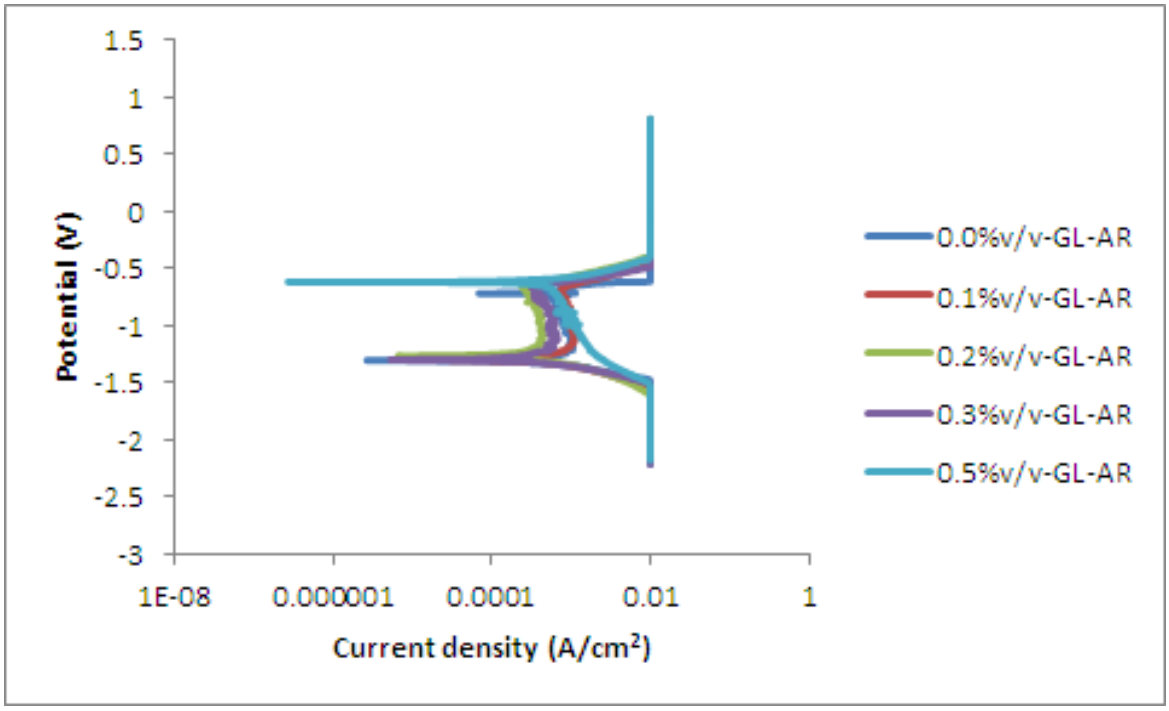

Figure 4.35: Potentiodynamic polarization curves for as-received Al-Si-Mg (SSM-HPDC) alloy in 3.5wt%NaCl / Guava (*Psidium guajava*) leaf extracts environment.

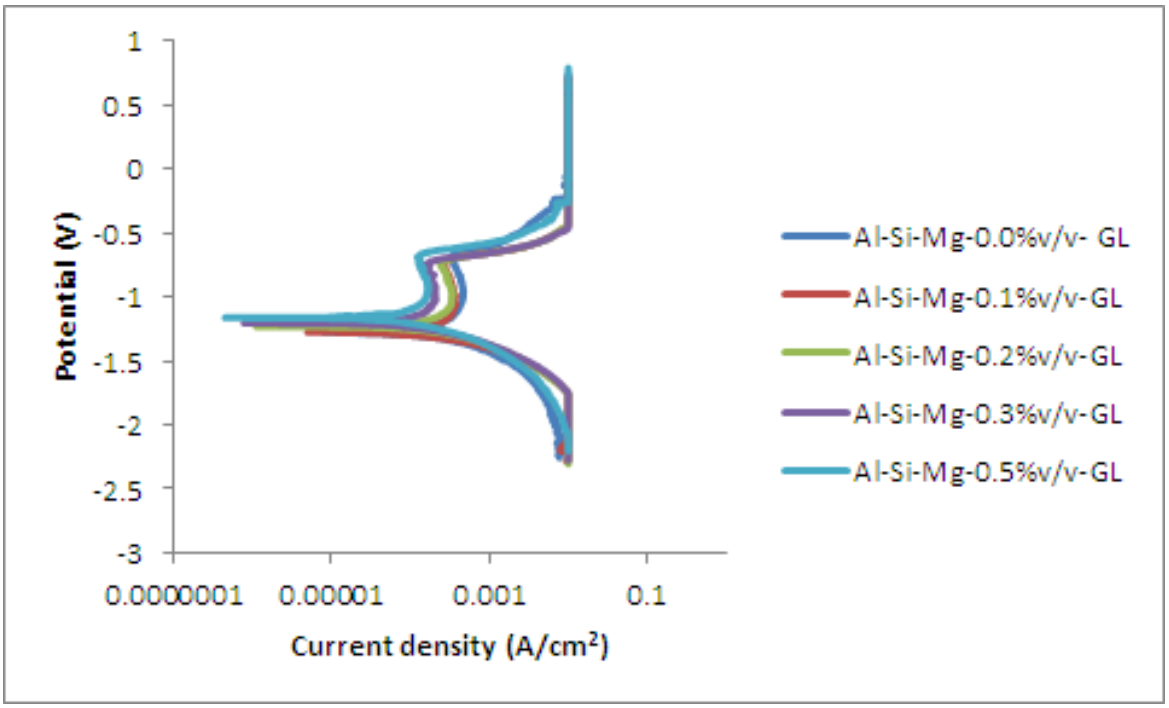

Figure 4.36: Potentiodynamic polarization curves for double thermally aged Al-Si-Mg (SSM-HPDC) alloy in 3.5wt%NaCl /Guava (*Psidium guajava)* leaf extract environment.

.

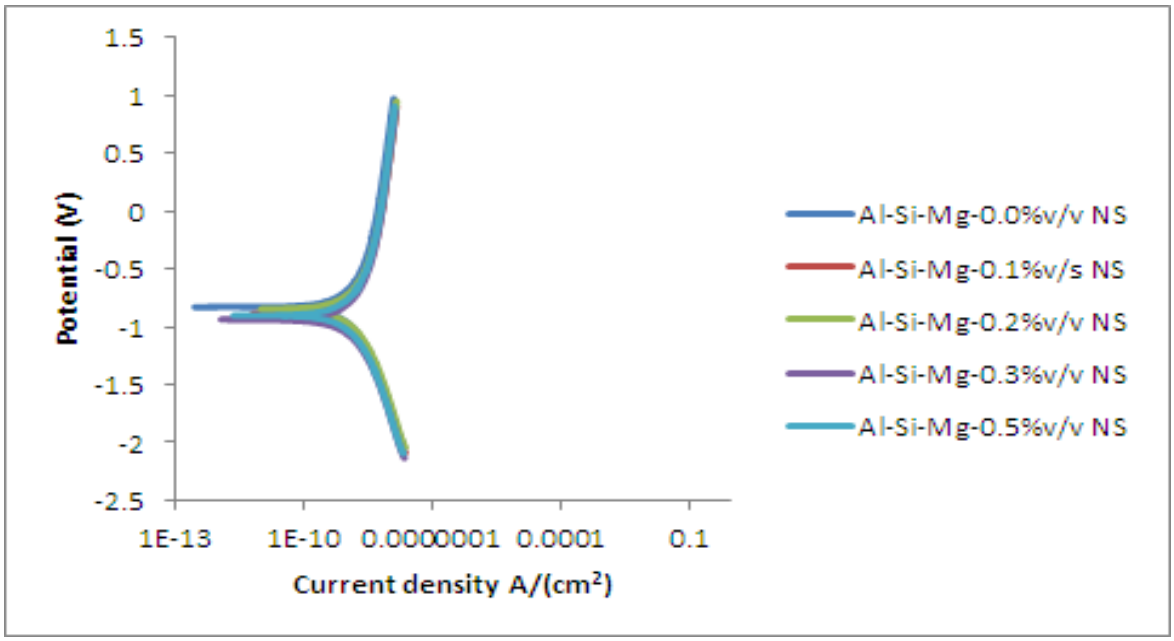

Figure 4.37: Potentiodynamic polarization curves for as-received Al-Si-Mg (SSM-HPDC) alloy in 3.5wt% NaCl /Neem (*Azadirachta indica*) seed extract environment.

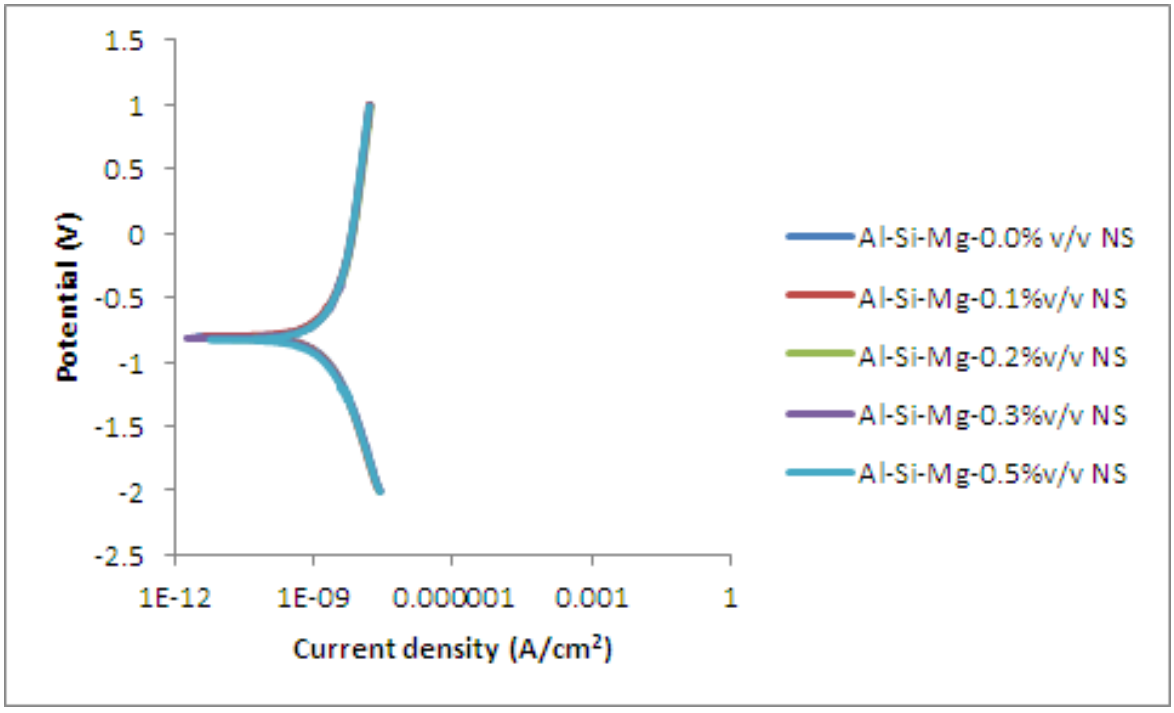

Figure 4.38: Potentiodynamic polarization curves for double thermally aged Al-Si-Mg (SSM-HPDC) alloy in 3.5wt% NaCl / Neem (*Azadirachta indica*) seed extract environment.

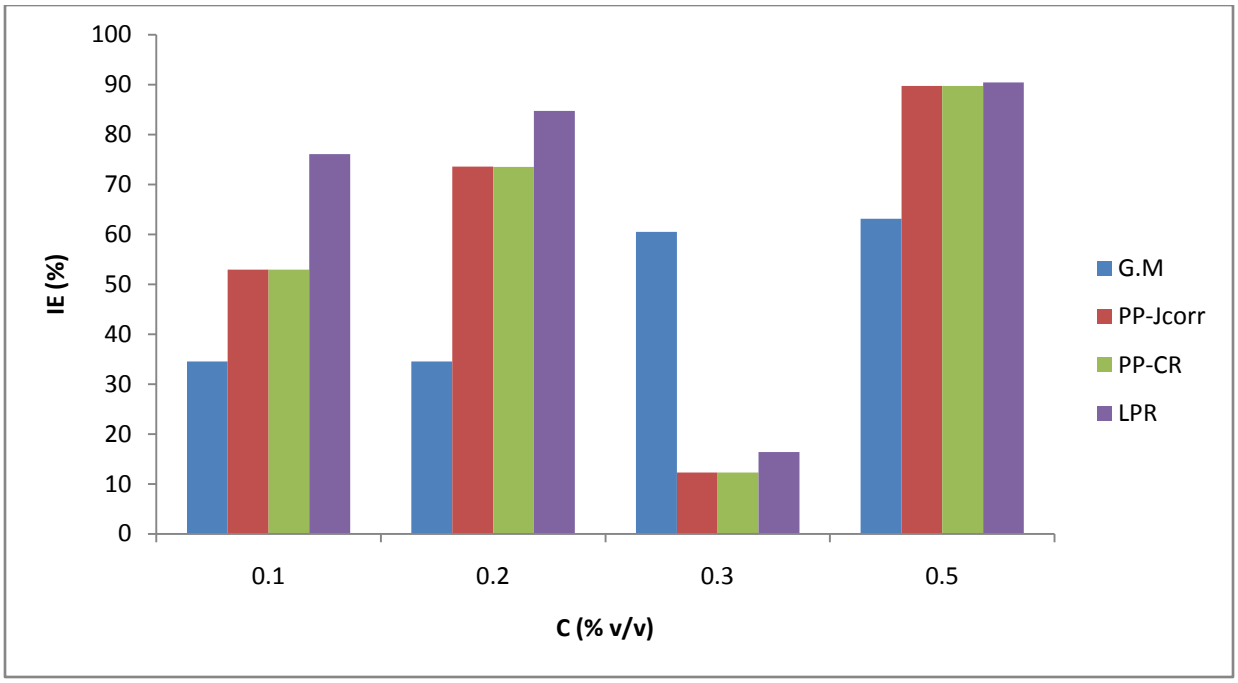

Figure 4.39: Comparative chart of inhibitor efficiency (IE) for Al-Si-Mg-3.5%wt NaCl solution/ *Psidium guajava* concentration obtained by gravimetric G.M, PP-CR, PP-Jcorr and LPR.

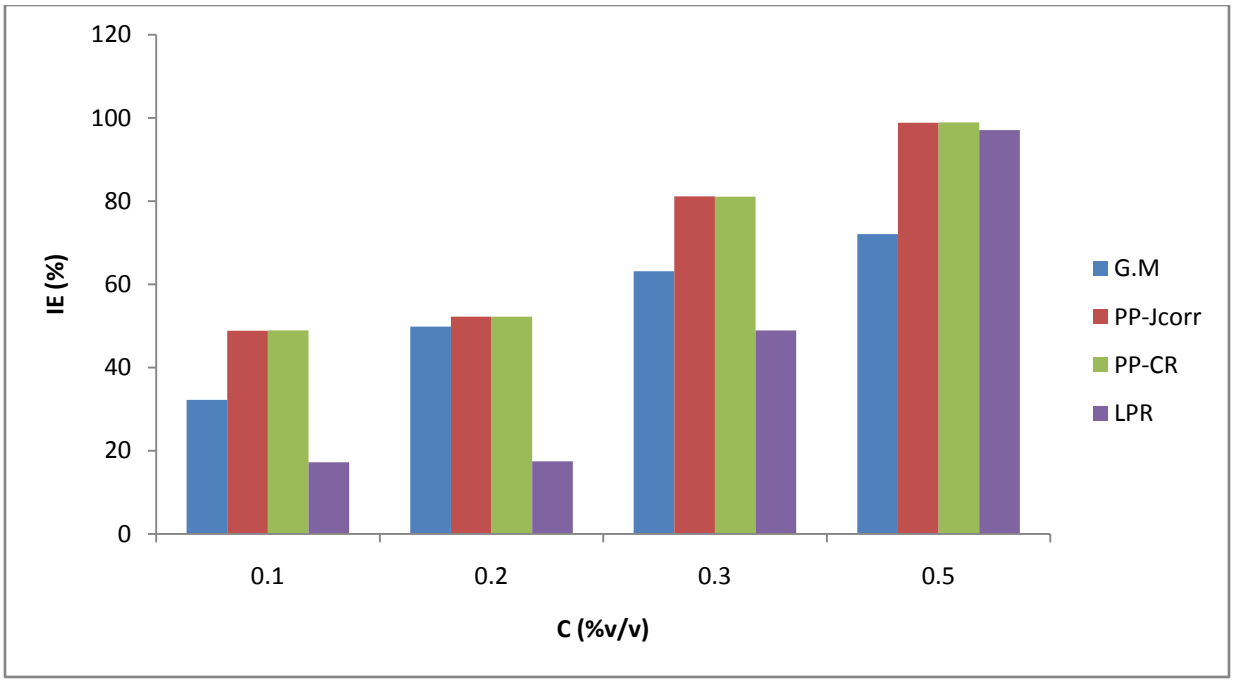

Figure 4.40: Comparative chart of inhibitor efficiency (IE) for double thermally-aged Al-Si-Mg-3.5%wt NaCl solution/ *Psidium guajava* concentration obtained by G.M, PP-CR, PP-Jcorr and LPR.

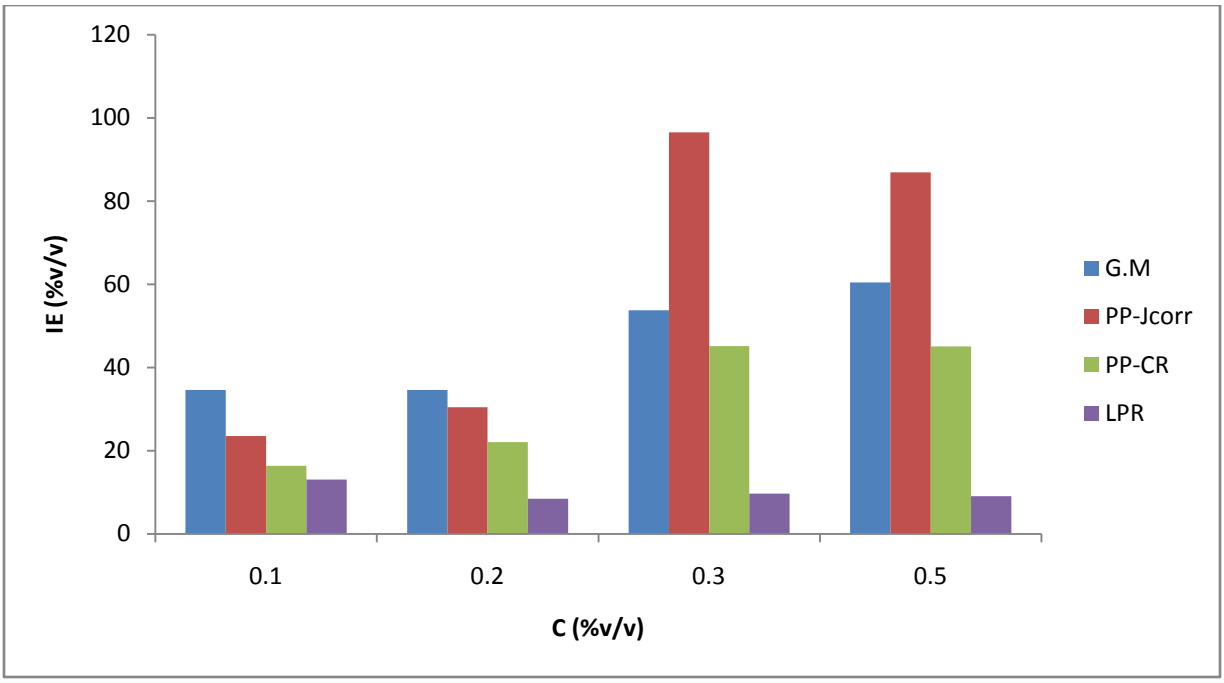

Figure 4.41: Comparative chart of inhibitor efficiency (IE) for Al-Si-Mg-3.5%wt NaCl solution/ *Azadirachta indica* concentration obtained by G.M, PP-CR, PP-Jcorr and LPR.

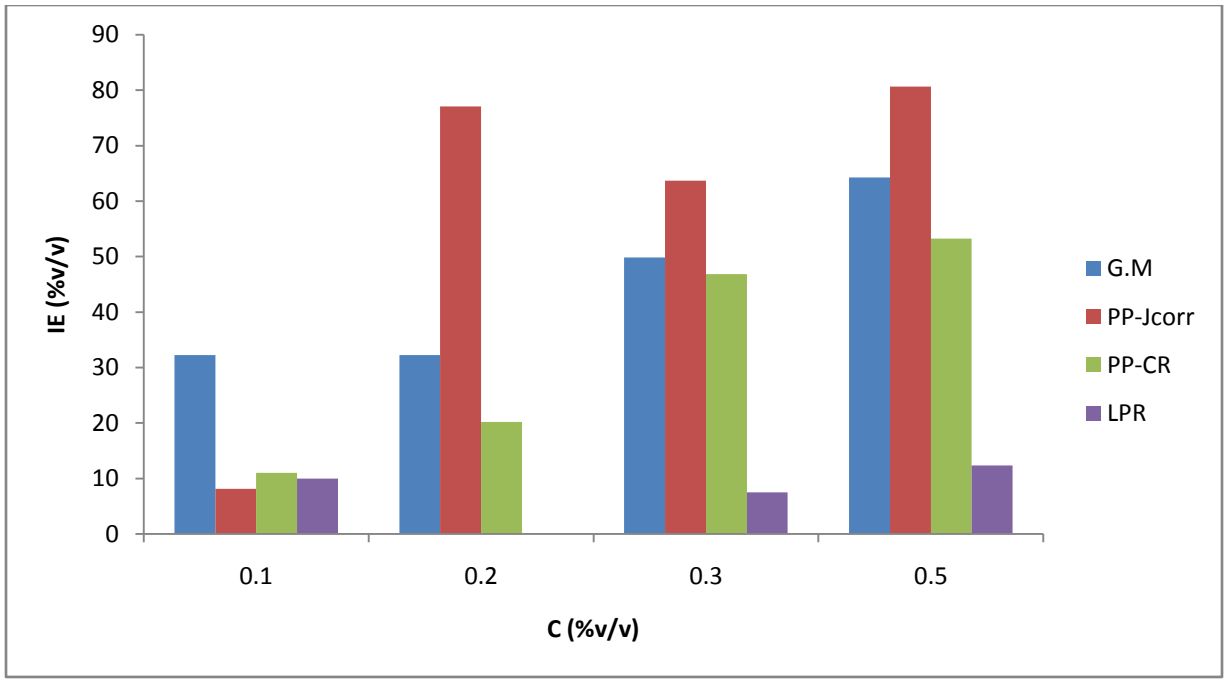

Figure 4.42: Comparative chart of inhibitor efficiency (IE) for double thermally-aged Al-Si-Mg-3.5%wt NaCl solution/*Azadirachta indica* concentration obtained by G.M, PP-CR, PP-Jcorr and LPR.

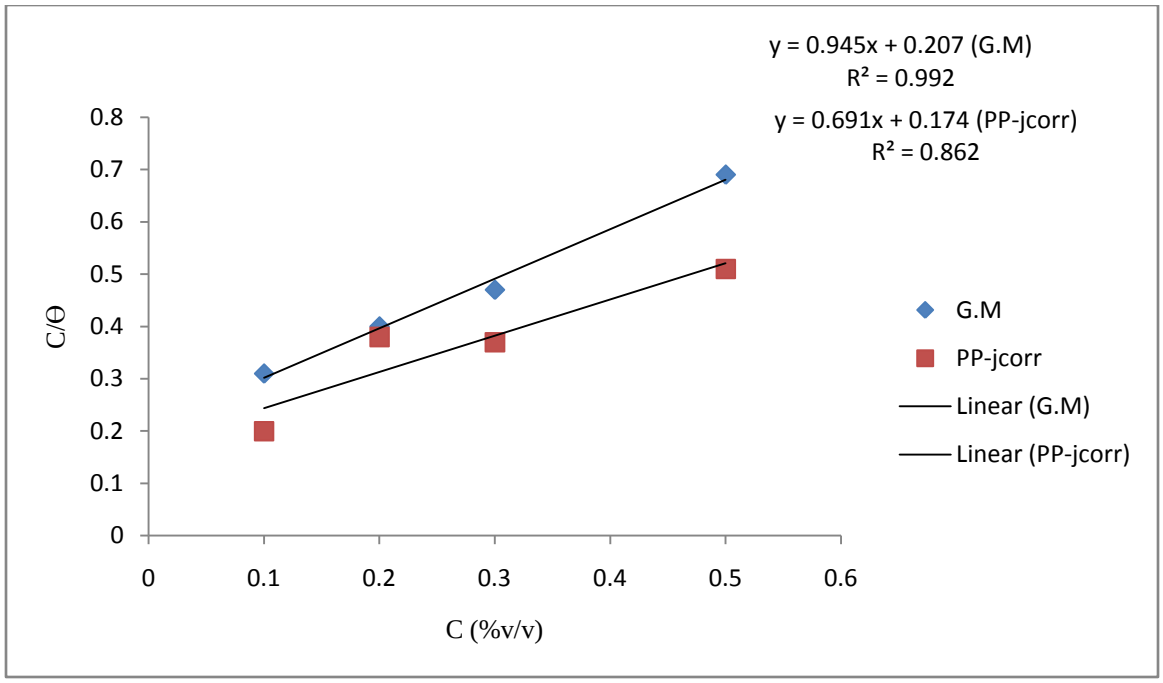

Figure 4.43: Langmuir isotherm for the adsorption of guava (*Psidium guajava*) leaf extract on double thermally-aged Al-Si-Mg (SSM-HPDC) alloy obtained by gravimetric and potentiodynamic polarization method.

.

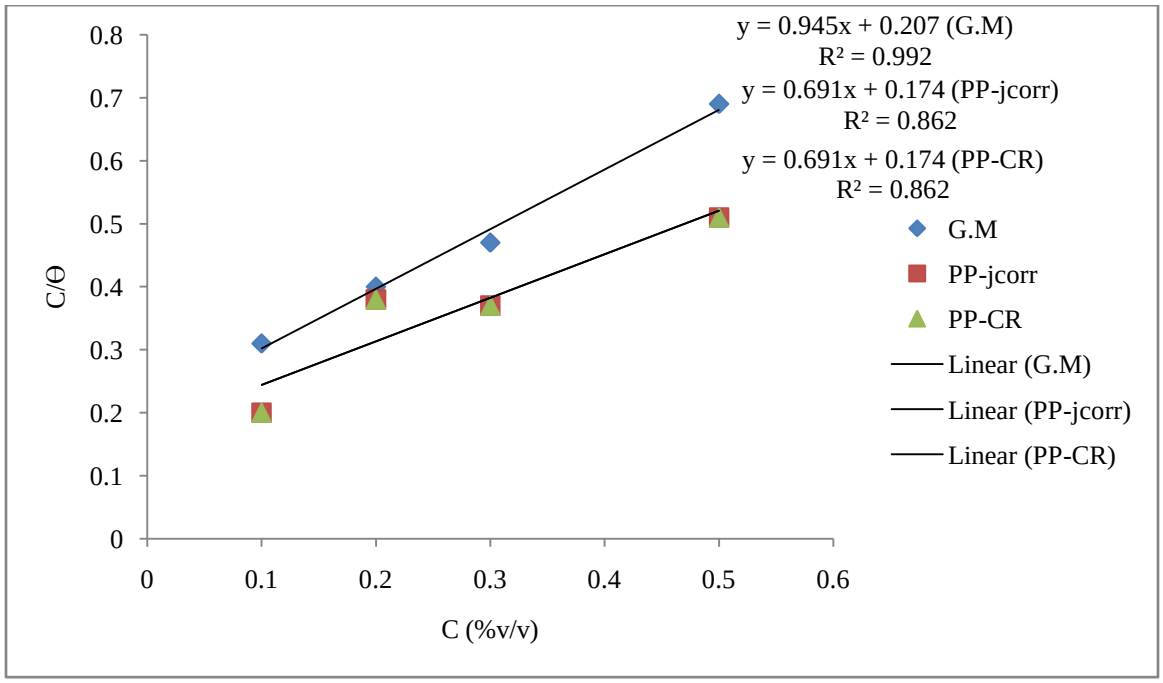

Figure 4.44: Langmuir isotherm for the adsorption of neem (*Azadirachta indica*) seed extract on Al-Si-Mg (SSM-HPDC) alloy obtained by gravimetric and potentiodynamic polarization method.

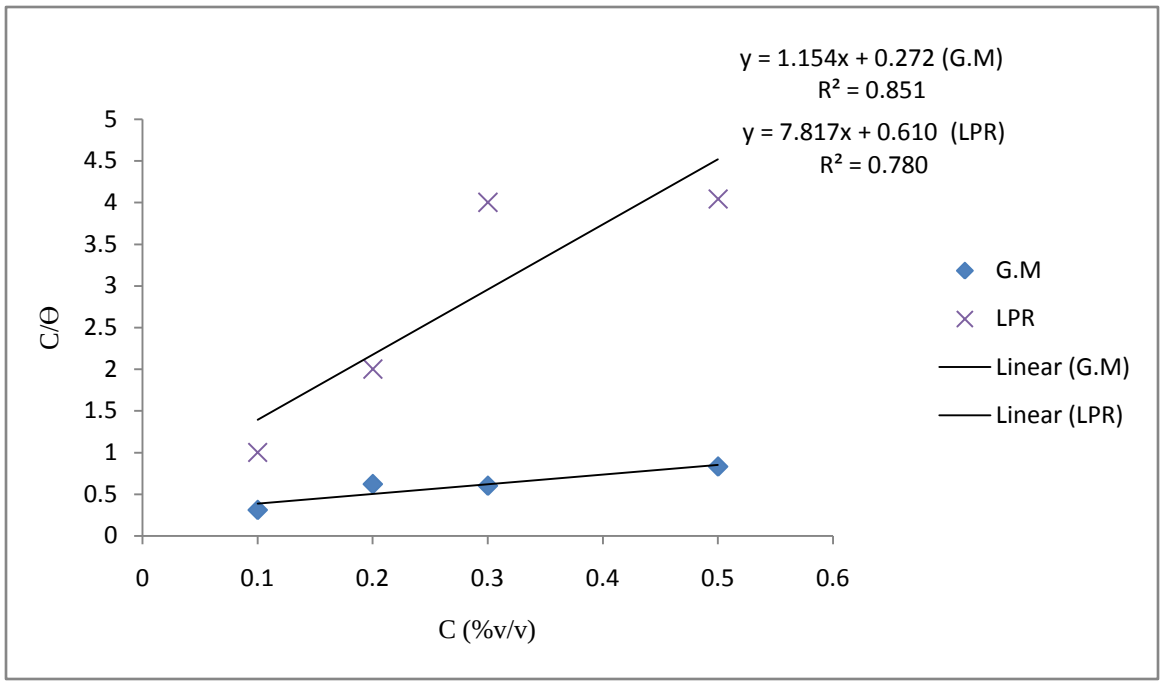

Figure 4.45: Langmuir isotherm for the adsorption of neem (*Azadirachta indica*) seed extract on the double thermally-aged Al-Si-Mg (SSM-HPDC) alloy obtained by gravimetric and potentiodynamic polarization method.

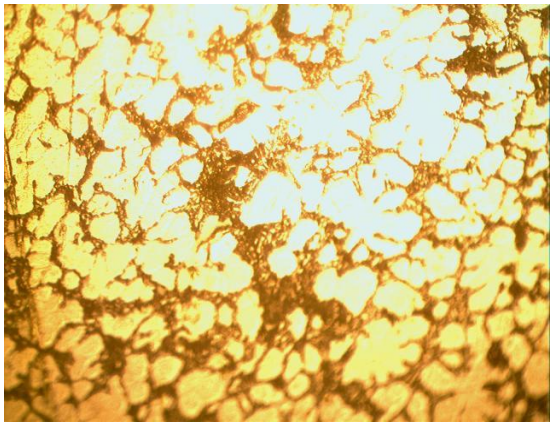

Plate 1

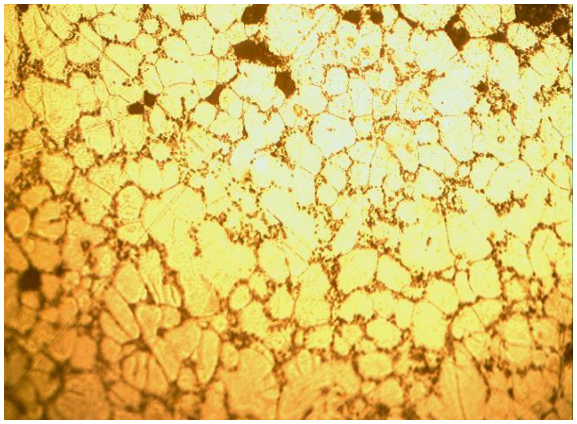

Plate 2

Plate 1: OPM microstructure of as-received Al-Si-Mg (SSM-HPDC) alloy (× 100). The structure consists of eutectic silicon and intermetallic particles in Al matrix.

Plate 2: OPM microstructure of double thermally-aged Al-Si-Mg (SSM-HPDC) alloy (× 100) showing refinement of precipitated constituent particles with enhanced grain boundaries.

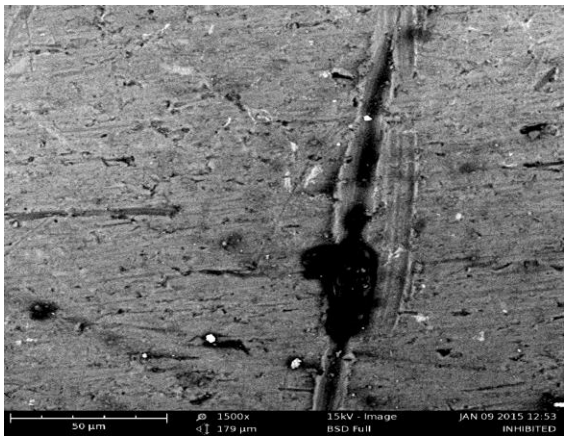

Plate 3

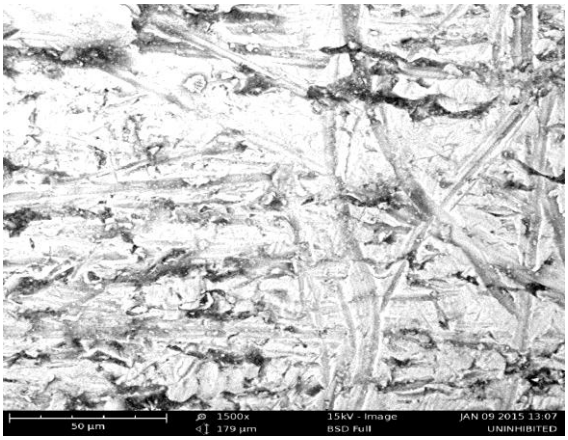

Plate 4

Plate 3: SEM micrograph of double thermally-aged Al-Si-Mg alloy in 3.5wt% NaCl-0.5%v/v guava (*Psidium guajava*) leaf extract after 3hrs.

Plate 4: SEM micrograph of uninhibited double thermally-aged Al-Si-Mg alloy in 3.5wt% NaCl after 3hrs (Control).

;

CHAPTER FIVE

5.0 DISCUSSION

5.1 Fourier Transform Infrared Spectroscopy (FTIR) Analysis

In Figure 4.1, the FTIR analysis results of guava leaf extracts confirmed the presence of OH (Phenols, Hydroxyl group), C=O (Aldehyde, Ketones, acids), C=C (Alkene), $CH(CH_3)_2$ (Alkyls), O=C-O-C (Esters), Aromatic C-H bend, C-I (Alkyl halide) compounds which shows major peaks at 3855.83, 3412.19, 2930.93, 1724.42, 1628.94, 1447.67, 1291.39,1173.72,847.74, 708.86 and 461cm^{-1} respectively (Table 4.1). The absorption due to the presence of hydroxyl group (OH), C=C stretching, C-H bend is similar to earlier observation by Sunganya *et al.*, 2007 and Bansode *et al.,* 2014. While in Figure 4.2, the FTIR analysis results of neem seed extracts confirmed the presence of OH (Phenols), C≡C (Alkynes), C=C (Alkene), $CH(CH_3)_2$ (Alkyls), O=C-O-C (Esters), C-F (Alkyl halide), C-I (Alkyl halide) which show major peaks at 3985.01, 3422.8, 3363.97, 2117.91, 1637.62, 1413.87, 1257.63, 1061.85, and 456.18cm^{-1} respectively (Table 4.2). The absorption due to presence of OH (Phenols), C≡C (Alkynes), C=C (Alkene) is also similar to that of Ameh et al., 2013.

There is no absorbance in between the region 2220-2260 cm^{-1} which indicates that no cyanide groups in both extracts. (Ragavendran *et al.*, 2011; Thangarajan *et al* 2012).

Comparing Tables 4.1 and 4.2 we observed that C=O (Aldehyde, Ketones), Aromatic C-H bend present in guava leaf extracts are not present in neem seed extracts. While the C≡C (Alkynes) present in neem seed extracts was not found in guava leaf extracts.

The adsorption of inhibitor on alloy surface is accredited to lone pair of electrons present in functional groups of neem seed and guava leaf extracts (Nnabuk *et al.*, 2011). The phenol group of the extracts donates electrons to the metal to achieve its noble state of orbits, while the alloy

would receive the electron to become more stable. This indirectly retard further redox reaction and could resist alloy from corrosion attack (El-Etre *et al*., 2005). Hence it is obvious from analysis that inhibition is due to -OHstretch, C=Ostretch, C≡Cstretch, C=Cstretch, O=C-O-Cstretch and aromatic C-H bend.

5.2 Hardness Measurement and Double Thermal Ageing Treatment

Table 4.3 presents the average hardness value for Al-Si-Mg (SSM-HPDC) alloy, the result of the age-hardened sample showed an increase in hardness value (82.8 HRF) compared to the as-receive sample (59.1 HRF) indicating an increase of 40%. The age-hardening mechanisms responsible for strengthening are based on formation of intermetallic compounds during decomposition of metastable supersaturated solid solution obtained by solution treatment and quenching (Hossain and Kurny, 2014). The improvement in hardness can be attributed to fine coherent clusters precipitates which serve as an obstacle to dislocation movement (Umaru, 2009).

5.3 Gravimetric Based-Mass Loss Measurement

5.3.1 Effect of inhibitor concentration and time on corrosion rate

Figures 4.3-4.14 showed the variation of corrosion rate of as-received and age-hardened alloy for guava leaf and neem seed extract respectively. In Figures 4.3-4.8 it was observed that there was a decrease in corrosion rate with increase in concentration of guava leaf extract from 0.1-0.5%v/v with least values obtained at 0.5%v/v. From Tables 1 and 4 it was seen that the least values of corrosion rates were both associated with 0.5%v/v, their values were 425, 265, 177, 133 and 189 mpy for as-received alloy and 332, 213, 133 and 185mpy for age-hardened alloy with time 1-5hrs respectively at 30^{o}C. In Tables 2, 3, 5 and 6 the same trend was observed with corrosion rate at 50^{o}C and 70^{o}C respectively.

Figures 4.9-4.14 showed the corrosion rate in the presence of neem seed extract for both the as-received and age-hardened alloy. The result showed a decrease in corrosion rate with variation in concentration from 0.1-0.5%v/v. In tables 7 and 10 the least values of corrosion rate were found on 0.5%v/v of neem seed with values of 456, 320,210,189 and 225mpy for as-received and 456, 228, 210, 189 and 225 mpy with time of 1-5hrs at 30^{o}C. In tables 8, 9, 11 and 12 the same trend was observed with corrosion rate at temperatures of 50^{o}C and 70^{o}C respectively. The significant decrease in corrosion rate at 0.5%v/v inhibitor concentration can be attributed to the adsorption of inhibitor molecules on alloy surface which act as physical barrier to restrict the diffusion of ions to and from the alloy surface and prevent the alloy atoms (ions) from precipitating in further anodic or cathodic reactions, hence resulting in decrease in corrosion rate (Ayeni *et al.*, 2012).

5.3.2 Effect of inhibitor concentration and time on inhibitor efficiency.

Figures 4.15-4.20 showed the variations of inhibitor efficiency with time for guava leaf extract. The values from Tables 13 and 16 showed that the maximum inhibitor efficiencies of 63.17, 61.71, 61.69, 61.67 and 28.41% for as-received and 72.10, 66.61, 67.10, 60.30, 29.92% for age-hardened with time of 1-5hrs respectively were obtained at concentration of 0.5%v/v at 30^{o}C. Tables 14,15,17,18 followed the same trend with temperatures of 50^{o}C and 70^{o}C respectively.

Figures 4.21-4.25 showed the variation of inhibitor efficiency with time for neem seed extract. The maximum inhibitor efficiency was obtained at concentration of 0.5%v/v. From Tables 19 and 22 their values are 60.49, 53.76, 54.55, 45.53, 14.77% for as-received and 60.49, 64.26, 54.55, 43.58 and 14.77% for age-hardened with time 1-5hrs respectively at a temperature of 30^{o}C. Table 20, 21, 23 and 24 followed the same trend with temperatures of 50^{o}C and70^{o}C respectively.

The inhibition behavior of the neem seed and guava leaf extracts can be attributed to the presence of phenolic O-H, aromatic C=C, C=O, O=C-O-C, C≡C, as characterized by IR spectroscopy (Rajendran *et al.,* 2009)

5.3.3 Effect of temperature on inhibitor efficiency

Figures 4.26-4.2 showed the variation of inhibitor efficiency with temperature for guava leaf and neem seed extract respectively. It is evident from these figures that inhibition efficiency decreases with increasing temperature. The decrease in inhibitor efficiency with increase in temperature can be attributed to the fact that at a lower temperature the inhibitor molecules adsorbed onto the alloy surface, while at higher temperature increased rate of dissolution process takes place along with partial desorption of inhibitor molecules from the alloy surface as a result of dissociation of constituents of inhibiting substance (Olasehinde *et al*., 2013; Asuke *et al*., 2010).

5.3.4 Thermodynamic consideration

Thermodynamic model could be used to explain the corrosion inhibition of the inhibitors. Thus, The free energy of adsorption (ΔG_{ads}) and heat of adsorption (Q_{ads}) were calculated using equations 3.6 and 3.7 respectively. The values of ΔG_{ads} obtained are presented in Tables 29-34. The negative values of ΔG_{ads} ensure the spontaneity of the adsorption process and stability of the adsorbed layer on the alloy surface. Generally, the values of ΔG_{ads} around 20kJ/mol or lower are consistent with physiosorption, while those around 40kJ/mol or higher involve chemisorptions (Olasehinde *et al.,* 2013). As shown in the Tables, results obtained indicate that the values of ΔG_{ads} are all negative in all cases and less than 20kJ/mol. This is consistent with literature survey and therefore authenticates physical adsorption. (Ebenso *et al.,* 2008; Quraishi *et al.,* 2009).

Tables 35 and 36 showed that Q_{ads} are of the negative indicating that the adsorption of the extracts is exothermic (Ebenso *et al.*, 2008). The obtained values of heat of adsorption (Q_{ads}) were more negative than -10kJ/mol for both the as-received and age-hardened samples, suggesting that the adsorption is probably chemical.

5.3.5 Kinetic consideration

The activation energies of the inhibited system were higher than the uninhibited system. This indicates that the energy barrier for corrosion reaction increased in the presence of the extract (Quraishi *et al.*, 2009). It also indicates a change in the rate determining step brought about by the presence of various chemical components of the inhibitors (Asuke *et al.*, 2010). The increase in activation energy in the presence of extract denotes physical adsorption while the reverse is attributed to chemical adsorption (Olusegun *et al.*, 2013).

In Table 37, the values of activation energy (E_a) for the as-received and age-hardened samples were found to be - 14.30, -20.71,-20.69, -20.69, -19.88 and -13.61, -24.09, -20.69, -18.27, -10.76 in free solution for 1-5 hrs respectively. But in the presence of guava leaf extract they increased to -32.69, -22.56, -32.08, -30.94, -16.33 and -39.12, -13.63, -38.40, -36.22 and -14.93 for 1-5hrs respectively. Table 38 follows the same trend in the presence of neem seed extracts with values of -28.76, -31.57, -32.24, -21.62, -14.63 and -28.76, -25.88, -32.22, -21.62 and -14.64 at 0.5% v/v respectively for 1-5 hrs.

It has been reported that when the values of E_a >80 KJ/mol indicates chemical adsorption whereas E_a <80 kJ/mol infers physical adsorption (Ismail et al., 2011; Adeyemi and Olubomehin, 2010). On the bases of the experimentally determined activation energy values of E_a <80 KJ/mol in this study, we propose that the extracts are physically adsorbed on the coupons.

5.4 Potentiodynamic Polarization Studies

In Figures 4.35-4.38, the anodic and cathodic polarization curves for the as-received and age-hardened Al-Si-Mg (SSM-HPDC) alloy in the presence of guava leaf and neem seed respectively are shown.

Considering the corrosion condition of both the as-received and aged-hardened Al-Si-Mg (SSM-HPDC) alloy in 3.5wt%NaCl in the presence of guava leaf and neem seed extracts. It can be seen that current density (j_{Corr}) decreased with increased in inhibitor concentration without causing significant change in corrosion potential (E_{Corr}) suggesting that these extracts are mixed types inhibitors within the studied environment(Quraishi *et al.*,2009).

In Table 39, the corrosion potential of the as-received alloy in blank solution was -1.3069 V but at various concentration of guava leaf extract, the corrosion potential values shifted towards the anodic side (-1.3006 V,-1.2663 V,-1.3033 V,-0.6180 V) indicating that the extract affects the anodic reaction predominantly. The same trend was observed in Table 40 for the age-hardened alloy in the presence and absence of guava leaf extract. In Table 41 the corrosion potential of the as-received alloy in blank solution was -0.83089 V but at various concentration of neem seed extracts, the corrosion potential values shifted towards the cathode side (-0.88954 V,-0.84847 V,-0.93878 V,-0.903 V) indicating that neem seed extract controls the cathodic reaction predominantly. In Table 42 the same trend was observed for the age-hardened alloy in the presence of neem seed extract at concentration of 0.2% v/v-0.5% v/v.

The linear polarization values (Tables 39 and 40) showed that addition of guava leaf extract resulted in an increase in polarization resistance value (R_p) for the as-received alloy from 118.51Ω (uninhibited) to 1244.7Ω (inhibited) condition with an IE of 90.48% while for the age-hardened, it increased from 195.58Ω (uninhibited) to 6736.6Ω (inhibited) condition with an IE of

97.10%. The linear polarization resistance (LPR) values from Table 41 and 42 showed that addition on neem seed extract resulted to a decrease in corrosion current density (j_{Corr}) for the as-received alloy from 1.74E-09 (uninhibited) to 2.28E-10 (inhibited) with an IE of 86.90% while the age-hardened alloy decrease from 5.15E-09 (uninhibited) to 9.95E-10 (inhibited) with an IE of 80.68%. The increase in R_p and corresponding decrease in j_{Corr} generally suggested an improvement in corrosion resistance of the alloy (as-received and age-hardened condition) in the presence of inhibitors. This shows that the alloy in both the as-received and age-hardened condition was protected within the immersion time considered (Popoola *et al.,* 2012).

5.4.1 Inhibition efficiency and adsorption behaviour

The computed percentage inhibition efficiency (% IE) of the as-received and age-hardened Al-Si-Mg-3.5%wt NaCl solution with variation in concentration of *Psidium guajava* and *Azadirachta indica* respectively using the equation reported in chapter three (Wan *et al.*, 2012).

The variation in the % IE using the gravimetric (G.M), potentiodynamic polarization-corrosion rate (PP-CR), potentiodynamic polarization-corrosion density (PP-J_{corr}), and linear polarization resistance (LPR) are presented in Figures 4.39-4.42 for *Psidium guajava* and *Azadirachta indica*. The results show that addition of the extracts increase the IE with an increase in inhibitor concentrations. This may be attributed to the fact that, as the extract addition increases, the surface area covered by the inhibitor increased hence higher IE was achieved (Popoola *et al.,* 2012). Guava (*Psidium guajava*) leaf and Neem (*Azadirachta indica*) seed extracts can be said to exhibit a mixed-type corrosion inhibition because of the simultaneous change in the anodic and cathodic region during the potentiodynamic polarization measurement. This is in agreement with previous studies (Popoola *et al.,* 2012; Abdulwahab *et al.,* 2012). The adsorption mechanism of the extracts in Figure 4.43-4.45 showed that the relationship between C/θ and C is linear for

both extracts in simulated seawater environment. Since the linear regression coefficient/or correction factors (R^2) close to unity: G.M (0.992, 0.851), PP (0.862, 0.780) the adsorption behavior is assumed to have obeyed Langmuir adsorption isotherms. In this case, the adsorption of inhibitor molecules belongs to a monolayer adsorption, assuming that lateral interactions between the inhibitor molecules are ignored.

5.5 Microstructure and Surface Morphology Analyses

From microstructure analysis, it can be seen that the microstructure of the age-hardened alloy (Plate II) has finer grains and enhanced grain boundaries than the as-received alloy (Plate I). This is based on the fact that there was an increase in volume of the precipitated intermetallic compounds during ageing process and also refinement of the precipitated constituent particles (Hossain *et al*., 2014).

The SEM micrographs of uninhibited Al-Si-Mg sample in 3.5%NaCl solution (Plate III) indicate severe surface degradation and pit formation compared to the inhibited sample (Plate IV) .This indicates that the guava leaf extract was able to exhibit some degrees of inhibition which retarded the corrosion rate of the Al-Si-Mg alloy. This occurrence has been attributed to formation of thin oxides on the alloy surface which interfere with the reaction sites, thus impede the formation of pits and their growths (Abdulwahab *et al.,* 2012).

CHAPTER SIX

6.0 SUMMARY, CONCLUSIONS AND RECOMMENDATIONS

6.1 Summary

Gravimetric-based mass loss and potentiodynamic polarization techniques of corrosion control have been employed to study the effect of neem seed and guava leaf extracts on the corrosion be inhibition of high pressure die cast (SSM-HPDC) Al-Si-Mg alloy in the as-received and age-hardened conditions. Also the hardness measurement of the alloy in both conditions was done.

From the experimental results obtained for the gravimetric-based mass loss and potentiodynamic polarization method, it was clarified that neem seed and guava leaf extracts decrease the corrosion rates of the alloy at various concentrations with maximum inhibition efficiency obtained at 0.5%v/v. The results of hardness measurement show an increase in hardness value of the alloy as a result of the double thermal ageing treatment.

6.2 Conclusions

The study of the corrosion inhibition of double thermally aged high pressure die cast (SSM-HPDC) Al-Si-Mg alloy with neem seed and guava leaf extracts has led to the following conclusions:

1. The heat treatment improved the hardness of the alloy by 40%.
2. The result of gravimetric based-mass loss and potentiodynamic polarization technique indicates that neem seed and guava leaf extracts improved the corrosion resistance of the alloy.
3. The adsorption of the extracts onto the surface of both the as-received and age-hardened alloy was exothermic, spontaneous and favours the physical adsorption.
4. Potentiodynamic polarization measurements show that the extracts are mixed- type inhibitors but predominant to the anodic and cathodic branches for guava leaf and neem seed extracts respectively.

6.3 Recommendations

1. Effort should be made to identify more natural plants which could be used as corrosion inhibitors for Al-Si-Mg alloy.
2. Electrochemical impedance spectroscopy (EIS) studies of the action of the inhibitors on the as-received and double thermally aged Al- Si-Mg (SSM-HPDC) alloy in other media is recommended
3. The effect of step quenching and ageing treatment on Al-Si-Mg alloy in neem seed and guava leaf extracts is recommended.

REFERENCES

Abdulwahab, M., Madugu I.A., Yaro S.A., Popoola A.P.I (2011). Degradation Behaviour of High Chromium Sodium-Modified A356.0 type Al-Si-Mg alloy in Simulated Seawater

Environment. Journal of Minerals Characterization & Engineering Vol 10 No 6 PP 535-551.

Abdulwahab, M. (2007). Effect of Chromium and Manganese on the Mechanical properties and Corrosion Resistance of Al-Si-Fe Alloy in 0.5M HCl Solution. An M.Sc Thesis, Department of Metallurgical and Materials Engineering, Ahmadu Bello University, Zaria, Nigeria.PP 1-19.

Abdulwahab, M. (2011). The Effect of Multiple-Step Thermal Ageing Treatment on the Hardness and corrosion characteristics of A356.0 Type Al-Si-Mg Alloy. A PhD Dissertation, department of Metallurgical & Material Engineering, Ahmadu Bello University, Zaria, Nigeria.PP 7-13.

Abdulwahab, M., Madugu, I.A., Yaro, S.A., Hassan, S.B and Papola, A.P.I (2011). Effect of Multiple-Step thermal ageing treatment on the hardness characteristics of A356.0 type Al-Si-Mg alloy. Materials and Design, 32, 1159-1165.

Adams, M.S (2012).Inhibition and alloying as means of controlling corrosion of Al-Cu-Ni alloy. An M.sc Thesis Department of Metallurgical and Materials Engineering, Ahmadu Bello University Zaria, Nigeria.PP 6-7.

Ajanaku, K.O., Aladesuyi, O., Ajanaku, C.O., Ajanaku, C.O., Adedapo, E.A., Akinsiku, A.A., Sodiya, F.E., (2015). Adsorption Properties of Azadirachta indica extract on the corrosion of Aluminium in 1.85M Hydrochloric acid. Journal of the International Association of Advanced Technology and Science. Vol 16, PP 5563-1682.

Ameh , A.O., Muhammad, J.A and Audu H.G (2013).Synthesis and characterization of antiseptic soap from neem oil and shea butter oil. African journal of Biotechnology.Vol 12(29), pp 4656-4662.

Amitha, R.B.E and Bharati, B.J.B. (2012). Green inhibitors for corrosion protection of metal and alloys. An over view. International Journals of Corrosion, doi:10.1155/2012/380217.

Andretta. F., Terryn, H., and Wit, J (2004). Corrosion Behaviour of Different Tempers of AA7075 Aluminum alloys. Electrochimica Acta, 49, 2851-2862.

Asuke, F., Yaro, S.A., Oloche, O.B and Aigbodion, V.S (2009). Potential of palm exudate (Palmwine) as corrosion inhibitor for Al-Si alloy in caustic soda solution. Journal of Metallurgy and Materials Engineering, Vol 4, No 2, PP48-54.

Atkinson, H.V (2005).Modeling the semi-solid processing of metallic alloys. Progress in Materials science, 50(3): 341-412.

Awolu, O.O., Obafaye, R.O and Ayodele, B.S (2013).Optimization of solvent extraction of oil from neem (Azadirachta indica) and its characterizations. Journal of Scientific Research and Reports. 2(1):304-314.

Ayeni, F.A., Madugu, I.A., Sukop,P., Ihom A.P., Alabi, O.O., Okara ,R., Abdulwahab.,M (2012). Effect of Aqueous Extracts on Bitter leaf powder on corrosion inhibition of Al-Si alloy in0.5M caustic soda solution. Journal of Minerals and Materials characterization and Engineering 11,667-670.

Bangyikhan, K (2005). Effect of oxide film, Fe-rich phase, porosity and their interactions on tensile properties of cast Al-Si-Mg alloys. Doctoral dissertation Thesis, Faculty of Engineering, University of Birmingham, Birmingham.PP-1-3.

Bansode, D. S and Chavan M. D (2014). Screening of Guava (Psidium guajava) For Effective Phytomedicines and study on its Antimicrobial effect against Selected Enteric Pathogens. International Journal of Advances in Pharmacy, Biology and Chemistry. Vol. 3(3), PP 802-806.

Birol, Y (2009). Response to Artificial Ageing of Dendritic and Globular Al-7Si-Mg alloys. Journal of Alloys and compounds, 484, PP 164-167.

Cabott, P.L., Centellas, J.A., Garrdo, J.A., Perez, Z.E and Vidal, H (1991). Electrochemical study of aluminium corrosion acid chloride solutions. Electrochinica Acta, vol 36, PP 179-187.

Caceras, C.H., Djurdjevic, M.B., Stockwell, T.J and Sokolowski (1999).Effect of Cu content on the Level of Microporosity in Al-Si-Cu-Mg casting Alloys. Scripta Mater.40 (5), PP 631-637.

Dauda, K.T., Atasie, V.N and Adetimilehin ,A.A (2013). Kinetics of the inhibitory Effects of Ethanolic Extract of *Vernonia amydgalina* on the corrosion of Aluminium in 1.0M HCl. Chemistry Journal, vol.03 (3) PP 86-89.

Djurdjevil, M.B. (2001). Quantification of Cu Enriched phases in synthetic 3xx Aluminum Alloys. International Journal of Cast Metals Research 12, 1-12.

Ebenso, E.E., Eddy, N.O and Odiongenyi, A.O (2008). Corrosion inhibitive properties and adsorption behavior of ethanol extract of pipper guinensis as a green corrosion inhibitor for mild steel in H_2SO_4 . African journal of pure and Applied chemistry vol. 2(11) PP 107-115.

El-Etre, A.Y., Abdallah, M and El-Tantawy (2005). Corrosion inhibition of some metals using lawsonia extract. Corrosion Science 47, 385-395.

Escalera-Lozano, R., Pench-Canul ,M.I., Montoya-Davila, M and Uribe-Salas, A (2010). The Role of Mg_2Si in the corrosion Behaviour of Al-Si-Mg Alloys for pressureless infiltration. The open corrosion journal, vol 8, PP 73-79.

Ernst, F (2006). Precipitation Hardening of Al-Si-Mg Alloy. Materials Laboratory III, Spring Semester Lecture Note EMSE-290.

Fagbohun, I.R., Adekeye, T.J, and Akinbola, J.P (2013). Effect of aqueous extract of leaves and bark of guava (*Psidium guajava)* on Fugi Microsporum gypseum and Trichophyton mentagrophytes, and bacteria staphylococcus aureus and staphylococcus epidermidis. Advancement in Medicinal Plant Research vol 1(2), PP 45-48.

Fontana, M.G, Greene N.D (1987). Corrosion Engineering Mc Grawc-Hill book Company. New York, PP 8-29.

Flemings, M.C and Martinez R.A (2006).Principles of microstructural formation in semi-solid metal processing. Solid State Phenomena. 116/117:1-8

Fracasso Federico (2010). Influence of quench rate on the hardness obtained after artificial ageing of an Al-Si-Mg. Doctoral dissertation, Jonkoping Institute of Technology, Tekniska Hogskolan.PP 5-13.

Govender G. and Moller H (2008). Evaluation of surface chemical segregation of semi-solid cast Aluminium alloy A356.Solid State Phenomena. Vols 141/143:433-438.

Hagerman, A.E. (1988) Extraction of Tannis from Fresh and preserved leaves. Journal of Chemical Ecology 14:453-461.

Haizhi, Y. (2003).An overview of the Development of Al-Si alloy based material for Engine Applications. Journal of Materials Engineering and performance. Volume 12(3), 288-297.

Hongwei, S., Han, E.H., Lamaka, S.V., Zheludkevich, M.L and Liu, F (2014). Cerium cinnamate as an environmentally benign inhibitor pigment for epoxy coating on AA2024-T3. Progress in organic coatings, vol. 77, PP 765-773.

Howida, A.F., Tarek, M.A and Mohamed, S.E. (2014). Novel plant extracts as green inhibitors for 7075-T6 aluminium alloy in an aqueous medium. International Journal of Electrochemical Science, vol. 9, PP 1565-1582.

Hulya, K. and Cevdet, M.(2007). Age-hardening behavior of powder metallurgy AA2014 alloy. Materials and Design 28, 982-986.

Johnson, .S., Morgan, E.D and Paris, C.N (1996).Development of the Major Triterpenoids and oil in the fruit and seeds of neem (*Azadirachta indica*). Journal of Annal Botany.78: 383-388.

Khomamizadeh, F. and Ghasemi A. (2004). Evaluation of quality index of A356 aluminum alloy by Microstructural Analysis. Scientia Iranica 11(4) 386-391.

Kuznetsov, Y.I (2004). Physico-Chemical aspect of metal corrosion inhibition in aqueous solutions. Russian chemical reviews 73(1):75-87.

Liauw, M.Y., Natan, F.A., Widiyanti, P., Ikarasari, .D., Indraswati, N and soetaredjo, F.E(2008).Extraction of oil quality, kinetics and thermodynamic. ARPN Journal of Engineering and Applied Chemistry. 3(3): 49-54.

Loto, C.A (1998). The effect of Bitter leaf extracts on the corrosion of Mild steel in 0.5M HCl and H_2SO_4 solutions. Nigeria Corrosion Journal International vol 1, PP19-20.

Loto, C.A, Loto R.T and Popoola (2011).Effect of neem leaf (*Azadirachita indica*) extract on the corrosion inhibition of Mild steel in dilute acids. International journal of physical sciences vol. 6(9) PP 2249-2257.

Madugu, I.A and Abdulwahab, M (2007). The Mechanical properties of As-cast Al-Si-Fe-Mn alloy. Nigerian journal of research and production, Vol 10, No2, PP72-79.

Maria, Y.L., Natan, F.A., Ikasari, D, Indraswati, N., Soetaredjo, F.E (2008). Extraction of Neem oil (*Azadirachta indica*) using N-Hexane and ethanol studies of oil Quality, kinetic and thermodynamic. Asian Research Publishing net work. Vol 3, No 3 PP49-53.

Micheal, J. Kroes., James, R. Rardon (1993): Aircraft Basic Science, 7th Edition Published by Glencoe/Mc Graw-Hill, New York.

Mohammed, R.A., Abdulwahab, M., Madugu, I.A., Gaminana, J.O., Asuke F (2013).Inhibitive effect by natural *Cyperus esculentus* oil on the corrosion of A356.0 type Al-Si-Mg alloy in simulated seawater environment. J.Mater.Environ.Sci. 4(1) PP93-98.

Moller, H., Curle, U.A, Masuka, E.P (2010). Characterization of surface liquid segregation in SSM-HPDC aluminium alloy 7075, 2024, 6082 and A201. Transaction of Non ferrous Metal Society of China. 20:847-851.

Moller H and Masuka E.P (2009) .The Influence of liquid segregation on the pitting corrosion behavior of semi-solid metal high pressure die cast alloy F357.The Open Corrosion Journal. Volume 2, 216-220.

Moller, H., Stumpf, W.E., Pistorius, P.C(2010).Influence of elevated Fe,Ni and Cr levels on the tensile properties of SSM-HPDC Al-Si-Mg alloy F357.Transaction of Nonferrous Metals Society of China, 20:842-846.

Nnabuk, O.E., Paul, A., Casmir, E.G., Eno, E.E (2011). GCMS Studies On Anogessus Leocarpus (Al) Gum and Their Corrosion Inhibition Potential for Mild Steel in 0.1 M HCl. International Journal of Electrochemical Science, 6: 5815-5829.

Nnanna, L.A., Obasi, V.O., Nwadiuku, O.C., Mejeh,K.J., Ekekwe,N.D, Udensi (2012).Inhibition by *Newbouldia leavis* leaf Extract of the corrosion of Aluminium in HCl and H_2SO_4 solutions. Archives of Applied science Research 4(1): 207-217.

Nwinyi, O.C., Chinedu, N.S., Ajani, O.O (2008). Evaluation of antibacterial activity of *Psidium guajava and Gongronema latifolium*. J Med Plants Res, 2(8):189-192.

Noyel, S. V., Rohith, P., Manivannan, R., (2015). *Psidium Guajava* Leaf Extract as Green Corrosion Inhibitor for Mild steel in Phosphoric Acid. International Journal of Electrochemical Science. Vol 10. PP 2220-2238.

Olusegun, S. J., Adeiza, B.A ., Ikeke, K.I. and Bodunrin, M.O (2013). *Jatropha curcas* leaves Extract as corrosion inhibitor for Mild steel in 1M Hydrochloric Acid. Journal of Emerging Trends in Engineering and Applied sciences (JETEAS) 4(1):138-143.

Omotoyinbo, J.A., Oluruntoba, D.T., Olusegun, S.J (2013). Corrosion inhibition of Pulverised *Jatropha curcas* leaves on Medium Carbon Steel in 0.5M H_2SO_4 and NaCl Environments. International journal of Science and Technology volume 2 No.7, PP 510-514.

Peter, C. Okafor., Eno, E. Ebonso., Udofot, J. Ekpe (2010). Azadirachta indica Extract as Corrosion Inhibitor for Mild steel in Acid Medium. International Journal of Electrochemical Science. 5: 978-993.

Popoola, A.P.I., Fayomi, O.S.I., Abdulwahab, M. (2012). Degradation Behaviour of Aluminum in 2M HCl/HNO_3 in the presence of *Arachis hypogeae* Natural oil. International Journal of Electrochemical Science, Vol 7, PP 5817-5827

Quraishi, M.A., Dileep, K. Y and Ishtiaque, A. (2009).Green Approach to corrosion inhibition by Black pepper Extract in Hydrochloric Acid Solution. The open journal, 2, 56-60.

Ragavendran, P., Sophia, D., Arul, C and Gopalarkrishnan, V. (2011). Functional group analysis of various extracts of *Aerva lanata* by FTIR spectrum. Phamacologyonline 1:358-364.

Ragasa, C.V., Nacpil Z.D., Natividad G.M., Tada M., Coll J.C., RideoutJ.A (1997). Tetranortriterpenoids from *Azadirachta indica*. Journal of Phytochemistry 46:555-558.

Rawajfeh, A.E. and Qawabah, S.M.A. (2009). Investigation of copper addition on the mechanical properties and corrosion resistance of commercially pure aluminum. Emirates Journal for Engineering Research Vol 14, No.1, PP 47-52.

Reda,Y., Abdel-Karim., Elmahallawi (2008). Improvement in mechanical and stress corrosion cracking properties in Al-alloy 7075 via retrogression and reagings. Materials Science and Engineering A485, 468-475.

Rekha, N.N., Shashi, S., Sharma, I.K., Verma, P.S and Alka, S. (2010). Inhibitory Efficacy of *Piper nigrum linn* extract on corrosion of AA1100 IN HCl. RASAYAN J.Chem. Vol.3, No.4, PP 783-795.

Roy, N, Samuel, A.M and Samuel, F.H (1996). Porosity formation in Al-9wt%Si-3wt%Cu alloy system: Metallurgraphic observations.Metall. Mater. Trans. 27A, PP 415-429.

Sheng-Long, L., Yin-chun, C., Cheng-Kuo, L., Ah-Hung, T. (2012). Effect of Strontium and Heat treatment on the wear corrosion property of Al-7Si-0.3Mg alloy. Materials chemistry and physics 135,503-509.

Stephen, G.Y., Sylvester, O. A., Tersoo G. T., Ungwanen, J. A and Joseph A. G. (2014).Thermodynamic, Kinetic and Adsorptive parameters of corrosion inhibition of Aluminium using *sorghum bicolar* leaf extract in H_2SO_4.International Journal of Advanced Research in Chemical Science (IJARCS).Volume 1 PP 38-46.

Suganya, T., Fumio, I and Siriporn, O. (2007). Antioxidant Active Principles Isolated from Psidium guajava Grown in Thailand. Scientia Pharmaceutica (Sci. Pharm). vol 75, PP 179-193.

Tahamtan,S and Boostani, A.F (2009). Qualitative analysis of pitting corrosion behavior of thixoformed A356 alloy in chloride medium using electrochemical techniques. Mater Des 30:2483-2489.

Tash, M., Samuel, F.H., Mucciardi,.F & Doty, H. W (2007). Effect of Metallurgical Parameters on the hardness and microstructural characterization of as-cast and heat-treated 356 and 319 aluminum alloys. Materials science and Engineering A 443, 155-201.

Tavitas,M. F.J., Gruzleski, J.E., Samuel, F.H., Valtierra, S and Doty, H.W. (2008). Effect of Mg and Sr-modification on the mechanical properties of 319-type aluminum cast alloys subjected to artificial aging. Materials Science and Engineering A 450, 356 – 364.

Thangarajan, S., Paramasivam, R., Chinthamony A., Palanisamy C and Velliyur K.G (2012). Element and functional group analysis of *lchnocarpus frutescens*. International journal of pharmacy and pharmaceutical sciences. Vol 4(5) PP 343-345.

Toliwal, S.D., Kalpesh, J., Pavagadhi, T (2010).Inhibition of corrosion of Mild steel in HCl solutions by Schiff Base Derived from Non Traditional oil. Journal of Applied chemical research 12:24-36.

Umaru, B.O. (2013).Effect of Pre-ageing condition on the Hardness and Corrosion characteristics of Double-Thermally-Aged Al-Si-Mg alloy. An Msc Thesis, Department of Metallurgical and Materials Engineering, Ahmadu Bello University, Zaria, Nigeria.PP 6, 9& 22.

Wan Nik, W.B., Sulaiman, O., Ayob, A.F., Ahmad, M.F., Rahman, M.M (2012). Marine Extracts as Corrosion Inhibitor for Aluminium in Seawater Applications. International Journal of Engineering Research and Applications . vol.1. PP 723-728.

APPENDIX

Table 1: Corrosion rate of as-received Al-Si-Mg (SSM-HPDC) alloy in 3.5wt% NaCl using guava (*Psidium guajava*) leaf extract as inhibitor at 30^{o}C.

Concentration	Corrosion rate (mpyx10^{2})				
(%v/v)	1hr	2hr	3hr	4hr	5hr
0.0	11.54	6.92	4.62	3.47	2.64
0.1	9.14	4.62	3.32	2.27	2.25
0.2	8.86	4.62	3.20	2.27	2.25
0.3	4.56	3.20	2.52	1.89	2.01
0.5	4.25	2.65	1.77	1.33	1.89

Table 2: Corrosion rate of as-received Al-Si-Mg (SSM-HPDC) alloy in 3.5wt% NaCl using guava (*Psidium guajava*) leaf extract as inhibitor at 50^{o}C.

Concentration	Corrosion rate (mpyx10^{2})				
(%v/v)	1hr	2hr	3hr	4hr	5hr
0.0	16.28	11.39	7.60	5.70	4.26
0.1	13.67	9.11	6.08	4.68	3.74
0.2	13.67	6.84	4.56	4.68	3.20
0.3	9.11	6.84	4.56	3.18	3.20
0.5	9.11	4.56	3.83	2.80	2.80

Table 3: Corrosion of as-received Al-Si-Mg (SSM-HPDC) alloy in 3.5wt% NaCl using guava (*Psidium guajava*) leaf extract as inhibitor at 70^{o}C.

Concentration	Corrosion rate (mpyx10^{2})				
(%v/v)	1hr	2hr	3hr	4hr	5hr
0.0	18.79	13.67	9.11	6.84	5.47
0.1	16.28	11.39	7.60	5.70	4.56
0.2	16.28	9.11	6.08	5.70	4.56
0.3	13.67	9.11	6.08	5.70	4.56
0.5	13.67	9.11	5.70	4.56	4.56

Table 4: Corrosion rate of double thermally aged Al-Si-Mg (SSM-HPDC) alloy in 3.5wt%NaCl using guava (*Psidium guajava*) leaf extract at 30^{o}C.

Concentration	Corrosion rate (mpyx10^{2})				
(%v/v)	1hr	2hr	3hr	4hr	5hr
0.0	11.54	6.38	4.62	3.35	2.64
0.1	9.24	4.62	3.20	2.27	2.25
0.2	8.86	3.20	3.04	1.86	2.01
0.3	4.25	2.65	2.52	1.33	2.01
0.5	3.32	2.13	1.52	1.33	1.85

Table 5: Corrosion rate of double thermally aged Al-Si-Mg (SSM-HPDC) alloy in 3.5wt%NaCl using guava (*Psidium guajava*) leaf extract at 50^{o}C.

Concentration	Corrosion rate (mpyx10^{2})				
(%v/v)	1hr	2hr	3hr	4hr	5hr
0.0	16.01	11.39	7.60	5.20	3.42
0.1	13.67	9.11	6.08	4.42S	3.20
0.2	9.11	6.84	4.56	3.40	3.20
0.3	9.11	4.56	3.83	3.18	3.20
0.5	8.51	4.56	3.83	3.18	2.65

Table 6: Corrosion rate of double thermally aged Al-Si-Mg (SSM-HPDC) alloy in 3.5wt%NaCl using guava (*Psidium guajava*) leaf extract at 70^{o}C.

Concentration	Corrosion rate (mpyx10^{2})				
(%v/v)	1hr	2hr	3hr	4hr	5hr
0.0	20.58	11.39	9.11	6.18	5.47
0.1	18.46	9.11	7.60	5.70	4.56
0.2	13.67	9.11	6.08	5.70	4.56
0.3	12.35	8.56	5.50	4.56	4.56
0.5	12.35	8.23	5.50	4.56	4.40

Table 7: Corrosion rate of as-received Al-Si-Mg (SSM-HPDC) alloy in 3.5wt%NaCl using neem (*Azadirachta indica*) seed extract as inhibitor at 30^{o}C

Concentration	Corrosion rate (mpyx10^{2})				
(%v/v)	1hr	2hr	3hr	4hr	5hr
0.0	11.54	6.92	4.62	3.47	2.64
0.1	9.14	4.62	3.20	2.27	2.25
0.2	9.14	4.62	3.20	2.27	2.25
0.3	8.86	3.20	2.52	2.27	2.25
0.5	4.56	3.20	2.10	1.89	2.25

Table 8: Corrosion rate of as-received Al-Si-Mg (SSM-HPDC) alloy in 3.5%wtNaCl using neem (*Azadirachta indica*) seed extract as inhibitor at 50^{o}C.

Concentration	Corrosion rate (mpyx10^{2})				
(%v/v)	1hr	2hr	3hr	4hr	5hr
0.0	16.28	11.39	7.60	5.70	4.26
0.1	15.67	9.11	6.08	4.68	3.74
0.2	13.28	7.84	6.08	4.68	3.74
0.3	13.28	6.84	4.56	3.18	3.74
0.5	9.11	6.84	4.56	3.18	3.20

Table 9: Corrosion rate of as-received Al-Si-Mg (SSM-HPDC) alloy in 3.5%wtNaCl using neem (*Azadirachta indica*) seed extract as inhibitor at 70^{o}C.

Concentration	Corrosion rate (mpyx10^{2})				
(%v/v)	1hr	2hr	3hr	4hr	5hr
0.0	22.79	13.67	9.11	6.84	5.47
0.1	18.79	11.39	6.08	5.70	4.56
0.2	18.24	11.39	6.08	5.70	4.56
0.3	18.24	9.11	6.08	4.56	4.56
0.5	13.67	9.11	5.50	4.56	4.56

Table 10: Corrosion rate of double thermally aged Al-Si-Mg (SSM-HPDC) alloy in 3.5wt%NaCl using neem (*Azadirachta indica*) seed extract as inhibitor at 30^{o}C.

Concentration	Corrosion rate (mpyx10^{2})				
(%v/v)	1hr	2hr	3hr	4hr	5hr
0.0	11.54	6.38	4.62	3.35	2.64
0.1	9.24	4.62	3.20	2.27	2.25
0.2	8.23	4.62	3.20	2.27	2.25
0.3	8.23	3.20	2.52	1.89	2.25
0.5	4.56	2.28	2.10	1.89	2.25

Table 11: Corrosion rate of double thermally aged Al-Si-Mg (SSM-HPDC) alloy in 3.5wt%NaCl using neem (*Azadirachta indica*) seed extract as inhibitor at 50^{o}C.

Concentration	Corrosion rate (mpyx10^{2})				
(%v/v)	1hr	2hr	3hr	4hr	5hr
0.0	16.01	11.39	7.60	5.20	3.42
0.1	13.67	10.29	6.08	4.68	3.20
0.2	13.67	10.29	4.56	3.42	3.20
0.3	9.11	9.11	4.56	3.42	3.20
0.5	9.11	4.25	4.56	3.18	3.20

Table 12: Corrosion rate of double thermally aged Al-Si-Mg (SSM-HPDC) alloy in 3.5wt%NaCl using neem (*Azadirachta indica*) seed extract as inhibitor at 70^{o}C.

Concentration	Corrosion rate (mpyx10^{2})				
(%v/v)	1hr	2hr	3hr	4hr	5hr
0.0	18.46	11.39	9.11	6.18	5.47
0.1	16.24	10.29	7.60	5.70	4.56
0.2	13.67	9.23	7.60	5.70	4.56
0.3	12.35	9.23	6.08	5.70	4.56
0.5	12.35	8.86	6.08	4.56	4.56

Table 13: Inhibition efficiency of as-received Al-Si-Mg (SSM-HPDC) alloy in 3.5wt% NaCl using guava (*Psidium guajava*) leaf extract as inhibitor at 30^{o}C.

Concentration	Inhibition efficiency (%)				
(%v/v)	1hr	2hr	3hr	4hr	5hr
0.0	-	-	-	-	-
0.1	20.80	33.24	28.14	34.58	14.77
0.2	23.22	33.24	30.74	34.58	14.77
0.3	60.49	53.76	45.45	45.53	23.86
0.5	63.17	61.71	61.69	61.67	28.41

Table 14: Inhibition efficiency of as-received Al-Si-Mg (SSM-HPDC) alloy in 3.5wt% NaCl using guava (*Psidium guajava*) leaf extract as inhibitor at 50^{o}C.

Concentration	Inhibition efficiency (%)				
(%v/v)	1hr	2hr	3hr	4hr	5hr
0.0	-	-	-	-	-
0.1	16.03	20.02	20.00	17.89	12.21
0.2	16.03	39.95	40.00	17.89	24.88
0.3	44.04	39.95	40.00	44.21	24.88
0.5	44.04	59.96	49.61	50.88	34.27

Table 15: Inhibition efficiency of as-received Al-Si-Mg (SSM-HPDC) alloy in 3.5% NaCl using guava (*Psidium guajava*) leaf extract as inhibitor at 70^{o}C.

Concentration	Inhibition efficiency (%)				
(%v/v)	1hr	2hr	3hr	4hr	5hr
-	-	-	-	-	-
0.1	13.36	16.68	16.58	16.67	16.64
0.2	13.36	33.36	33.26	16.67	16.64
0.3	27.25	33.36	33.26	16.67	16.64
0.5	27.25	33.36	37.43	33.33	16.64

Table 16: Inhibition efficiency of double thermally aged Al-Si-Mg (SSM-HPDC) alloy in 3.5wt% NaCl using guava (*Psidium guajava*) leaf extract as inhibitor at 30^{o}C.

Concentration	Inhibition efficiency (%)				
(%v/v)	1hr	2hr	3hr	4hr	5hr
0.0	-	-	-	-	-
0.1	23.22	27.59	30.74	32.24	14.77
0.2	23.22	49.84	34.20	44.48	23.86
0.3	63.17	58.46	45.45	60.30	23.86
0.5	72.10	66.61	67.10	60.30	29.92

Table 17: Inhibition efficiency of double thermally aged Al-Si-Mg (SSM-HPDC) alloy in 3.5wt% NaCl using guava (*Psidium guajava*) leaf extract as inhibitor at 50^{o}C.

Concentration	Inhibition efficiency (%)				
(%v/v)	1hr	2hr	3hr	4hr	5hr
0.0	-	-	-	-	-
0.1	14.62	20.02	20.00	15.00	6.43
0.2	43.03	39.95	40.00	34.23	6.43
0.3	43.03	59.96	49.60	38.85	6.43
0.5	46.85	59.96	49.60	38.85	22.51

Table 18: Inhibition efficiency of double thermally aged Al-Si-Mg (SSM-HPDC) alloy in 3.5wt% NaCl using guava (*Psidium guajava*) leaf extract as inhibitor at 70^{o}C.

Concentration	Inhibition efficiency (%)				
(%v/v)	1hr	2hr	3hr	4hr	5hr
0.0	-	-	--	-	-
0.1	10.30	20.02	16.58	7.77	16.64
0.2	33.58	20.02	33.26	7.77	16.64
0.3	39.99	24.85	39.63	26.21	16.64
0.5	39.99	27.74	39.63	26.21	19.56

Table 19: Inhibition efficiency of as-received Al-Si-Mg (SSM-HPDC) alloy in 3.5wt% NaCl using neem (*Azadirachta indica*) seed extract as inhibitor at 30^{o}C.

Concentration	Inhibition efficiency (%)				
(%v/v)	1hr	2hr	3hr	4hr	5hr
0.0	-	-	-	-	-
0.1	20.80	33.24	30.74	34.58	14.77
0.2	20.80	33.24	30.74	34.58	14.77
0.3	23.22	53.76	45.45	34.58	14.77
0.5	60.49	53.76	54.55	45.53	14.77

Table 20: Inhibition efficiency of as-received Al-Si-Mg (SSM-HPDC) alloy in 3.5wt% NaCl using neem (*Azadirachta indica*) seed extract as inhibitor at 50^{o}C.

Concentration	Inhibition efficiency (%)				
(%v/v)	1hr	2hr	3hr	4hr	5hr
0.0	-	-	-	-	-
0.1	3.75	20.02	20.00	17.89	12.21
0.2	18.43	31.17	20.00	17.89	12.21
0.3	18.43	39.95	40.00	44.21	12.21
0.5	44.04	39.95	40.00	44.21	24.88

Table 21: Inhibition efficiency of as-received Al-Si-Mg (SSM-HPDC) alloy in 3.5wt% NaCl using neem (*Azadirachta indica*) seed extract as inhibitor at 70^{o}C.

Concentration	Inhibition efficiency (%)				
(%v/v)	1hr	2hr	3hr	4hr	5hr
0.0	-	-	-	-	-
0.1	17.55	16.68	33.26	16.67	16.64
0.2	19.96	16.68	33.26	16.67	16.64
0.3	19.96	33.36	33.26	33.33	16.64
0.5	40.00	33.36	39.63	33.33	16.64

Table 22: Inhibition efficiency of double thermally aged Al-Si-Mg (SSM-HPDC) alloy in 3.5wt% NaCl using neem (*Azadirachta indica*) seed extract as inhibitor at 30^{o}C.

Concentration	Inhibition efficiency (%)				
(%v/v)	1hr	2hr	3hr	4hr	5hr
0.0	-	-	-	-	-
0.1	19.93	27.59	30.74	32.24	14.77
0.2	28.68	27.59	30.74	32.24	14.77
0.3	28.68	49.84	45.45	43.58	14.77
0.5	60.49	64.26	54.55	43.58	14.77

Table 23: Inhibition efficiency of double thermally aged Al-Si-Mg (SSM-HPDC) alloy in 3.5wt% NaCl using neem (*Azadirachta indica*) seed extract as inhibitor at 50^{o}C.

Concentration	Inhibition efficiency (%)				
(%v/v)	1hr	2hr	3hr	4hr	5hr
0.0	-	-	-	-	-
0.1	14.62	9.66	20.00	10.00	6.43
0.2	14.62	9.66	40.00	34.23	6.43
0.3	43.10	20.02	40.00	34.23	6.43
0.5	43.10	59.44	40.00	38.85	6.43

Table 24: Inhibition efficiency of double thermally aged Al-Si-Mg (SSM-HPDC) alloy in 3.5wt% NaCl using neem (*Azadirachta indica*) seed extract as inhibitor at 70^{o}C.

Concentration	Inhibition efficiency (%)				
(%v/v)	1hr	2hr	3hr	4hr	5hr
0.0	-	-	-	-	-
0.1	12.03	9.66	16.58	7.77	16.64
0.2	25.95	18.96	16.58	7.77	16.64
0.3	33.10	18.96	33.26	7.77	16.64
0.5	33.10	22.21	33.26	26.21	16.64

Table 25: Inhibition efficiency of as-received Al-Si-Mg (SSM-HPDC) alloy for immersion time of 1hr at different operating temperatures

Concentration guava leaf extract (%)	Inhibition efficiency (%)		
	$30^{O}C$	$50^{O}C$	$70^{O}C$
0.0	-	-	-
0.1	20.80	16.03	13.36
0.2	23.22	16.03	13.36
0.3	60.49	44.04	27.25
0.5	63.17	44.04	27.25

Table 26: Inhibition efficiency of double thermally aged Al-Si-Mg (SSM-HPDC) alloy for immersion time of 1hr at different operating temperatures .

Concentration guava leaf extract (%)	Inhibition efficiency (%)		
	$30^{O}C$	$50^{O}C$	$70^{O}C$
0.0	-	-	-
0.1	23.22	14.62	10.30
0.2	23.22	43.03	33.58
0.3	63.17	43.03	39.99
0.5	72.10	46.85	39.99

Table 27: Inhibition efficiency of as-received Al-Si-Mg (SSM-HPDC) alloy for immersion time of 1hr at different operating temperatures

Concentration neem seed extract (%)	Inhibition efficiency (%)		
	$30^{O}C$	$50^{O}C$	$70^{O}C$
0.0	-	-	-
0.1	20.80	3.75	17.55
0.2	20.80	18.43	19.96
0.3	23.22	18.43	19.96
0.5	60.49	44.04	40.00

Table 28: Inhibition efficiency of double thermally aged Al-Si-Mg (SSM-HPDC) alloy for immersion time of 1hr at different operating temperatures

Concentration neem seed extract (%)	Inhibition efficiency (%)		
	$30^{O}C$	$50^{O}C$	$70^{O}C$
0.0	-	-	-
0.1	27.59	9.66	9.66
0.2	27.59	9.66	18.96
0.3	49.84	20.02	18.96
0.5	64.26	59.44	22.21

Table 29: Change in free energy of adsorption at different concentration of guava (*Psidium guajava*) leaf extract at 30^{o}C

Free energy of adsorption (ΔGads) kJ/mol										
Conc.	As-received					Age-hardened				
(%v/v)	1hr	2hr	3hr	4hr	5hr	1hr	2hr	3hr	4hr	5hr
0.1	-12.54	-14.15	-13.55	-14.31	-11.50	-14.62	-12.91	-13.87	-14.04	-11.50
0.2	-11.15	-12.41	-12.37	-12.56	-12.70	-11.15	-12.41	-13.06	-13.61	-14.04
0.3	-14.21	-13.52	-12.68	-12.69	-10.31	-14.50	-14.00	-12.68	-14.20	-10.31
0.5	-13.22	-13.06	-13.06	-13.06	-9.53	-14.25	-13.59	-13.65	-12.91	-9.72

Table 30: Change in free energy of adsorption at different concentration of guava (*Psidium guajava*) leaf extract at 50^{o}C

Free energy of adsorption (ΔGads) kJ/mol										
Conc.	As-received					Age-hardened				
(%v/v)	1hr	2hr	3hr	4hr	5hr	1hr	2hr	3hr	4hr	5hr
0.1	-12.52	-13.24	-13.24	-12.87	-10.94	-12.22	-13.24	-13.24	-14.87	-9.77
0.2	-10.66	-14.01	-14.01	-11.01	-12.11	-14.35	-14.01	-14.01	-13.35	-7.92
0.3	-13.37	-12.92	-12.92	-13.40	-11.05	-13.26	-15.10	-13.35	-12.79	-6.82
0.5	-12.00	-13.73	-12.60	-11.95	-10.89	-12.30	-13.73	-12.60	-11.42	-9.32

Table 31: Change in free energy of adsorption at different concentration of guava (*Psidium guajava*) leaf extract at 70^{o}C

Free energy of adsorption (ΔGads) kJ/mol										
Conc.	As-received					Age-hardened				
(%v/v)	1hr	2hr	3hr	4hr	5hr	1hr	2hr	3hr	4hr	5hr
0.1	-12.68	-13.64	-13.42	-13.12	-13.42	-11.84	-14.06	-13.42	-10.93	-13.42
0.2	-10.70	-14.06	-14.05	-11.45	-11.45	-15.24	-12.09	-14.05	-13.04	-11.45
0.3	-12.08	-12.90	-12.89	-10.29	-10.29	-8.98	-11.73	-13.68	-11.93	-10.29
0.5	-10.62	-11.45	-11.60	-11.45	-8.83	-12.27	-10.69	-12.21	-10.47	-9.39

Table 32: Change in free energy of adsorption at different concentration of neem (*Azadirachta indica*) seed extract at 30^{o}C

Free energy of adsorption (ΔGads) kJ/mol										
Conc.	As-received					Age-hardened				
(%v/v)	1hr	2hr	3hr	4hr	5hr	1hr	2hr	3hr	4hr	5hr
0.1	-12.54	-14.15	-13.87	-13.87	-11.50	12.41	-14.33	-13.87	-14.44	-11.50
0.2	-10.80	-12.41	-12.37	-12.56	-9.75	11.87	-6.94	-12.87	-12.30	-9.75
0.3	-10.15	-13.52	-13.52	-11.54	-12.70	10.83	-13.13	-12.37	-12.49	-12.70
0.5	-12.93	-12.24	-12.24	-11.41	-7.45	-12.93	-12.82	-12.68	-11.21	-7.45

Table 33: Change in free energy of adsorption at different concentration of neem (*Azadirachta indica*) seed extract at 50^{o}C.

Free energy of adsorption (ΔGads) kJ/mol										
Conc.	As-received					Age-hardened				
(%v/v)	1hr	2hr	3hr	4hr	5hr	1hr	2hr	3hr	4hr	5hr
0.1	-12.22	-13.24	-13.87	-13.24	-10.24	12.22	-10.96	-13.24	-12.87	-10.94
0.2	-10.36	-12.97	-14.01	-14.01	-9.81	-10.36	-9.10	-14.01	-11.01	-9.77
0.3	-10.02	-12.92	-12.92	-12.92	-8.717	-13.27	-10.29	-12.92	-13.40	-6.82
0.5	-12.00	-11.55	-12.02	-12.02	-9.67	-11.90	-13.67	-12.16	-11.42	--5.45

Table 34: Change in free energy of adsorption at different concentration of neem (*Azadirachta indica*) seed extract at 70^{o}C

Free energy of adsorption (ΔGads) kJ/mol										
Conc.	As-received					Age-hardened				
(%v/v)	1hr	2hr	3hr	4hr	5hr	1hr	2hr	3hr	4hr	5hr
0.1	-13.60	-13.64	-12.08	-13.12	-13.42	-12.87	-11.33	-13.42	-10.93	-13.42
0.2	-12.08	-11.45	-13.42	-11.45	-11.45	-13.05	-11.89	-11.43	-13.04	-11.45
0.3	-12.28	-12.90	-14.05	-12.90	-10.29	-12.87	-10.74	-12.89	-8.96	-10.29
0.5	-12.27	-11.45	-12.22	-11.45	-8.83	-11.42	-9.85	-11.44	-10.47	-8.83

Table 35: Heat of adsorption (Q_{ads}) kJ/mol at different concentration of guava (*Psidium guajava*) leaf extract.

Heat of adsorption (Q_{ads}) kJ/mol										
Conc.	As-received					Age-hardened				
(%v/v)	1hr	2hr	3hr	4hr	5hr	1hr	2hr	3hr	4hr	5hr
0.1	-12.97	-27.98	-18.25	-36.00	-8.94	-23.14	-17.09	-23.34	-40.33	-36.80
0.2	-18.71	-11.78	-16.55	-36.00	-26.34	-37.23	-16.31	-10.14	-17.54	-36.80
0.3	-69.68	-15.87	-9.07	-2.17	-2.25	-33.34	-2.53	-6.77	-35.45	-36.80
0.5	-31.69	-6.86	-20.00	-11.88	-11.11	-21.54	-33.00	-15.84	-8.99	-90.21

Table 36: Heat of adsorption (Q_{ads}) kJ/mol at different concentration of neem (*Azadirachta indica*) seed extract.

Heat of adsorption (Q_{ads}) kJ/mol										
Conc.	As-received					Age-hardened				
(%v/v)	1hr	2hr	3hr	4hr	5hr	1hr	2hr	3hr	4hr	5hr
0.1	-77.61	-27.97	-23.34	-36.04	-96.46	-15.22	-51.69	-23.31	-59.57	-37.63
0.2	-6.12	-3.85	-23.24	-36.04	-96.46	-34.72	-51.69	-16.75	3.65	-37.63
0.3	-8.06	-22.70	-8.87	-16.47	-96.46	-34.72	-56.07	-8.87	-16.05	-37.63
0.5	-27.07	-22.84	-23.70	-2.17	-26.34	-28.62	-8.36	-23.71	-7.95	-37.63

Table 37: Activation energy (Ea) kJ/mol at different concentration of guava (*Psidium guajava*) leaf extract.

Activation energy (Ea) kJ/mol										
Conc.	As-received					Age-hardened				
(%v/v)	1hr	2hr	3hr	4hr	5hr	1hr	2hr	3hr	4hr	5hr
Control	-14.30	-20.71	-20.69	-20.63	-19.88	-13.61	-24.09	-20.69	-18.27	-10.76
0.1	-16.73	-28.22	-25.14	-30.07	-21.12	-16.28	-28.22	-26.67	-27.69	-14.64
0.2	-14.86	-16.31	-14.72	-30.07	-14.64	-1.16	-31.57	-16.85	-25.07	-19.32
0.3	-28.76	-31.57	-24.65	-21.62	-19.32	-31.69	-22.56	-17.40	-36.22	-19.32
0.5	-32.69	-22.56	-32.08	-30.94	-16.33	-39.12	-31.63	-38.40	-36.22	-14.93

Table 38: Activation energy (Ea) kJ/mol at different concentration of of neem (*Azadirachta indica*) seed extract.

Activation energy (Ea) kJ/mol										
Conc.	As-received					Age-hardened				
(%v/v)	1hr	2hr	3hr	4hr	5hr	1hr	2hr	3hr	4hr	5hr
Control	-14.30	-20.71	-20.69	-20.63	-19.88	-13.61	-24.09	-20.69	-18.27	-10.76
0.1	-22.40	-28.22	-26.67	-30.07	-21.12	-16.28	-33.28	-26.67	-30.07	-14.64
0.2	-15.53	-21.98	-26.67	-30.07	-21.12	-21.09	-33.28	14.72	-17.03	-14.64
0.3	-17.13	-10.75	-24.65	-14.01	-21.12	-4.22	-43.28	-24.65	-24.65	-14.64
0.5	-28.76	-31.57	-32.24	-21.62	-14.63	-28.76	-25.88	-32.22	-21.62	-14.64

Table 39: The potentiodynamic polarization parameters for the corrosion of as-received Al-Si-Mg (SSM-HPDC) in 3.5wt% NaCl / Guava (*Psidium guajava)* leaf extract environment.

S/N	**Conc. (%v/v)**	**$E_{corr,}$ obs(v)**	**j_{corr} (A/cm^2) (Ω)**	**Corrosion rate (mm/yr)**	**Polarization resistance**
1	0.0	-1.3069	8.22E-05	0.95536	118.51
2	0.1	-1.3006	3.87E-05	0.44955	496.15
3	0.2	-1.2663	2.17E-05	0.25269	776.27
4	0.3	-1.3033	7.21E-05	0.83804	101.82
5	0.5	-0.6180	8.42E-06	0.097876	1244.7

Table 40: The potentiodynamic polarization parameters for the corrosion of double thermally aged Al-Si-Mg (SSM-HPDC) in 3.5wt% NaCl / Guava (*Psidium guajava)* leaf extract environment.

S/N	Conc. (%v/v)	$E_{corr,}$ obs(v)	j_{corr} (A/cm^2) (Ω)	Corrosion rate (mm/yr)	Polarization resistance
1	0.0	-1.2771	8.06E-05	0.936820	195.58
2	0.1	-1.2760	4.12E-05	0.478450	166.87
3	0.2	-1.2325	3.85E-05	0.447600	166.49
4	0.3	-1.2070	1.52E-05	0.176970	383.17
5	0.5	-1.1649	9.03E-07	0.010488	6736.6

Table 41: The potentiodynamic polarization parameters for the corrosion of as-received Al-Si-Mg (SSM-HPDC) in 3.5wt% NaCl / Neem (*Azadirachta indica*) seed extract environment.

S/N	Conc. (%v/v)	$E_{corr,}$ obs(v)	j_{corr} (A/cm^2) (Ω)	Corrosion rate (mm/yr)	Polarization resistance
1	0.0	-0.83089	1.74E-09	0.71516	1.30E+08
2	0.1	-0.88954	2.15E-09	0.83233	1.15E+08
3	0.2	-0.84847	1.21E-09	0.57068	1.42E+08
4	0.3	-0.93878	1.06E-10	0.39195	1.44E+08
5	0.5	-0.90300	2.28E-10	0.39274	1.43E+08

Table 42: The potentiodynamic polarization parameters for the corrosion of double thermally aged Al-Si-Mg (SSM-HPDC) in 3.5wt% NaCl / Neem (*Azadirachta indica*) seed extract environment.

S/N	Conc. (%v/v)	$E_{corr,}$ obs(v)	j_{corr} (A/cm^2) (Ω)	Corrosion rate (mm/yr)	Polarization resistance
1	0.0	-0.80409	5.15E-09	0.76671	9.99E+07
2	0.1	-0.80205	4.73E-09	0.68238	1.11E+08
3	0.2	-0.81871	1.18E-09	0.40766	1.00E+08
4	0.3	-0.81638	1.87E-09	0.58899	1.08E+08
5	0.5	-0.82908	9.95E-10	0.35851	1.14E+08

Table 43: Comparative table of inhibitor efficiency (IE) for as-received alloy-3.5wt%NaCl solution / Guava (*Psidium guajava*) leaf extract concentration obtained by G.M, PP-J_{corr}, PP-CR, and LPR.

Conc.(%v/v)	G.M (%)	PP-J_{corr} (%)	PP-CR (%)	LPR (%)
0.0	-	-	-	-
0.1	34.58	52.92	52.94	76.11
0.2	34.58	73.60	73.55	84.73
0.3	60.49	12.29	12.29	-16.39
0.5	63.17	89.76	89.76	90.48

Table 44: Comparative table of inhibitor efficiency (IE) for age-hardened alloy-3.5wt%NaCl solution / Guava (*Psidium guajava*) leaf extract concentration obtained by G.M, PP-J_{corr}, PP-CR, and LPR.

Conc.(%v/v)	G.M (%)	PP-J_{corr} (%)	PP-CR (%)	LPR (%)
0.0	-	-	-	-
0.1	32.24	48.88	48.92	-17.21
0.2	49.84	52.23	52.22	-17.47
0.3	63.17	81.14	81.11	48.96
0.5	72.10	98.88	98.89	97.10

Table 45: Comparative table of inhibitor efficiency (IE) for as-received alloy-3.5wt%NaCl solution/Neem (*Azadirachta indica*) seed extract concentration obtained by G.M, PP-J_{corr}, PP-CR, and LPR.

Conc.(%v/v)	G.M (%)	PP-J_{corr} (%)	PP-CR (%)	LPR (%)
0.0	-	-	-	-
0.1	34.58	-23.56	-16.38	-13.04
0.2	34.58	30.46	22.11	8.45
0.3	53.76	96.55	45.19	9.72
0.5	60.49	86.90	45.08	9.09

Table 46: Comparative table of inhibitor efficiency (IE) for age-hardened alloy-3.5wt%NaCl solution/Neem (*Azadirachta indica*) seed extract concentration obtained by G.M, PP-J_{corr}, PP-CR, and LPR.

Conc.(%v/v)	G.M (%)	PP-J_{corr} (%)	PP-CR (%)	LPR (%)
0.0	-	-	-	-
0.1	32.24	8.16	11.00	10.00
0.2	32.24	77.09	20.20	0.10
0.3	49.84	63.69	46.83	7.50
0.5	64.26	80.68	53.24	12.37

Thermodynamic model could be used to explain the corrosion inhibition of the inhibitors. Thus, the heat of adsorption (Q_{ads}) and free energies of adsorption (ΔG_{ads}) were calculated, using equations 17 and 18 respectively. The values of ΔG_{ads} obtained are presented in Table…….. The negative values of ΔG_{ads} ensure the spontaneity of the adsorption process and stability of the adsorbed layer on the……. surface. Generally, the values of ΔG_{ads} around 20KJ/mol or lower are consistent with physiosorption, while those around 40KJ/mol or higher involve chemisorptions (Olasehinde *et al.*, 2013). As shown in the Tables, results obtained indicate that the values of ΔG_{ads} are all negative in all cases and less than 20KJ/mol. This is consistent with literature survey and therefore authenticates physical adsorption.

The obtained values of heat of adsorption (Q_{ads}) were more negative than -10KJ/mol for both the as-received and age-hardened samples, suggesting that the adsorption is probably chemical.

Kinetic consideration

The values of activation energy (E_a) of as-received and age-hardened samples were found to be -14.30, -20.71,-20.69, -20.69, -19.88 and -13.61, -24.09, -20.69, -18.27, -10.76 in free solution for 1-5 hrs respectively. But in the presence of guava leaf extract it increased to -32.69, -22.56, -32.08, -30.94, -16.33 and -39.12, -13.63, -38.40, -36.22 and -14.93 for 1-5hrs respectively. The same trend follows in the presence of neem seed extracts with values of -28.76, -31.57, -32.24, -21.62, -14.63 and -28.76, -25.88, -32.22, -21.62 and -14.64 at 0.5% v/v respectively for 1-5 hrs. It has been reported that when the values of E_a >80 KJ/mol indicates chemical adsorption whereas E_a <80 KJ/mol infers physical adsorption (Ismail et al., 2011; Adeyemi and Olubomehin, 2010). On the bases of experimentally determined activation energy values of E_a <80 KJ/mol in this study, we propose that the extracts are physically adsorbed on the coupons.